
**Characterization of the *Lotus japonicus* nuclear pore
NUP107-160 subcomplex in plant-microbe symbiosis**

Dissertation
der Fakultät für Biologie der
Ludwig-Maximilians-Universität München

vorgelegt von
Andreas Binder
München, im Juli 2014

Dissertation eingereicht am: 3. Juli 2014

Tag der mündlichen Prüfung: 17. November 2014

Erstgutachter: Prof. Dr. Martin Parniske

Zweitgutachter: Prof. Dr. Ute C. Vothknecht

Eidesstattliche Versicherung

Ich versichere hiermit an Eides statt, dass die vorgelegte Dissertation von mir selbstständig und ohne unerlaubte Hilfe angefertigt ist.

München, den 3. Juli 2014

Andreas Binder

Erklärung

Hiermit erkläre ich, dass die Dissertation nicht ganz oder in wesentlichen Teilen einer anderen Prüfungskommission vorgelegt worden ist. Ich habe nicht versucht, anderweitig eine Dissertation einzureichen oder mich einer Doktorprüfung zu unterziehen.

München, den 3. Juli 2014

Andreas Binder

Table of Contents

1. Abbreviation index	3
2. List of Publications	4
3. Declaration of Contribution as Co-Author	5
4. Summary	7
5. Introduction	9
5.1. Arbuscular mycorrhiza and root nodule symbiosis	9
5.2. Symbiotic crosstalk and establishment of root endosymbioses	10
5.3. Signal transduction in root endosymbiosis	13
5.3.1. Signal perception at the plant plasma membrane	13
5.3.2. Signaling from plasma membrane to nucleus	14
5.3.3. Generation of nuclear calcium spiking	15
5.3.4. Decoding the calcium signal	17
5.3.5. Transcription factors in symbiotic signaling	18
5.3.6. Common symbiosis genes involved in microbial accommodation	20
5.4. The plant nuclear pore complex in symbiotic signaling and plant defense	21
6. Aim of the thesis	24
7. Part I: Analysis of the <i>Lotus japonicus</i> nuclear pore NUP107-160 subcomplex reveals pronounced structural plasticity and functional redundancy	25
8. Part II: A modular plasmid assembly kit for multigene expression, gene silencing and silencing rescue in plants	35
9. Part III: Characterization of nucleoporin mutants in symbiotic signaling	50
9.1. Results	50
9.1.1. Measurement of nod factor induced calcium spiking in <i>Lotus japonicus</i> lines stably expressing localized yellow cameleons	50
9.1.2. <i>nup85</i> and <i>nup133</i> mutants show residual calcium signatures in response to nod factor and chitin tetramer elicitation	52
9.1.3. CASTOR, POLLUX, NUP85 and NUP133 peptide antibodies	54
9.1.4. <i>nup107</i> LORE1 insertion mutants are deficient in nodulation	57
9.1.5. CASTOR and POLLUX localize to the inner nuclear membrane in <i>N. benthamiana</i>	60
9.1.6. Differential nuclear and cytosolic protein localization by complementation of superfolder GFP	62
9.1.7. Simultaneous overexpression of CASTOR and POLLUX complements the nodulation phenotype in <i>L. japonicus nup</i> mutants	63
9.2. Discussion	66
9.2.1. Transgenic <i>L. japonicus</i> calcium reporter lines for analysis of symbiotic calcium responses	66
9.2.2. Nuclear calcium signaling in <i>nup85</i> and <i>nup133</i> mutants	68
9.2.3. A LORE1 line with an insertion in <i>L. japonicus</i> NUP107 is defective in nodulation	68
9.2.4. Are CASTOR and POLLUX the targets that affect symbiotic signaling in <i>L. japonicus nup</i> mutants?	70
9.3. Material and methods	74

9.3.1.	Media	74
9.3.2.	Bacterial strains	75
9.3.3.	Plant lines	75
9.3.4.	<i>Lotus japonicus</i> mutant alleles and transgenic lines	75
9.3.5.	Oligonucleotides	75
9.3.6.	Bacterial growth conditions.....	77
9.3.7.	Plant germination and growth.....	77
9.3.8.	Transformation of <i>E. coli</i> cells	77
9.3.9.	Transformation of <i>Agrobacterium</i> cells.....	77
9.3.10.	<i>N. benthamiana</i> transformation	78
9.3.11.	Hairy root transformation	78
9.3.12.	Nodulation assay	79
9.3.13.	Crossing	79
9.3.14.	Extraction of genomic plant DNA.....	79
9.3.15.	Plant genotyping.....	80
9.3.16.	Polymerase-chain reaction.....	81
9.3.17.	Sequencing.....	81
9.3.18.	Plasmid isolation.....	81
9.3.19.	Molecular Cloning.....	81
9.3.20.	SDS page	83
9.3.21.	Whole-mount immunolocalization.....	84
9.3.22.	Microscopy	84
9.3.23.	Calcium imaging	84
10.	General Discussion	86
10.1.	Analysis of symbiotic signaling and flexible construct adaptation via Golden Gate cloning.....	86
10.2.	A window into the NPC - Study of <i>L. japonicus</i> NUP107-160 subcomplex mutants.....	87
10.3.	Proposed function of the NUP107-160 subcomplex in symbiotic signaling	88
11.	Appendix.....	92
11.1.	Supplementary Figure.....	92
11.2.	List of Figures.....	93
11.3.	List of Tables	93
12.	Acknowledgements	94
13.	Curriculum Vitae	95
14.	References.....	96

1. Abbreviation index

aa	amino acid
AM	arbuscular mycorrhiza
Amp	ampicillin
AOM	autoregulation of mycorrhization
AS	alternative splicing
BiFC	bimolecular fluorescence complementation
CaM	calmodulin
CAPs	cleaved amplified polymorphic sequences
CFP	cyan fluorescent protein
CLSM	confocal laser scanning microscopy
dCAPs	derived cleaved amplified polymorphic sequences
ddH ₂ O	double distilled water / Millipore filtered water
DNA	deoxyribonucleic acid
GA	gibberellic acid
Gent	gentamycin
GFP	green fluorescent protein
GG	golden gate
HRP	horse radish peroxidase
INM	inner nuclear membrane
IPTG	isopropyl β -D-thiogalactopyranoside
IT	infection thread
Kan	kanamycin
Kb	kilo base
kDa	kilodalton
LB	lysogeny broth / Luria-Bertani broth
LCO	lipochitooligosaccharide
LysM	lysine motif
MAP	mitogen-activated protein
MAPKK	mitogen-activated protein kinase kinase
MF	mycorrhiza factor
myc	mycorrhiza
NBS-LRR	nucleotide-binding site leucine-rich repeat
NES	nuclear export signal
NF	nodulation factor
NLS	nuclear localization signal
nod	nodulation
NUP	nucleoporin
ONM	outer nuclear membrane
p35S	cauliflower mosaic virus 35S promoter
PAM	periarbuscular membrane
PBS	phosphate-buffered saline
PCR	polymerase chain reaction
PPA	prepenetration apparatus
RLK	receptor like kinase
RNS	root nodule symbiosis
RT	room temperature
SD	standard deviation
Spec	spectinomycin
TEM	transmission electron microscope
TF	transcription factor
wt	wild type
X-Gal	5-Brom-4-chlor-3-indoxyl- β -D-galactopyranosid
YFP	yellow fluorescent protein

2. List of Publications

- **Binder, A.**, and Parniske, M. (2014). Analysis of the *Lotus japonicus* nuclear pore NUP107-160 subcomplex reveals pronounced structural plasticity and functional redundancy. *Frontiers in Plant Science* 4.
- **Binder, A.**, Soyano, T., Hayashi, M., Parniske, M., and Radutoiu, S. (2014). "Plant Genes Involved in Symbiotic Signal Perception/Signal Transduction," in *The Lotus japonicus Genome*, eds. S. Tabata & J. Stougaard. Springer Berlin Heidelberg, 59-71.
- **Binder, A.**, Lambert, J., Morbitzer, R., Popp, C., Ott, T., Lahaye, T., and Parniske, M. (2014). A modular plasmid assembly kit for multigene expression, gene silencing and silencing rescue in plants. *PLoS ONE* 9, e88218.
- De Lange, O., **Binder, A.**, and Lahaye, T. (2014). From dead leaf, to new life: TAL effectors as tools for synthetic biology *Plant Journal* 5, 753-771.
- **Binder, A.**, and Parniske, M. (2013). "The nuclear pore complex in symbiosis and pathogen defence," in *Annual Plant Reviews*. John Wiley & Sons Ltd, 229-254.
- Antolín-Llovera, M., Ried, M.K., **Binder, A.**, and Parniske, M. (2012). Receptor kinase signaling pathways in plant-microbe interactions. *Annual Review of Phytopathology* 50, 451-473.
- Krebs, M., Held, K., **Binder, A.**, Hashimoto, K., Den Herder, G., Parniske, M., Kudla, J., and Schumacher, K. (2012). FRET-based genetically encoded sensors allow high-resolution live cell imaging of Ca²⁺ dynamics. *Plant Journal* 69, 181-192.
- Perry, J., Brachmann, A., Welham, T., **Binder, A.**, Charpentier, M., Groth, M., Haage, K., Markmann, K., Wang, T.L., and Parniske, M. (2009). TILLING in *Lotus japonicus* identified large allelic series for symbiosis genes and revealed a bias in functionally defective ethyl methanesulfonate alleles toward glycine replacements. *Plant Physiology* 151, 1281-1291.

Manuscript submitted

- Banhara A., Ried M.K., **Binder A.**, Gust A.A., Höfle C., Hüchelhoven R., Nürnberger T., and Parniske M. Symbiosis-related genes sustain the development of a Downie Mildew pathogen on *Arabidopsis thaliana*

3. Declaration of Contribution as Co-Author Erklärung über die erbrachte Leistung als Koautor

*Andreas Binder, the author of this thesis, contributed to the following publications as listed:
Andreas Binder, der Autor der vorliegenden Dissertation, hat die folgenden Leistungen zu den
aufgeführten Veröffentlichungen beigetragen:*

Publication I: Analysis of the *Lotus japonicus* nuclear pore NUP107-160 subcomplex reveals pronounced structural plasticity and functional redundancy

Reference: **Binder, A.**, and Parniske, M. (2014). Analysis of the *Lotus japonicus* nuclear pore NUP107-160 subcomplex reveals pronounced structural plasticity and functional redundancy. *Frontiers in Plant Science* 4.

Andreas Binder

- designed and performed the experiments presented in the manuscript
- wrote the manuscript, which was marginally modified by Martin Parniske

- entwarf sämtliche im Manuskript präsentierten Experimente und führte sie durch
- schrieb das Manuskript, welches von Martin Parniske geringfügig verändert wurde

Publication II: A Modular Plasmid Assembly Kit for Multigene Expression, Gene Silencing and Silencing Rescue in Plants

Reference: **Binder, A.**, Lambert, J., Morbitzer, R., Popp, C., Ott, T., Lahaye, T., and Parniske, M. (2014). A modular plasmid assembly kit for multigene expression, gene silencing and silencing rescue in plants. *PLoS ONE* 9, e88218.

Andreas Binder

- designed the general concept of the cloning toolkit together with Robert Morbitzer, Claudia Popp and Jayne Lambert
- designed 120 and cloned 98 out of the 131 published toolkit constructs
- designed and performed all experiments presented in the manuscript
- created the figures and wrote the manuscript, which was edited by Thomas Lahaye and Martin Parniske.

- Erstellte das generelle Konzept des Klonierungs-Baukastens zusammen mit Robert Morbitzer, Claudia Popp und Jayne Lambert
- Entwarf 120 und klonierte 98 der insgesamt 131 publizierten Konstrukte.
- Entwarf sämtliche im Manuskript präsentierten Experimente und führte sie durch.
- Erstellte die Abbildungen und schrieb das Manuskript, welches von Thomas Lahaye und Martin Parniske editiert wurde.

Publication III: FRET-based genetically encoded sensors allow high-resolution live cell imaging of Ca²⁺ dynamics (integrated into part II of the thesis)

Reference: Krebs, M., Held, K., **Binder, A.**, Hashimoto, K., Den Herder, G., Parniske, M., Kudla, J., and Schumacher, K. (2012). FRET-based genetically encoded sensors allow high-resolution live cell imaging of Ca²⁺ dynamics. *Plant Journal* 69, 181-192.

Andreas Binder

- screened stable transformands of *L. japonicus* expressing NLS-YC3.6 and NES-YC3.6 cameleon constructs and propagated homozygous individuals.
- performed calcium measurements in *L. japonicus* as presented in Figure 6 of the manuscript.
- wrote the part of the manuscript related to Figure 6 (methods, results & discussion)

- Wählte geeignete stabile *L. japonicus* Transformanden aus, die NLS-YC3.6 und NES-YC3.6 Cameleon-Konstrukte exprimierten und propagierte homozygote Individuen.
- Führte die in Abbildung 6 des Manuskripts präsentierten Calciummessungen in *L. japonicus* durch.
- Schrieb den Teil des Manuskript der sich auf Figure 6 bezieht (Methoden, Ergebnisse & Diskussion)

Note: Publications I & II are not included as part of the thesis. The experiments of publication III that were performed by Andreas Binder (Figure 6 of the paper) have been added to part III of the thesis (licence agreement granted by John Wiley and Sons).

4. Summary

Plants engage in beneficial root nodule symbiosis (RNS) with rhizobial bacteria and arbuscular mycorrhiza (AM) symbiosis with fungi of the phylum glomeromycota. Genetic analyses in *Lotus japonicus* and *Medicago truncatula* have revealed a shared common program underlying establishment of both RNS and AM. Three of the identified common symbiosis genes of *L. japonicus*, *NUP85*, *NUP133* and *NENA* code for components of the nuclear pore complex (NPC). Mutations in these plant nucleoporins (NUPs) abolish symbiotic calcium spiking and cause temperature dependent defects in nodulation and mycorrhiza colonization. Homologs of *NUP85*, *NUP133* and *NENA* are part of the NUP107-160 (vertebrates) and *NUP84* (yeast) subcomplex, a vital part of the NPC scaffold. Loss or knock-down of NUP107-160/*NUP84* subcomplex components has been correlated with pleiotropic phenotypes in plants, animals and fungi. However, the symbiotic defects in *L. japonicus* appear to be surprisingly specific.

Investigation of the *L. japonicus nup* mutants indicated that the NUP107-160 sub-complex can tolerate the loss of individual members remarkably well. Immunolocalization in *L. japonicus* roots confirmed a nucleoporin-like localization for *NUP133*, which was not affected in the *nup85* mutant. In contrast to the NPC clustering phenotype in *Saccharomyces cerevisiae*, transmission electron microscopy analysis of *L. japonicus nup85*, *nup133*, *nena* and wild-type plants revealed only a slight reduction in the average distances between neighboring NPCs in *nup133* and no significant changes in *nup85* and *nena*. Despite the limited visible effects, quantitative immunodetection on protein blots demonstrated a reduction in the protein levels of other NUP107-160 complex members in *nup85* and *nena* mutants, suggesting a change in the subcomplex composition. Unlike the single *nup* mutants, *nup85/nup133* double mutants exhibited severe temperature dependent growth and developmental defects, suggesting that the loss of multiple NUP107-160 members affects more basal functions of the NPC.

Transgenic *L. japonicus* plants expressing the calcium reporter yellow cameleon 3.6 (YC3.6) were generated to analyze symbiotic calcium spiking. Rare atypical nuclear calcium transients, but no wild type like calcium oscillations could be detected in *nup85* and *nup133* mutants following treatment with rhizobial nod factor and fungal chitin tetramer, indicating that the mutations in the NPC lead to a disturbance in the nuclear calcium spiking machinery. The nuclear ion channels CASTOR and POLLUX were investigated as potential targets, which could be affected by mutations in the NUPs. A bimolecular fluorescence assay based on the dimerization domain of the bZIP63 transcription factor showed INM localization of CASTOR and POLLUX in *N. benthamiana* and simultaneous overexpression of both ion channels was able to restore nodulation in *L. japonicus nup85*, *nup133* and *nena* mutants. Taken together the data suggested that mutations in NUP107-160 subcomplex members could lead to a quantitative import defect of CASTOR and POLLUX into the inner nuclear membrane, thereby affecting nuclear calcium spiking and symbiotic signaling.

Flexible assembly of multigene constructs was facilitated by development of a cloning toolkit based on the Golden Gate method. General functionality of the system was demonstrated by assembly and testing of constructs for co-expression of three fluorophores as well as by gene silencing and complementation.

4. Zusammenfassung

Pflanzen gehen Symbiosen mit Rhizobien (Wurzelknöllchensymbiose) und Pilzen des Phylums Glomeromycota (Arbuskuläre Mykorrhiza) ein. Genetische Untersuchungen in *Lotus japonicus* und *Medicago truncatula* zeigten die Existenz eines gemeinsamen genetischen Programmes auf, welches sowohl für die Etablierung der Wurzelknöllchensymbiose (RNS) als auch der arbuskulären Mykorrhiza (AM) verantwortlich ist. Drei der identifizierten *L. japonicus* „common symbiosis“ Gene, *NUP85*, *NUP133* und *NENA* kodieren für Proteine des Kernporenkomplexes (NPC). Mutationen in diesen Nukleoporinen (NUPs) verhindern symbiotische Calciumoszillationen („Calcium Spiking“) und führen zu temperaturabhängigen Defekten in der Wurzelknöllchenbildung und Kolonisierung durch Mykorrhiza-Pilze. Homologe von *NUP85*, *NUP133* und *NENA* sind Teil des NUP107-160 (Vertebraten) und *NUP84* (Hefe) Subkomplexes, eines essentiellen Bestandteils des Kernporengerüsts. Der komplette oder teilweise Verlust von *NUP107-160/NUP84* Subkomplexproteinen führt in Pflanzen, Tieren und Pilzen zu pleiotropen Phänotypen. Demgegenüber erscheinen die symbiotischen Defekte in *L. japonicus* überraschend spezifisch.

Die Untersuchung der *L. japonicus nup* Mutanten ließ darauf schließen, dass der *NUP107-160* Subcomplex den Verlust einzelner Komponenten erstaunlich gut kompensieren kann. Immunfluoreszenzfärbungen in *L. japonicus* Wurzeln bestätigten, dass *NUP133* eine für ein Nukleoporin typische Lokalisierung aufwies und diese in *nup85* Mutanten unverändert blieb. Im Gegensatz zur beobachteten Anhäufung von NPCs in *Saccharomyces cerevisiae* zeigten transmissionselektronenmikroskopische Untersuchungen in *L. japonicus nup85*, *nup133*, *nena* und Wildtyp Pflanzen nur eine geringe Verkleinerung des Abstandes zwischen benachbarten Kernporen in *nup133* und keine signifikanten Unterschiede in *nup85* und *nena*. Trotz dieser geringen sichtbaren Differenzen zeigten quantitative Immunoblots eine Abnahme von anderen *NUP107-160* Nukleoporinen in *nup85* und *nena* Mutanten an, was auf eine veränderte Zusammensetzung des *NUP107-160* Subkomplexes schließen ließ. Anders als einzelne *nup* Mutanten, wiesen *nup85/nup133* Doppelmутanten schwerwiegende temperaturabhängige Wachstums- und Entwicklungsdefekte auf, folglich beeinträchtigt der Verlust von mehreren *NUP107-160* Proteinen in verstärktem Maße grundlegende Funktionen der Kernpore.

Zur Untersuchung von symbiotischem „Calcium Spiking“, wurden transgene *L. japonicus* Pflanzen erzeugt, die den Calcium Reporter „yellow cameleon 3.6“ (YC3.6) stabil exprimieren. In *nup85* und *nup133* Mutanten konnten damit nach Zugabe von Nodfaktor und Chitintetramer vereinzelte atypische Calciumsignale nachgewiesen werden, jedoch keine Calciumoszillationen wie in den Wildtyp-Pflanzen. Dies gab einen Hinweis darauf, dass die Mutationen in Kernporenkomponenten die Calciumspikingmaschinerie beeinträchtigen. Die nukleären Ionenkanäle CASTOR und POLLUX wurden als mögliche Ziele untersucht, welche durch Mutationen in den NUPs in Mitleidenschaft gezogen sein könnten. Die Analyse mittels bimolekulare Komplementation von YFP, basierend auf der Dimerisierung des Transkriptionsfaktors bZIP63, zeigte an, dass CASTOR und POLLUX in *N. benthamiana* in der inneren Kernmembran lokalisiert sind. Durch die gleichzeitige Überexpression von beiden Ionenkanälen wurde die Knöllchenbildung in *L. japonicus nup85*, *nup133* und *nena* Mutanten wiederhergestellt. Diese Daten legen nahe, dass die Mutationen in Proteinen des *NUP107-160* Subkomplexes zu einem quantitativen Importdefekt von CASTOR und POLLUX in die innere Kernmembran führen, wodurch nukleäres „Calcium Spiking“ und die symbiotische Signaltransduktion gestört werden.

Die flexible Erzeugung von Multigenkonstrukten wurde durch die Entwicklung eines Klonierungs-Baukastens nach der Golden Gate (GG) Methode ermöglicht. Die Funktionalität des Systems wurde durch den Zusammenbau und Test von Konstrukten zur Co-Expression von drei Fluorophoren und zum Gen-Silencing und zur Silencing-Komplementation demonstriert.

5. Introduction

5.1. Arbuscular mycorrhiza and root nodule symbiosis

Root endosymbioses with microbial partners serve an important function in plant nutrition and fitness. Arbuscular mycorrhiza (AM) and root nodule symbiosis (RNS) with legumes are of particular ecological and economic importance (Udvardi et al., 2005; Smith and Smith, 2011). AM is an ancient association between biotrophic fungi of the phylum *Glomeromycota* and the majority of land plants (Schüßler et al., 2001). It is considered the most widespread symbiosis (Fitter, 2005) and can be traced back to the emergence of land plants 400 million years ago (Remy et al., 1994). In exchange for fixed carbon from the plant, AM fungi provide their hosts with phosphorus, sulfur, nitrogen, water and other inorganic nutrients from the surrounding soil via an extended hyphal network (Figure 1). Fungal hyphae enter the root epidermis and grow into the cortex, where they spread longitudinally in the apoplastic space to form tree-shaped arbuscules inside inner cortical root cells (Gutjahr and Parniske, 2013). Nutrient exchange is assumed to primarily take place in the arbusculated cells (Parniske, 2008; Smith and Read, 2008).

Root nodule symbiosis (RNS) between nitrogen fixing bacteria and plants is evolutionary much younger than AM (58 million years ago; Sprent, 2007; Doyle, 2011) and restricted to plant species of the eurosoid I subclade of angiosperms (Fabales, Fagales, Cucurbitales, Rosales; Soltis et al., 2000). Legumes form RNS with diverse bacteria collectively referred to as rhizobia (Sprent, 2007), whereas plants of the orders Fagales, Curcubiales and Rosales primarily interact with actinobacteria of the genus *Frankia* (Pawlowski and Sprent, 2008). In RNS, atmospheric nitrogen is fixed by differentiated bacteria inside of specialized root organs, the nodules. In exchange for the supplied nitrogen the plant provides the microsymbiont with a variety of nutrients, including dicarboxylates (primarily malate) and amino acids (White et al., 2007). Analyses of symbiotic mutants in the model legumes *Lotus japonicus* and *Medicago truncatula* (Parniske, 2008; Venkateshwaran et al., 2013) identified a common genetic program underlying both RNS and AM. The existence of the shared symbiosis (SYM) genes indicated that AM genes were recruited during the evolution of RNS (Kistner and Parniske, 2002; Markmann and Parniske, 2009).

AM and RNS share noteworthy similarities in the mechanisms leading to symbiotic establishment. A mutual exchange of signal molecules between plant and symbiotic partner is followed by activation of the plant's symbiotic signaling pathway, calcium spiking and expression of symbiosis associated genes. Ultimately, the microbes gain entry to the host and symbiotic organs are formed.

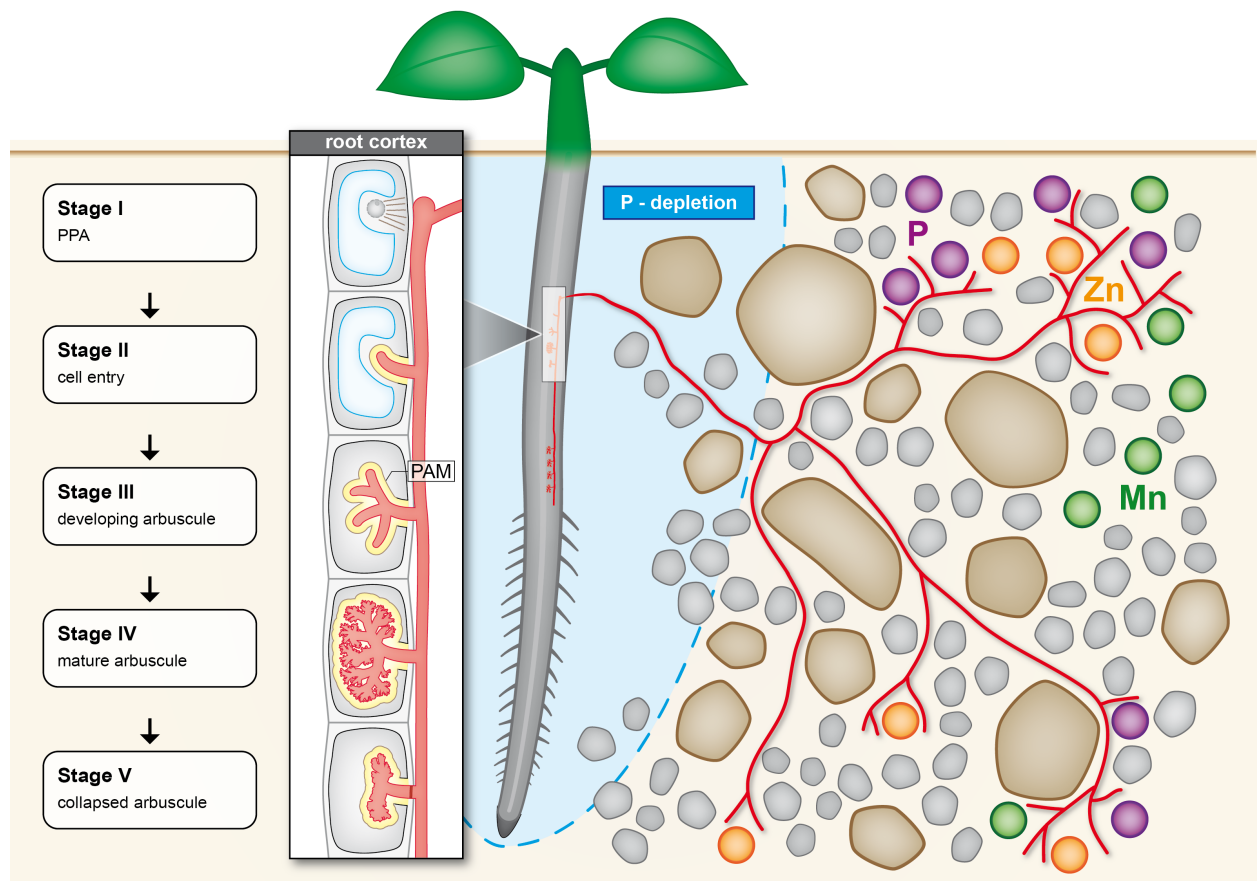


Figure 1: Arbuscule development and nutrient provision. During establishment of AM, fungal hyphae penetrate the root and enter the cortex, where they spread along the apoplastic space. Arbuscule development takes place in cortical cells. First PPA-like structures are formed upon hyphal contact, then hyphae enter the cell and generate finely branched arbuscules, which are separated by a periarbuscular membrane (PAM) from the plant cell's cytosol. Dying arbuscules are separated from the hyphae by septa. An extended hyphal network in the surrounding soil provides the plant with water and nutrients, primarily phosphorous (P). Nutrient exchange is assumed to take place inside of arbusculated cells. Figure was inspired by Arthur Schüßler. Arbuscule development stages are based on Gutjahr and Parniske (2013).

5.2. Symbiotic crosstalk and establishment of root endosymbioses

AM fungi exist in the soil as spores. In the presymbiotic AM stage the plant exudes carotenoid-derived phytohormones, the strigolactones (SL; Ruyter-Spira et al., 2013), into the vicinity of the root. SLs act as “branching factors”, inducing AM fungal spore germination, cell proliferation and hyphal branching (Akiyama et al., 2005; Besserer et al., 2006). Phosphate-limiting conditions promote the biosynthesis and exudation of SLs and lead to increased AM colonization (Yoneyama et al., 2012), whereas high phosphate levels negatively regulate AM development (Menge et al., 1978; Balzergue et al., 2010; Breuillin et al., 2010). Following germination, AM fungi release diffusible signals, which trigger various plant responses, including induction of a set of plant genes (Kosuta et al., 2003; Kuhn et al., 2010; Ortu et al., 2012), nuclear calcium spiking (Kosuta et al., 2008; Chabaud et al., 2011; Sieberer et al., 2012), formation of lateral roots (Oláh et al., 2005) and starch accumulation (Gutjahr et al., 2009). Different chitooligosaccharides (N-acetylglucosamine oligosaccharides), which are present in AM fungal exudates, were identified as active signaling molecules (myc factors, MF). Sulphated and non-sulphated

lipochitooligosaccharides (LCOs), structurally very similar to rhizobial nodulation factors, were shown to trigger root hair branching and induction of the symbiotic *ENOD11* promoter (Maillet et al., 2011). Additionally, short-chain chitin oligomers (tetramers and pentamers) were able to induce calcium spiking in both legumes and non-legumes (Genre et al., 2013).

Upon contact with a compatible plant, AM fungal hyphae differentiate into a hyphopodium at the root surface and penetrate the rhizodermis (Gutjahr and Parniske, 2013). Fungal penetration and progression through the root is actively controlled by the host. A plant derived accommodation structure comprised of microtubules, microfilaments and ER, the so-called prepenetration apparatus (PPA; Genre et al., 2005) determines the fungal path through rhizodermal and cortical cells (Genre et al., 2005; Genre et al., 2008). Structurally, the PPA resembles the preinfection threads formed during establishment of RNS (Genre et al., 2005; Fournier et al., 2008). In the inner cortex, fungal hyphae grow longitudinally in the apoplast (Figure 1), then branch out to form arbuscules in cortical cells (Demchenko et al., 2004; Harrison, 2012). Mature arbuscules are highly branched structures, separated from the cytosol of the plant by a periarbuscular membrane (PAM). Albeit continuous with the plant plasma membrane, the PAM harbors distinct protein compositions. Based on the local enrichment of proteins, at least two different PAM domains can be distinguished: the phosphate transporter 4 (PT4) localizes specifically to the arbuscule branches, while the blue copper-binding protein 1 (BCP1) is found in arbuscule trunks as well as the peripheral plasma membrane (Pumplin and Harrison, 2009).

In RNS, the symbiotic signal exchange between plant and bacterial partner is initiated under nitrogen limiting conditions by exudation of flavonoid and isoflavonoid compounds produced via the phenylpropanoid pathway of the plant (Weston and Mathesius, 2013). Compatible rhizobia recognize particular flavonoids, which leads to the activation of bacterial nodulation (*nod*) genes and the production of nodulation factors (NFs; Subramanian et al., 2007). Chemically NFs are N-acetylglucosamine (GlcNAc) based lipochito-oligosaccharides that can be decorated with different substituents, such as methyl, acetyl, fucosyl or sulphate groups (Dénarié et al., 1996; Miller and Oldroyd, 2012). NFs are critical for the association between rhizobia and their host plants and the types of NF produced determines the specificity of the interaction (Roche et al., 1991; Downie and Walker, 1999). Plant root hairs exhibit deformation upon NF perception and undergo polar growth directed towards the NF signal, which ultimately causes an entrapment of the rhizobia in the curled root hair (Esseling et al., 2003).

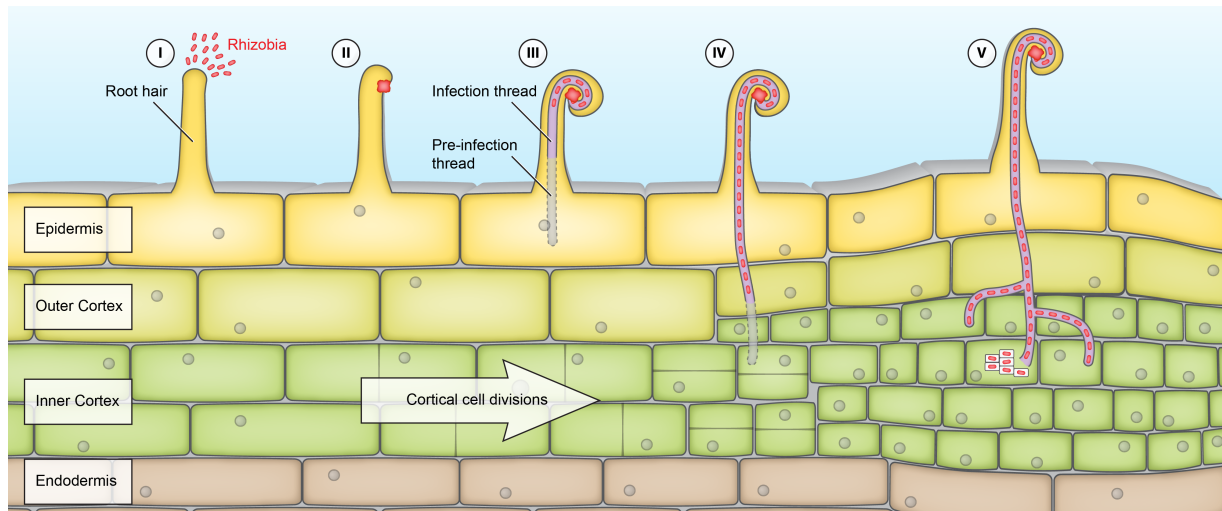


Figure 2: Establishment of root nodule endosymbiosis. I) Signal exchange between rhizobial soil bacteria and plants at root hairs initiates root colonization and nodule formation. II) Bacteria are entrapped by a curling root hair, forming a microcolony of dividing rhizobia. III-IV) From this site bacteria enter the root via infection threads (ITs), which grow through the root hair towards the cortex. IT growth is preceded by a pre-infection thread, consisting of dense cytoplasmic subdomains. Cortical cell divisions accompany IT progression, leading to the formation of the nodule primordium. V) Rhizobia are released into the cells of the nodule primordium, which later develops into the mature nodule. The bacteria are enclosed in vacuole-like symbiosomes inside the cells, where they differentiate into nitrogen fixing bacteroids. Illustration is loosely based on Oldroyd et al. (2011).

Other responses that are induced by application of NF include calcium influx into the root hair cytoplasm, membrane depolarization and intra- and extracellular alkalization (Ehrhardt et al., 1992; Felle et al., 1995; Felle et al., 1996; Felle et al., 1998), as well as calcium oscillations in and around the root hair nucleus (Ehrhardt et al., 1996; Sieberer et al., 2009). The enclosed bacteria continue to divide, thereby creating an infection focus. At this site, plant cell wall hydrolysis and invagination of the plasma membrane result in the formation of tubular infection threads (ITs), which allow entry of the rhizobia into the root (Figure 2). ITs progress from the rhizodermis through the outer root cortex into the inner cortex (Oldroyd et al., 2011). Their growth is preceded by pre-infection threads, which consist of ER rich cytoplasmic bridges aligned with cytoskeleton (structurally similar to the PPA in AM) (van Brussel et al., 1992; Yokota et al., 2009). In parallel to the progression of intracellular infection, cells of the inner cortex divide and redifferentiate, thereby forming a nodule primordium. Rhizobia inside ITs continue to divide until they reach the primordial cells, where they are released into the cytoplasm (Oldroyd et al., 2011). The bacteria are then enclosed in organelle-like symbiosomes and differentiate into symbiotically active nitrogen fixing bacteroids (Kereszt et al., 2011). Root hair infection via ITs is the most common mode of root colonization by rhizobia (Oldroyd et al., 2011). Other less effective infection pathways, such as NF independent single cell infection and NF dependent crack entry, are not as well characterized and assumed to represent more basal evolutionary stages (Sprent, 2007; Sprent and James, 2007; Madsen et al., 2010). In crack entry, rhizobia can enter cortical cells through epidermal breaches, thus circumventing the epidermal stages of root hair invasion, however, transcellular ITs in the

cortex are still formed (Held et al., 2010). While certain legume clades are restricted to these simpler infection modes, the pathways are very likely also retained in species that normally form root hair ITs. Certain tropical legumes, such as *Sesbania rostrata*, can switch from intracellular IT infection mode to intercellular crack entry under flooded conditions (Goormachtig et al., 2004). Moreover, residual nodulation due to alternative infection modes can be observed in certain *Lotus* mutants, in which normal IT based colonization is abolished (James and Sprent, 1999; Karas et al., 2005; Groth et al., 2010; Madsen et al., 2010).

5.3. Signal transduction in root endosymbiosis

5.3.1. Signal perception at the plant plasma membrane

The plant symbiotic programs leading to nodule organogenesis and intracellular infection as well as arbuscule formation are initiated by the perception of the symbiotic signals at the plasma membrane. In *L. japonicus* recognition of rhizobial NF and early symbiotic responses are dependent on the lysin motif (LysM) domain receptors NFR1 and NFR5 (Madsen et al., 2003; Radutoiu et al., 2003). Both proteins directly bind NF with high affinity (Broghammer et al., 2012), most likely via their three extracellular LysM domains. The Lys motif is known to be involved in binding of N-acetylglucosamine containing ligands such as NFs (Gust et al., 2012) and domain swap experiments demonstrated that the LysM domains of NFR1 and NFR5 mediate host specificity depended on different NF decorations (Radutoiu et al., 2007). NFR1 and NFR5 localize to the plasma membrane and form a heterocomplex, which is assumed to initiate signal transduction upon NF binding (Madsen et al., 2011). NFR1 contains an active intracellular kinase domain, which performs both autophosphorylation and transphosphorylation of NFR5 (Madsen et al., 2011). NFR5 on the other hand lacks certain kinase subdomains and does not show *in vitro* kinase activity, which suggests that it is likely a pseudokinase. The cytosolic domain of NFR5 is nevertheless important for RNS, since a deletion of nine amino acids abolishes symbiotic signaling (Madsen et al., 2011). The receptors mediating perception of chitin-derived MF signals (chitin oligomers and lipochitooligomers) have not been identified in legumes, however, they are probably related to the NFRs (Antolín-Llovera et al., 2012). The tropical tree genus *Parasponia* evolved RNS with rhizobia independently from legumes (Trinick, 1973; Op den Camp et al., 2012). In *Parasponia andersonii* a single NFR5-like receptor was shown to be required for both AM and RNS, suggesting that a mycorrhizal LysM-type receptor was recruited for RNS. In legumes a duplication of the original receptor gene might have driven a functional diversification to produce NF and MF specific receptors. Multiple loci encoding LysM proteins with a typical receptor kinase structure were identified in *L. japonicus* (Lohmann et al., 2010). Among these *Lys* genes are potential candidates for AM signal receptors as well as additional cortical NF receptors (Madsen et al., 2010).

A plasma membrane associated remorin, SYMREM1, which is involved in nodulation and infection, interacts with NFR1 and NFR5 in *L. japonicus* and with the orthologous

receptors LYK3 and NFP in *M. truncatula* (Lefebvre et al., 2010; Tóth et al., 2012). Remorins are a plant specific gene family assumed to act as scaffold proteins in the organization of membrane microdomains, SYMREM1 might therefore be required in the recruitment of a symbiotic receptor platform (Jarsch and Ott, 2011). The rho-like small GTPase ROP6 was identified as another interactor of NFR5 and silencing of the gene resulted in disturbed infection thread development and reduced nodulation (Ke et al., 2012). Additionally *M. truncatula* LYK3 phosphorylates and interacts with the E3 ubiquitin ligase PUB1 (Mbengue et al., 2010), a negative regulator in symbiotic signaling. Biochemical approaches previously identified a lectine nucleotide phosphohydrolase (LNP) as a NF binding protein (Quinn and Etzler, 1987). LNP is a peripheral membrane protein, localized at the surface of root hairs and treatment of roots with LNP antiserum impaired root hair deformation and nodulation (Etzler et al., 1999; Day et al., 2000; Kalsi and Etzler, 2000). More recent studies in *L. japonicus* demonstrated that an antisense line lacking LNP was deficient both in nodulation and in AM colonization (Roberts et al., 2013). Several hypothesis for the function of LNP in symbiotic signaling have been proposed: 1) It could be part of a signaling complex together with the NF and MF receptors; 2) function in parallel to the LysM receptor kinase pathway potentially utilizing its apyrase activity to hydrolyze extracellular ATP and/or ADP or 3) act downstream of the initial signal perception as a very early component of the common sym pathway (Roberts et al., 2013).

Besides *LNP*, at least eight other genes have been identified with a function in both early RNS and AM signaling in *L. japonicus*: *SYMRK*, *NUP85*, *NUP133*, *NENA*, *CASTOR*, *POLLUX*, *CCaMK* and *CYCLOPS* (Stracke et al., 2002; Mitra et al., 2004; Imaizumi-Anraku et al., 2005; Kistner et al., 2005; Kanamori et al., 2006; Saito et al., 2007; Groth et al., 2010). *LNP*, *SYMRK*, *NUP85*, *NUP133*, *NENA*, *CASTOR* and *POLLUX* are required for nuclear calcium spiking, whereas *CCaMK* and *CYCLOPS* act downstream of the calcium response (Figure 3). How this shared symbiotic pathway can integrate rhizobial and AM stimuli to activate specific downstream signaling events leading to nodulation and arbuscule formation still remains poorly understood. It is likely that parallel pathways exist in order to differentiate between the symbiotic programs.

5.3.2. Signaling from plasma membrane to nucleus

The receptor-like kinase (RLK) SYMRK (NORK/DMI2) mediates symbiotic signal transduction following Nod-factor perception and *symrk* mutants are deficient in both RNS and AM (Endre et al., 2002; Stracke et al., 2002). SYMRK is composed of an intracellular kinase, a transmembrane domain, and an extracytoplasmic region consisting of leucine-rich repeats (LRRs) and a malectin-like domain (MLD) (Antolín-Llovera et al., 2014). At least three distinct SYMRK variants with different sizes of the extracellular region exist in angiosperms. The longest version containing three LRRs is needed for RNS, while shorter versions are sufficient for AM (Markmann et al., 2008). SYMRK interacts with both SYMREM1 and NFR5, potentially acting as a coreceptor of NFR5 in symbiotic signaling (Tóth et al., 2012; Antolín-Llovera et al., 2014). The alteration of a conserved

extracellular “GDPC” sequence in the *symrk-14* mutant, affects symbiotic development in the epidermis, but not in the cortex (Kosuta et al., 2011). Depending on the “GDPC” sequence, full length SYMRK is cleaved *in planta*, resulting in the release of the extracellular MLD. The cleavage product lacking the MLD (SYMRK- Δ MLD) outcompetes full length SYMRK for NFR5 interaction, suggesting that the MLD interferes with NFR5 binding (Antolín-Llovera et al., 2014). Moreover, SYMRK- Δ MLD is rapidly degraded if the LRR region is present. Removal of the LRRs stabilizes the truncated SYMRK and results in an increased formation of infection threads (Antolín-Llovera et al., 2014). The degradation of SYMRK- Δ MLD is potentially mediated by the E3 ligase SINA, an interactor of SYMRK, whose ectopic expression was correlated with reduced SYMRK protein levels and impaired infection thread development (Den Herder et al., 2012).

The components involved in signal transduction from the PM receptors to the nuclear calcium spiking machinery have not been determined; however, screens for interaction partners of known signaling components identified candidates for missing pieces. Among the interactors of SYMRK, a 3-Hydroxy-3-Methylglutaryl Coenzyme A Reductase1 (HMGR1) coenzyme (Kevei et al., 2007) as well as the MAP Kinase Kinase (MAPKK) SIP2 (Chen et al., 2012) have been identified and silencing of either of the genes causes nodulation defects. MAP kinase or HMGR signaling might be involved in downstream signal transduction. HMGRs are the rate controlling enzymes of the mevalonate pathway that produces sterols, isoprenoids and in particular cytokinins, which are necessary for the induction of nodule morphogenesis (Oldroyd et al., 2011). Metabolites of the HMGR pathway could act as symbiotic secondary messengers (Kevei et al., 2007). Although HMGR1 is upregulated during initial stages of mycorrhizal symbiosis (Liu et al., 2003), neither HMGR1 nor SIP2 were implicated with a function in mycorrhiza colonization, indicating that additional pathways downstream of SYMRK might be involved in AM signal transduction.

5.3.3. Generation of nuclear calcium spiking

Nuclear and perinuclear calcium oscillations are initiated after contact with both rhizobia and AM fungi (Kosuta et al., 2008; Chabaud et al., 2011; Sieberer et al., 2012) and can be triggered directly by addition of rhizobial NFs (Ehrhardt et al., 1996; Miwa et al., 2006a; Sieberer et al., 2009) and short-chain chitoooligomers, which are present in AM fungal exudates (Genre et al., 2013). Forward and reverse genetic screens in legumes have identified proteins involved in the generation of the calcium response. The closely related ion channels CASTOR and POLLUX (*M. truncatula* DMI1) are required for calcium spiking and mutant alleles are deficient for RNS and AM colonization (Ané et al., 2004; Imaizumi-Anraku et al., 2005; Charpentier et al., 2008). The channels are located in the nuclear envelope (Riely et al., 2007; Charpentier et al., 2008), in case of DMI1 preferentially targeted to the inner side of the nuclear membrane (Capoen et al., 2011). Electrophysiological and functional analysis revealed that the proteins are cation channels. CASTOR showed a preference for K⁺ and POLLUX could complement a yeast K⁺ import and export mutant (Charpentier et al., 2008). Symbiotic signaling in *L. japonicus*

requires both CASTOR and POLLUX. In *M. truncatula* the POLLUX homologue DMI1 alone is sufficient and expression of DMI1 in *L. japonicus* was able to complement a *castor/pollux* double mutant (Venkateshwaran et al., 2012). This functional difference between POLLUX and DMI1 was pinpointed to a single amino acid exchange in the putative selectivity filter region of the channels (alanine in POLLUX, serine in DMI1), which resulted in an increased mean channel opening time of DMI1 compared to CASTOR. Exchanging the filter region of POLLUX to that of DMI1 allowed for the complementation of *dmi1* and *castor/pollux* double mutants, however the same was not true when the change was introduced into CASTOR, which failed to rescue either *dmi1* or *castor/pollux*, but was still able to rescue a *castor* single mutant (Venkateshwaran et al., 2012). This finding indicates a functional or regulatory difference between CASTOR and POLLUX/DMI1 that goes beyond their K⁺ conductivity. A mathematical model predicted that calcium dependent activation of DMI1 and voltage dependent opening of calcium channels in addition to the presence of a calcium pump are sufficient for sustained calcium oscillations (Granqvist et al., 2012). A sarco/endoplasmic reticulum type calcium pump (SERCA), *M. truncatula* Calcium ATPase8 (MCA8), was localized to both the inner and the outer nuclear membrane. Silencing of *MCA8* perturbed spiking and resulted in reduced mycorrhization (Capoen et al., 2011). The actual calcium channels that generate the calcium response have so far not been identified. Nuclear calcium release in animals is primarily linked to the activation of Inositol (1,4,5)triphosphate receptors (InsP₃Rs; Bootman et al., 2009), however in higher plants no sequences coding for InsP₃Rs homologous channels could be identified (Kudla et al., 2010).

Several hypotheses regarding the function of CASTOR and POLLUX/DMI1 in the calcium spiking machinery have been put forward. One model assumes that CASTOR and POLLUX/DMI1 are activated by secondary messengers, causing K⁺ to flow into the perinuclear space. This would cause hyperpolarization of the nuclear membranes and in turn could lead to the opening of voltage gated calcium channels (Venkateshwaran et al., 2012). In a slightly different model it was suggested that for continued calcium spiking both DMI1 and calcium channels would need to be simultaneously activated by binding of second messenger molecules. In this case DMI1 (as well as CASTOR and POLLUX) would predominantly act as a counter ion channel, but also initially contribute to the activation of the calcium channels by hyperpolarization of the nuclear membrane (Charpentier et al., 2013). Mutations in three nucleoporins genes, *NUP85*, *NUP133* and *NENA* (*SEH1*), also abolish calcium spiking and cause defects in both RNS and AM symbiosis, similar to the phenotypes observed in *castor* and *pollux* mutants (Kistner et al., 2005; Kanamori et al., 2006; Saito et al., 2007; Groth et al., 2010). More information about the NPC in symbiotic signaling is presented in the last chapter of the introduction.

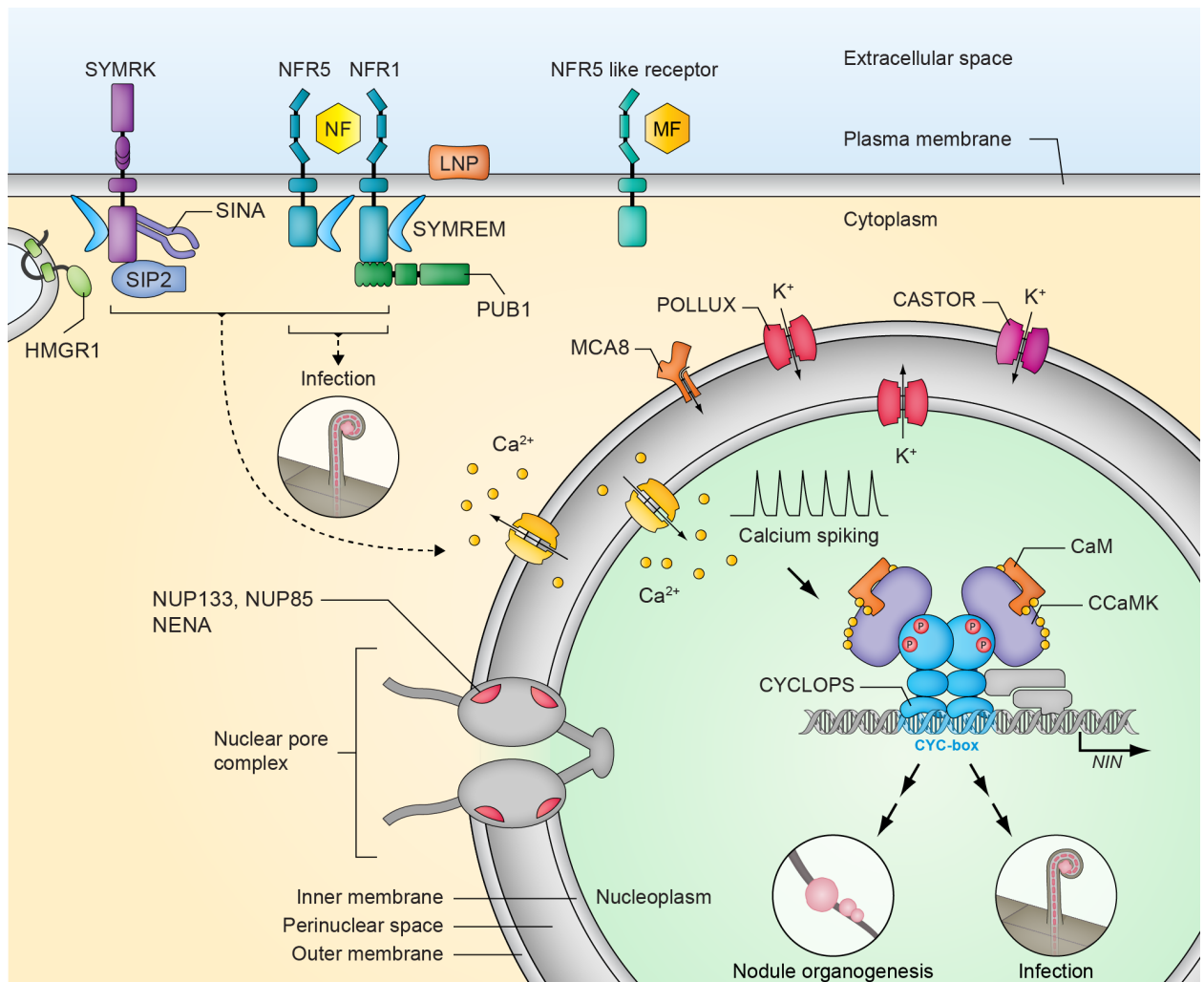


Figure 3: Symbiotic signal transduction. Signaling molecules are detected by plasma membrane bound receptors, initiating a signaling cascade to the nucleus. As a result, nuclear calcium spiking is activated, which is decoded by a complex involving CCaMK and CYCLOPS. Ultimately, symbiosis associated genes are induced leading to intracellular infection and nodule organogenesis or arbuscule development. For details on the individual signaling components see main text. Figure is based on Singh and Parniske (2012).

5.3.4. Decoding the calcium signal

As the likely primary decoder of symbiotic calcium signatures, a nuclear calcium- and calmodulin-dependent kinase (CCaMK) plays a central role in symbiotic signal transduction (Singh and Parniske, 2012). *ccamk* mutants do not form infection threads, nodules and arbuscules when inoculated with rhizobia or AM fungi (Levy et al., 2004; Mitra et al., 2004). A calmodulin (CaM) binding domain and three calcium binding EF-hands mediate CCaMKs regulation during calcium spiking (Swainsbury et al., 2012). Calcium binding induces a conformational change in the protein (Swainsbury et al., 2012) and promotes its autophosphorylation (Takezawa et al., 1996; Sathyanarayanan et al., 2000). Constitutive activation of CCaMK, caused by mutations in an autophosphorylation site (T265D, T265I), leads to spontaneous nodule development in the absence of rhizobia (Gleason et al., 2006; Tirichine et al., 2006). Negative regulation of CCaMK as a result of autophosphorylation within the calcium/CaM binding domain (Liao et al., 2012; Routray et al., 2013) is also required for normal cortical infection and AM development (Liao et al.,

2012), demonstrating an intricate modulation of CCaMK activity during symbiotic signaling. Autoactive CCaMK mutants are able to restore nodulation and AM symbiosis in the mutants *symrk*, *castor*, *pollux*, *nup85* and *nup133* (Hayashi et al., 2010; Madsen et al., 2010). This indicates that the primary function of these genes is the activation of calcium spiking and highlights the importance of calcium signaling in symbiotic signal transduction. It emerges that the calcium oscillations themselves may carry cell type and stage specific information. Live cell imaging demonstrated a transition from low to high frequency spiking during apoplastic cell entry that was very similar for both mycorrhizal and rhizobial symbionts (Sieberer et al., 2012). Previously calcium oscillations induced by AM fungal hyphae were described to be less regular than NF induced spiking (Kosuta et al., 2008; Chabaud et al., 2011), however, so far there has been no proof of differential decoding of AM and NF induced calcium signals by CCaMK.

5.3.5. Transcription factors in symbiotic signaling

Downstream of signal perception and calcium spiking, symbiotic signaling is coordinated and integrated at the level of transcriptional regulation. The activation of CCaMK appears to be the central regulatory mechanism, which initiates downstream activation of transcriptional networks both in RNS and mycorrhiza establishment (Hayashi et al., 2010; Madsen et al., 2010). So far, a set of transcription factors, including GRAS domain, ethylene response factor (ERF) and CAAT-box family members (Kaló et al., 2005; Smit et al., 2005; Combier et al., 2006; Andriankaja et al., 2007; Middleton et al., 2007; Vernié et al., 2008; Gobbato et al., 2012; Schaarschmidt et al., 2013; Soyano et al., 2013; Yu et al., 2014) as well as the transcription factor NIN (Schäuser et al., 1999; Marsh et al., 2007) and the DNA binding protein CYCLOPS (Singh et al., 2014) have been identified with symbiosis related functions.

CCaMK forms a complex with the nuclear CYCLOPS protein (*M. truncatula* IPD3) (Singh et al., 2014), which is essential for RNS and AM infection (Messinese et al., 2007; Yano et al., 2008). CYCLOPS was revealed to be a novel type of transcriptional activator, which upon phosphorylation by CCaMK binds to a CYCLOPS responsive *cis* element in the *NIN* promoter and activates *NIN* gene expression (Singh et al., 2014). Phosphorylation of CYCLOPS S50 and S154 is critical for promoter binding and symbiotic development. An autoactive phosphomimetic mutant version of CYCLOPS (S50D/S154D) triggers spontaneous nodule formation independent of CCaMK, indicating that CYCLOPS acts as a master regulator of root nodule organogenesis (Singh et al., 2014). As *cyclops* and *ipd3* mutants are able to form nodules in an autoactive CCaMK background (Yano et al., 2008; Horváth et al., 2011; Ovchinnikova et al., 2011), it is possible that other CCaMK targets are able to partially substitute for the function of CYCLOPS in organogenesis.

NIN is a RWP-RK domain-containing transcription factor essential for nodulation and infection during RNS, but not required in AM development (Schäuser et al., 1999; Marsh et al., 2007). Upon NF addition *NIN* is quickly upregulated, whereas its expression is severely reduced in the *cyclops/ipd3* mutant (Yano et al., 2008; Horváth et al., 2011). *NIN* expression is also activated in response to the photohormone cytokinin dependent on the

cytokinin receptor LHK1 and a gain of function version of LHK1 is able to spontaneously induce nodule formation without rhizobial infection (Tirichine et al., 2007). Induction of NIN depends on cytokinin only in the cortex, but not in the epidermis (Heckmann et al., 2011; Plet et al., 2011). NIN induces gene expression of *NF-YA1* and *NF-YB1* by direct binding to the genes promoters (Soyano et al., 2013). *NF-YA1* and *NF-YB1* are two subunits of the heteromeric CAAT-box binding protein complex Nuclear Factor Y (NF-Y; Mantovani, 1999). Knockdown of *NF-YA1* inhibits root nodule organogenesis, whereas ectopic overexpression of either *NIN* or *NF-YA1* and *NF-YB1* leads to increased cortical cell divisions and in case of *NIN* overexpression to formation of nodule primordium-like structures (Soyano et al., 2013). *NF-YA1* is orthologous to *M. truncatula* HAP2-1, which was previously shown to be involved in meristem persistence in root nodules (Combier et al., 2006). Besides their function in RNS, the NF-Ys also act as positive regulators in mycorrhization and their expression is downregulated during autoregulation of mycorrhization (AOM; Schaarschmidt et al., 2013). AOM serves to limit the number of infection events during mycorrhization via shoot-derived inhibitors, similar to autoregulation in nodulation (Staehelin et al., 2011). In addition to the NF-Ys, *NIN* was shown to target the promoter of a *L. japonicus* pectate lyase gene (*NPL*), which is induced in roots and root hairs during RNS (Xie et al., 2012). The pectate lyase activity of *NPL* is required for initiation of infection threads and penetration of the rhizobia into the root hair (Xie et al., 2012). *NSP1* and *NSP2* are GRAS type transcription factors that were originally identified with a specific role in RNS (Catoira et al., 2000; Oldroyd and Long, 2003; Kaló et al., 2005; Smit et al., 2005; Heckmann et al., 2006; Murakami et al., 2007), however more recent analyses also indicate a function of the NSPs in mycorrhiza signaling (Maillet et al., 2011; Delaux et al., 2013 Laressergues et al., 2012) and in the SL biosynthesis pathway (Liu et al., 2011). Since *NSP1* and *NSP2* are not required for *NIN* transactivation by *CYCLOPS* and neither autoactive *CYCLOPS* (*S50D/S154D*) nor autoactive *CCaMK* lead to the formation of spontaneous nodules in *nsp1* and *nsp2* mutants (Madsen et al., 2010; Singh et al., 2014), it is likely that the NSPs act downstream or in parallel pathways to the early induction of *NIN* by *CYCLOPS*. *NSP1* and *NSP2* form a heteromeric complex, which binds via *NSP1* to the promoters of *ERN1*, *NIN* and the early nodulin gene *ENOD11* (Hirsch et al., 2009). The *NSP1-NSP2* complex regulates the expression of *ENOD11* in concert with *ERN1*. Whereas *ERN1* is required for NF induced *ENOD11* expression during infection initiation, *NSP1-NSP2* regulate *ENOD11* expression during later stages of rhizobial infection by binding to a different promoter region than *ERN1* (Cerri et al., 2012). A closely related transcription factor, *ERN2* is only required during certain RNS infection stages, however, when expressed under the control of the *ERN1* promoter, it is able to complement NF induced *ENOD11* expression as well as nodule formation in an *ern1* mutant background (Cerri et al., 2012). *ERN* TFs are potentially also important in AM symbiosis, as *ERN2* is highly expressed during mycorrhiza colonization, particularly in cells harboring arbuscules and colonizing hyphae (Hogekamp et al., 2011; Young et al., 2011). *NSP2* also interacts with the AM specific

GRAS transcription factor RAM1, which regulates the expression of the *RAM2* gene by direct binding to its promoter (Gobbato et al., 2012). *RAM2* encodes a plant glycerol-3-phosphate acyl transferase (GPAT) that is involved in the production of cutin monomers and is required for hyphopodium and subsequent arbuscule formation (Wang et al., 2012). Besides the NSPs and RAM1, two additional GRAS type TFs, DELLA and DIP1 were recently identified with a function in AM (Floss et al., 2013; Yu et al., 2014). DELLA proteins act as repressors of gibberellic acid (GA) signaling and are degraded in response to GA treatment, which also inhibits mycorrhizal colonization (Harberd et al., 2009; Floss et al., 2013; Foo et al., 2013). DIP1 interacts with both DELLA and RAM1 and mutations in either of the genes inhibit arbuscule formation, suggesting that the TFs are part of a GRAS protein complex, which is involved in the regulation of mycorrhiza associated gene expression and colonization (Gobbato et al., 2012; Floss et al., 2013; Yu et al., 2014).

5.3.6. Common symbiosis genes involved in microbial accommodation

Several AM genes with putative functions in membrane trafficking are also involved in RNS. *M. truncatula VAPYRIN* (*Petunia PAM1*) is required for arbuscule formation and efficient fungal entry of the root (Reddy D. M. R. et al., 2007; Feddermann et al., 2010; Pumplin et al., 2010; Murray et al., 2011) and deletion of the gene prevents rhizobial infection threads from reaching the cortical cell layer, resulting in an increased number of uninfected nodule primordia (Murray et al., 2011). *VAPYRIN* encodes a protein with an N-terminal VAMP-associated protein (VAP)/major sperm protein (MSP) domain and a C-terminal ankyrin-repeat domain. Based on the domain structure and observed localization in the nucleus, cytosol and in distinct puncta in colonized cells, *VAPYRIN* was proposed to be involved in membrane trafficking and cellular rearrangement during symbiotic accommodation, however, this has not been experimentally verified (Pumplin et al., 2010; Murray et al., 2011). Two closely related *M. truncatula* vesicle associated membrane proteins (*VAMP*) are also implicated in rhizobium-legume symbiosis and AM (Ivanov et al., 2012). Silencing of both *VAMP721d* and *VAMP721e* inhibits arbuscule and symbiosome formation and blocks bacterial release from the infection thread. Both gene products localize to small vesicles, which accumulate at bacterial release sites near symbiosome membranes and *VAMP721e* also accumulates at the tips of arbuscule branches, potentially at the periarbuscular membrane (Ivanov et al., 2012). While other *VAMP72* proteins in *A. thaliana* are recruited during the interaction with biotrophic fungi (Kwon et al., 2008), *VAMP721d/e* are not present in the *Arabidopsis* genome. Considering that *Arabidopsis* has lost several symbiosis genes (Zhu et al., 2006), it is possible that the exocytotic pathway involving *VAMP721d/e* is specific to perimicrobial membrane synthesis.

5.4. The plant nuclear pore complex in symbiotic signaling and plant defense

Nuclear pore complexes (NPCs) are large macromolecular assemblies composed of multiple copies of about 30 distinct nucleoporins (NUPs) (Hoelz et al., 2011; Grossman et al., 2012). They are embedded into the nuclear envelope and mediate bidirectional transport of macromolecules, including proteins and RNA, in and out of the nucleus (Wente and Rout, 2010; Grünwald et al., 2011; Grünwald and Singer, 2012). Six distinct categories of NUPs can be classified, depending on their location in the NPC (Figure 4): 1) Integral membrane proteins that anchor the NPC to the nuclear envelope; 2) coat NUPs, which form the core NPC scaffold; 3) adaptor NUPs; 4) channel NUPs with unstructured phenylalanine-glycine (FG) repeat domains; 5) nuclear basket NUPs and 6) cytoplasmic filament NUPs (Hoelz et al., 2011). The last two both act as docking sites for transport factors. Besides their function in nucleocytoplasmic trafficking, NPCs and individual nucleoporins are also involved in a large number of cellular processes, including chromatin organization, cell cycle control, DNA repair and replication, kinetochore and spindle assembly, and regulation of gene expression (Capelson and Hetzer, 2009; Capelson et al., 2010; Strambio-De-Castillia et al., 2010; Wozniak et al., 2010; Van de Vosse et al., 2011; Van de Vosse et al., 2013; Bukata et al., 2013). NPCs are conserved across all eukaryotic lineages and can be traced back to the last eukaryotic common ancestor (Baptiste et al., 2005; Neumann et al., 2010).

Mutations in the *L. japonicus* nucleoporin genes *NUP85*, *NUP133* and *NENA* lead to temperature-dependent defects both in RNS and mycorrhiza symbiosis (Kistner et al., 2005; Kanamori et al., 2006; Saito et al., 2007; Groth et al., 2010). At non-permissive temperature (24°C or 26°C) the stronger mutant alleles form few or no nodules and AM infection and colonization are severely impaired, whereas at lower temperature (18°C) nodulation and AM phenotypes are less pronounced (Kanamori et al., 2006; Saito et al., 2007; Groth et al., 2010). Residual nodulation in the mutants is delayed in comparison to wild type plants and the majority of nodules remain uninfected by rhizobia. *nup* mutants fail to initiate NF elicited nuclear calcium spiking, however the earlier NF induced calcium influx into the cytosol at the root hair tip (Felle et al., 1998; Shaw and Long, 2003) is retained in *nup85* and *nup133* (Miwa et al., 2006a; *nena* was not tested). Cortical infection and development of mature nodules is not distinguishable in *nena* and wild type plants, suggesting that the nucleoporins are primarily required for rhizodermal root hair infection, but not in cortical nodule development (Groth et al., 2010). In *nena*, water-logging of the roots could significantly increase the number of infected nodules in an ethylene dependent manner, suggesting that a crack-entry infection mode (Sprent, 2007; Sprent and James, 2007; Madsen et al., 2010) is still active in the mutants (Groth et al., 2010).

Strikingly, the *nup* mutants only show mild phenotypes unrelated to symbiotic signaling, including defects in pollen tube growth and a reduction in seed yield, but no obvious additional growth or developmental defects (Kanamori et al., 2006; Saito et al., 2007;

Groth et al., 2010). The amino acid sequence identity between plant NUP133, NUP85 and SEH1/NENA compared to their receptive yeast and vertebrate homologs is fairly low, however, their predicted domain structures are conserved (Groth et al., 2010; Tamura et al., 2010). This is not unusual, as a high level of sequence divergence between homologous nucleoporins of different eukaryotic lineages in combination with the retention of an overall very similar structure is a typical feature of the NPC (Baptiste et al., 2005).

Yeast and vertebrate homologs of NUP85, NUP133 and NENA are part of the Y-shaped nuclear pore NUP107-160 (vertebrate) or NUP84 (yeast) subcomplex, which is the largest of the NPC subunits and present both on the cytosolic and nuclear side in a total of 16 copies per pore (Lutzmann et al., 2002; Alber et al., 2007). The complex is an essential NPC component involved in NPC assembly (Doucet et al., 2010) and its complete loss results in nuclei devoid of nuclear pores (Harel et al., 2003; Walther et al., 2003). Moreover, it is associated with a multitude of other functions, including mRNA export, gene activation, transcriptional elongation, kinetochore function, centrosome attachment, DNA repair, membrane stabilization, telomere anchoring and silencing (González-Aguilera and Askjaer, 2012). The subcomplex has not been fully characterized in plants, however, it is likely conserved, as homologs of all core NUP107-160 NUPs, namely NUP85, NUP96, NUP107, NUP133, NUP160, SEH1 and SEC13 (Belgareh et al., 2001; Lutzmann et al., 2002; Harel et al., 2003; Walther et al., 2003) are present in *Arabidopsis* (Wiermer et al., 2012). Moreover, yeast-two hybrid analysis confirmed an interaction of *L. japonicus* NENA (SEH1) and NUP85 (Groth et al., 2010), consistent with the arrangement of the nucleoporins in the yeast NUP84 subcomplex (Lutzmann et al., 2002). The role of the NPC in symbiotic signaling still remains enigmatic. The apparent lack of broad pleiotropic defects in the *nup* mutants suggests a rather specific function or target in symbiosis. Aberrations in structure or distribution of the NPCs might prevent on-going calcium oscillations by altering the electrophysiological properties of the nucleus. Alternatively, changes in the NPC scaffold could interfere with nucleo-cytoplasmic transport of symbiotic proteins or secondary messengers (reviewed in Binder and Parniske, 2013). CASTOR and POLLUX are probable candidates that could be affected in the *nup* mutants, given the similar mutant phenotypes, the relative position in the symbiotic signaling pathway and their subcellular localization in the nuclear envelope (Charpentier et al., 2008; Capoen et al., 2011). In *A. thaliana* mutations in genes coding for the nucleoporins NUP88 (MOS7), NUP96 (MOS3), NUP160 and to a lesser degree SEH1 cause defects in both basal and NBS-LRR (nucleotide-binding site-leucine-rich repeat) resistance (R) gene mediated defense (Zhang and Li, 2005; Cheng et al., 2009; Wiermer et al., 2012). Interestingly, NUP96, NUP160 and SEH1 are also putative members of the NUP107-160 subcomplex (Figure 4), suggesting a possible general function of the complex in plant-microbe signaling. In *nup88* there is strong circumstantial evidence that impaired nucleo-cytoplasmic transport is responsible for the observed defects in plant defense: *nup88/mos7* mutants exhibit an increase in nuclear export signal (NES) mediated nuclear export and a reduction in the nuclear accumulation of the NBS-LRR *snc1* (autoactive version of SNC1),

as well as a decrease in the nuclear levels of the defense regulators NPR1 and EDS1 (Cheng et al., 2009). Defense signaling appears to be susceptible to disturbances in nucleo-cytoplasmic transport in general, as mutations in an *Arabidopsis* importin α homolog (MOS6) also cause defects in plant innate immunity (Palma et al., 2005).

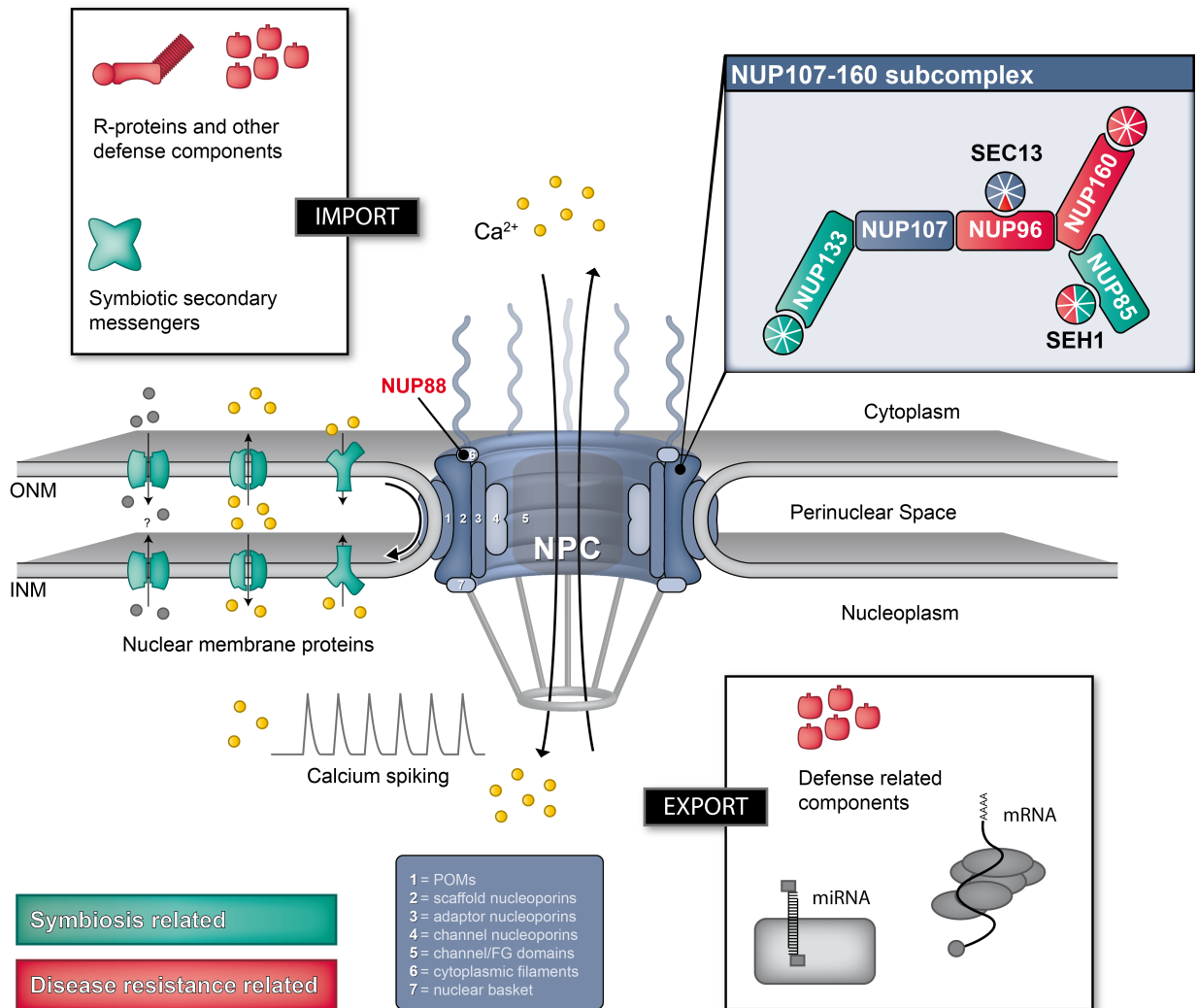


Figure 4: The nuclear pore complex in plant-microbe interactions. Components of the plant NUP107-160 subcomplex of the NPC are involved in plant-symbiosis in *L. japonicus* (NUP85, NUP133, SEH1/NENA) and plant defense signaling in *A. thaliana* (NUP96, NUP160, SEH1). Mutations in the nucleoporins could lead to disruptions in nucleo-cytoplasmic trafficking, thereby affecting components of symbiosis and plant immunity. Export and import of R proteins or other defense related proteins or RNAs could be disturbed, as demonstrated in the case of an *Arabidopsis nup88* mutant. Potential targets in symbiotic signaling include unidentified symbiotic secondary messengers or nuclear membrane proteins, such as the ion channels CASTOR and POLLUX (Charpentier et al., 2008), calcium channels or the calcium pump MCA8 (Capoen et al., 2011). Alternatively, symbiotic calcium spiking might be directly affected by structural changes in the *nup* mutants leading to altered electrophysiological properties of the NPC. The arrangement of the nucleoporins in the Y shaped NUP107-160 subcomplex is based on structural analysis of the yeast NUP84 complex (Kampmann and Blobel, 2009; Hoelz et al., 2011). POM = Pore membrane protein; FG domain = phenyl-alanine and glycine repeat domain; ONM = Outer nuclear membrane; INM = Inner nuclear membrane. Figure modified from Binder and Parniske (2013).

The defense phenotypes in *nup96*, *nup160* and *seh1* could therefore also be the result of disturbed nuclear import or export of defense regulators, R-proteins or defense related RNA transcripts, however, this has not been clearly demonstrated experimentally (Zhang and Li, 2005; Wiermer et al., 2012). Whereas the defense phenotype in *nup88/mos7* is very specific, mutations in *NUP96* and *NUP160* are associated with multiple pleiotropic impairments, including developmental defects, early flowering and nuclear mRNA accumulation (Zhang and Li, 2005; Wiermer et al., 2012). Moreover *NUP96* and *NUP160* are also involved in auxin signaling (Parry et al., 2006; Robles et al., 2012) and *NUP160* was implicated in the response of plants to cold stress (Dong et al., 2006).

6. Aim of the thesis

Nucleoporins (NUPs) have emerged with various functions in plant signaling processes. The majority of the characterized plant NUPs are part of the NUP107-160 subcomplex. Mutations in *L. japonicus* genes coding for NUP107-160 members *NUP85*, *NUP133* and *NENA* are deficient in RNS and AM symbiosis, but do not exhibit severe pleiotropic growth or developmental defects, despite the vital role of the NUP107-160 subcomplex in NPC biogenesis and stability.

The main goals of this thesis were to I) study the consequences of the *L. japonicus nup* mutations on the NUP107-160 complex and NPC in general and II) characterize possible targets or mechanisms which cause the observed symbiotic defects in the mutants. Prompted by the similar mutant phenotypes and nuclear membrane localization, the ion channels *CASTOR* and *POLLUX* were investigated as potential targets in symbiotic signaling. Polyclonal peptide antibodies against *CASTOR*, *POLLUX*, *NUP85* and *NUP133* were raised to study subcellular localization and protein expression in the native system. Additionally *LORE1* lines carrying insertions in genes encoding other proteins of the NUP107-160 subcomplex were analyzed to determine their symbiotic phenotypes. Calcium spiking analysis in the *nup* mutant background was performed to determine residual ability to generate nuclear calcium signals. To that end a toolset consisting of stable transgenic *L. japonicus* lines expressing targeted versions of yellowameleon calcium sensor was developed.

A requirement for the assembly of plasmids for expression of multiple genes prompted the assembly of a cloning toolkit based on the Golden Gate method. The system was intended for co-expression and subcellular localization analyses of *CASTOR* and *POLLUX* as well as for flexible and modular cloning in general.

7. Part I: Analysis of the *Lotus japonicus* nuclear pore NUP107-160 subcomplex reveals pronounced structural plasticity and functional redundancy

Published in:

Binder, A., and Parniske, M. (2014). Analysis of the *Lotus japonicus* nuclear pore NUP107-160 subcomplex reveals pronounced structural plasticity and functional redundancy. *Frontiers in Plant Science* 4.

doi: 10.3389/fpls.2013.00552

8. Part II: A modular plasmid assembly kit for multigene expression, gene silencing and silencing rescue in plants

Published in:

Binder, A., Lambert, J., Morbitzer, R., Popp, C., Ott, T., Lahaye, T., and Parniske, M. (2014). A modular plasmid assembly kit for multigene expression, gene silencing and silencing rescue in plants. *PLoS ONE* 9, e88218.

doi: 10.1371/journal.pone.0088218

9. Part III: Characterization of nucleoporin mutants in symbiotic signaling

9.1. Results

9.1.1. Measurement of nod factor induced calcium spiking in *Lotus japonicus* lines stably expressing localized yellow cameleons

Stable *L. japonicus* lines expressing targeted versions of yellow cameleon 3.6 (YC3.6) calcium sensors under the control of an optimized *Arabidopsis* *UBIQUITIN10* (*UBQ10*) promoter (Norris et al., 1993; Grefen et al., 2010) were generated by *A. tumefaciens* mediated transformation (Krebs et al., 2012), in order to study both nuclear and cytosolic calcium responses. One construct contained a nuclear localization signal (NLS-YC3.6), the other a nuclear export signal (NES-YC3.6). CLSM analysis of the respective lines revealed a clear nuclear localization of NLS-YC3.6 without cytosolic background signal (Figure 5A). The fluorescence was uniformly distributed within the nucleus, except for a slightly weaker signal in the nucleolus. For NES-YC3.6 transformed *L. japonicus* plants, fluorescence was exclusively observed in the cytoplasm (Figure 5B) and not in nuclei. Signal intensities were generally lower in plants transformed with the NES-YC3.6 construct compared to those transformed with NLS-YC3.6, except for root hair cells with a cytoplasmic accumulation in the tip region (Figure 5B). The localization of both cameleon constructs appeared to be ubiquitous throughout the plant and expression of the transgenes had no obvious effects on root hair or overall plant growth and morphology. Single cell measurements of calcium spiking were performed in *L. japonicus* using CLSM analysis. As the likely physiological targets of rhizobial NF perception (Oldroyd and Downie, 2008), the focus was put on growing root hair cells. Measurements were initiated 5 min prior to NF addition. After pipetting 10^{-8} M of aqueous NF solution directly onto the root, both nuclear (Figure 5A and C) and cytoplasmic spiking (Figure 5B and D) were observed in root hairs of NLS-YC3.6 and NES-YC3.6 expressing plants respectively. For the majority of root hair cells (>85%) calcium spiking continued for the duration of the 50-60 min measurement. In rare cases either no spiking could be detected (one in 20 cells) or spiking was arrested (two in 20 cells) after several min (Figure 5C). Measurements of random cells at later time points revealed that spiking continued several hours after NF addition. Previously NF induced calcium spiking was shown to be a cell-autonomous process (Ehrhardt et al., 1996; Sieberer et al., 2009), which was confirmed by the observation that adjacent root hair cell initialized calcium oscillations at different time points after NF addition and ongoing spiking was found to be independent and non-synchronous between the cells (Figure 5A and C). A typical biphasic asymmetric shape of symbiotic calcium spikes, as previously demonstrated in *M. truncatula* (Sieberer et al., 2009) and *L. japonicus* (Harris et al., 2003) was observed after NF treatment in NLS-YC3.6 transformed plants (Figure 5E). For cytoplasmic spiking in root hair cells this characteristic shape was less pronounced and instead showed a more symmetrical upward and downward slope (Figure 5E).

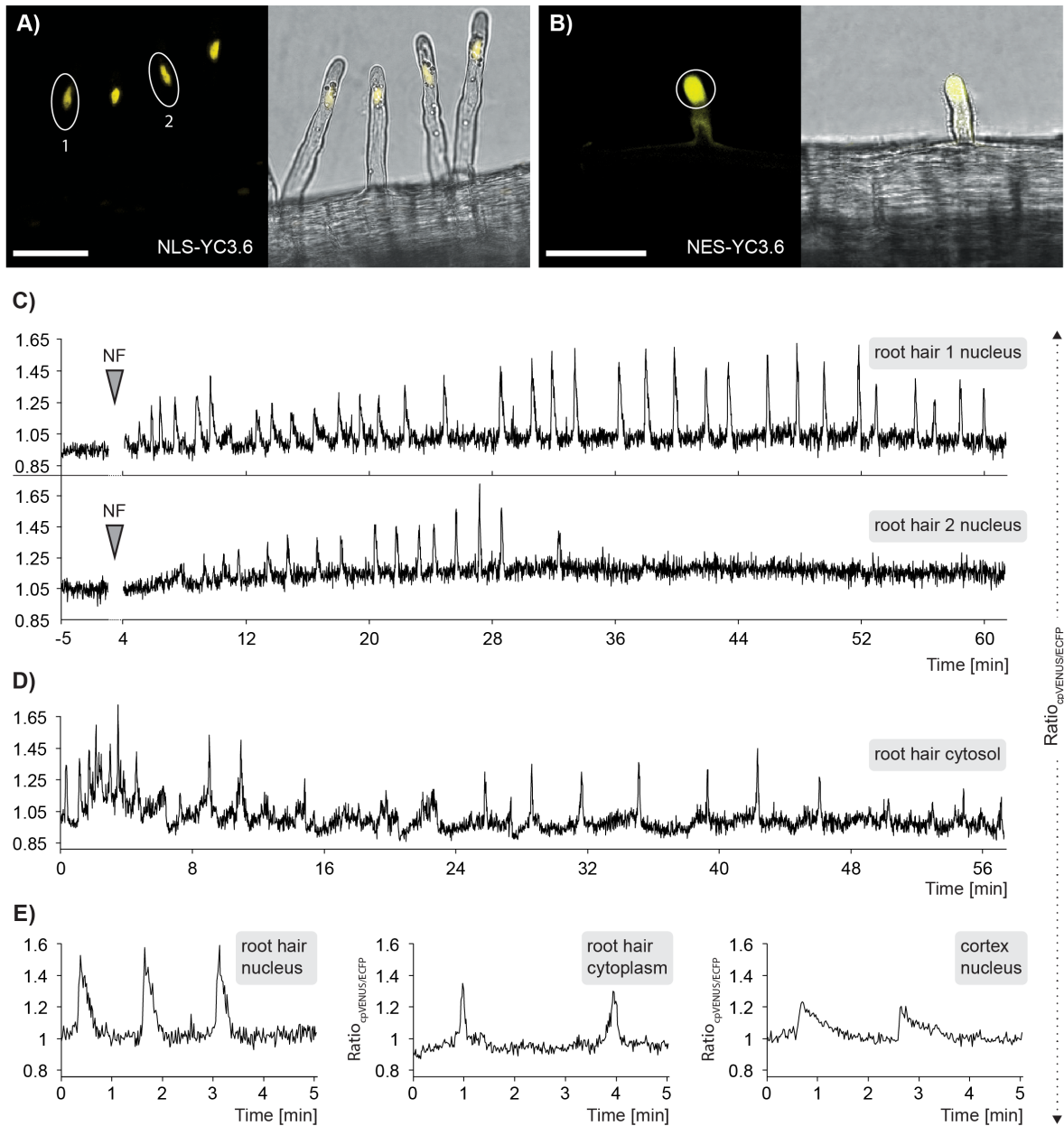


Figure 5: Nod factor induced calcium spiking in *L. japonicus*. Single cell calcium measurements were performed in *L. japonicus* roots stably expressing yellow cameleon 3.6 calcium reporters (YC3.6). cpVenus and merged cpVenus and bright field signals are shown for *L. japonicus* root hairs expressing (A) a YC3.6 construct with a nuclear localization signal (NLS-YC3.6) and (B) a YC3.6 reporter with a nuclear export signal (NES-YC3.6). Regions of interest for measurement of cpVenus and ECFP intensities are indicated by white circles. Nuclear calcium spiking could be detected in the NLS-YC3.6 line after elicitation with 10^{-8} M nod factor (NF) and continued for at least 60 minutes in root hair 1, whereas spiking was arrested after 30 minutes in root hair 2 (A;C). Following NF addition, continuous spiking was also observed in the cytoplasmic tip region of root hair cells using the NES-YC3.6 reporter construct (B; D). A side-by-side comparison (E) of 5 minute measurements between nuclear and cytoplasmic spiking and nuclear spiking in an upper cortex cell showed slight differences in the overall shape of the calcium transients. Scale bars represent 50 μ m (A; B). Figure 5 was slightly modified from Krebs et al. (2012).

9.1.2. *nup85* and *nup133* mutants show residual calcium signatures in response to nod factor and chitin tetramer elicitation

Nuclear calcium signatures were analyzed in *nup85-1* and *nup133-1* mutants in comparison to wild type plants, following addition of nod factor (NF) and chitin tetramer (CO4). Mutant lines stably expressing the nuclear localized NLS-YC3.6 calcium reporter were generated by crossing of *nup85-1* and *nup133-1* mutant plants to a *L. japonicus* Gifu NLS-YC3.6 line (Krebs et al., 2012).

Table 1: Analysis of calcium oscillations in wild type and nucleoporin mutant nuclei

Line	Treatment	Nuclei analyzed	Nuclei with single calcium responses	Nuclei with calcium spiking
Gifu wild type	NF (10^{-7} M)	38	0	36 (94.7 %)
<i>nup85-1</i>	NF (10^{-7} M)	84	6 (7.1%)	0
<i>nup133-1</i>	NF (10^{-7} M)	102	10 (9.8%)	0
Gifu wild type	CO4 (10^{-7} M)	31	2 (6.4%)	5 (16.1%)
Gifu wild type	CO4 (10^{-6} M)	77	4 (5.2%)	69 (89.6%)
<i>nup85-1</i>	CO4 (10^{-6} M)	69	3 (4.3%)	0
<i>nup133-1</i>	CO4 (10^{-6} M)	82	13 (15.9%)	1 (1.2%)

Calcium signals of individual nuclei of root hair and epidermal cells were recorded for at least 15 minutes, starting 15 minutes after application of the elicitor. In the wild type, 94.7 % of the cells responded to 10^{-7} M NF treatment with nuclear calcium spiking (≥ 4 successive spikes). Elicitation with 10^{-7} M CO4 resulted in calcium oscillations in only 16.1% of nuclei. When CO4 concentration was increased to 10^{-6} M, 89.7% of *L. japonicus* cells responded (Table 1). Consistent with a lack of calcium spiking in the root elongation zone after treatment with AM fungal spore exudate (Chabaud et al., 2011), the root tip region (approx. 0-0.5 mm) was not responsive to CO4 and was therefore not included in the measurements. In *nup85-1* and *nup133-1* mutants no wild-type like calcium spiking could be detected after addition of 10^{-7} M NF or 10^{-6} M CO4 (Figure 6, Table 1). However, individual nuclear calcium transients were observed in the timeframe of 15 minutes in 7.1% of *nup85-1* and 9.8% of *nup133-1* cells after NF elicitation and in 4.3% of *nup85-1* and 15.9% of *nup133-1* cells after CO4 elicitation. Similar transients were also detected in a low number of wild type plants after CO4 treatment. A single *nup133-1* cell responded to CO4 addition with calcium spiking like oscillations (four transients) over the course of 25 minutes. The transients in the *nup* mutants did not show a clear biphasic asymmetric shape typical for symbiotic calcium spikes (Harris et al., 2003; Sieberer et al., 2009), instead they were more symmetrical.

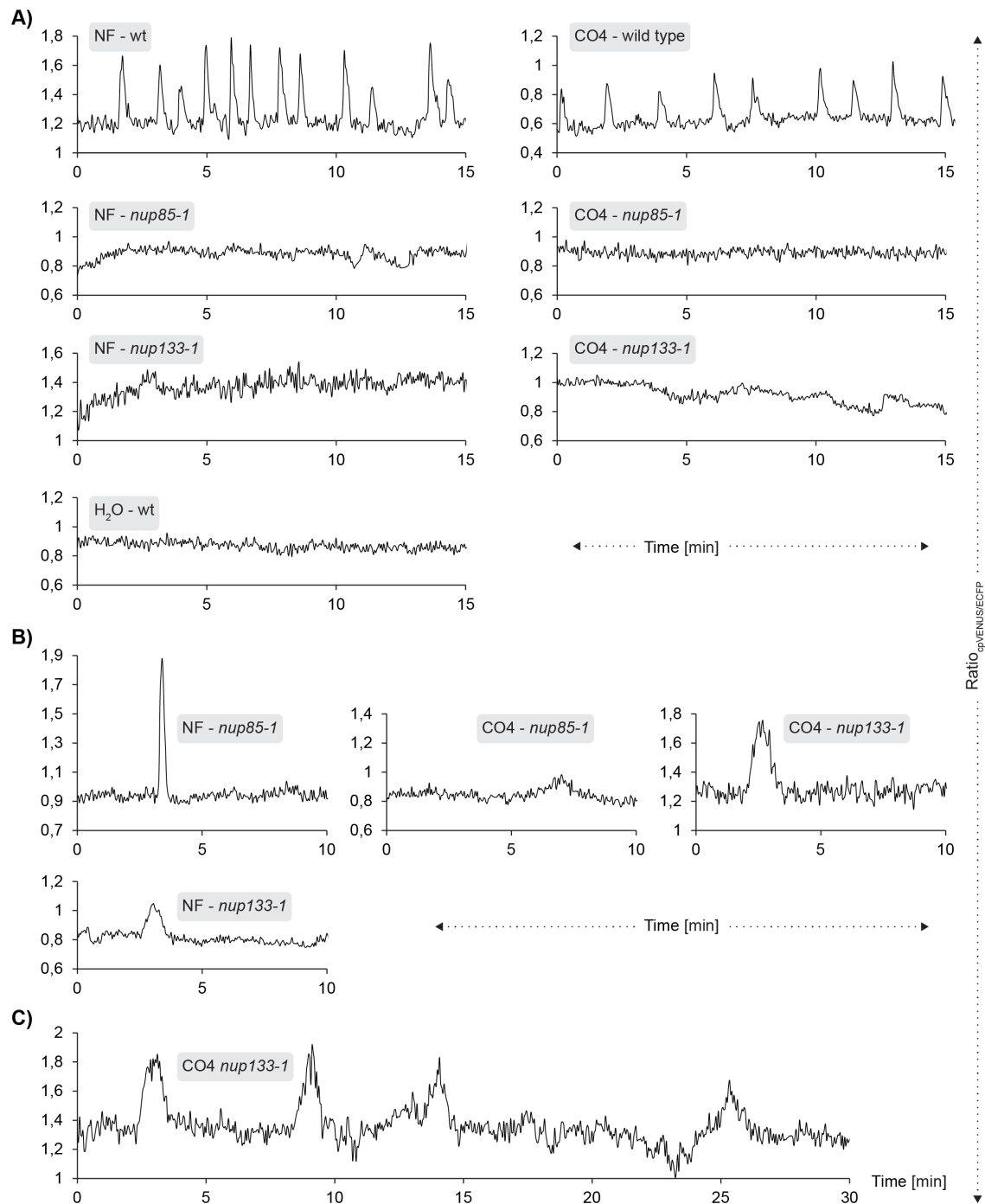


Figure 6: Residual calcium signatures in *nup85* and *nup133* nuclei. *L. japonicus* wild type (wt), *nup85-1* and *nup133-1* plants stably expressing the nuclear localized calcium reporter NLS-YC3.6 were treated with 10^{-7} M nod factor (NF) and 10^{-6} M chitin tetramer (CO4). A) Treatment with both NF and CO4 resulted in calcium spiking in the majority of wild type nuclei, but did not induce any signals in most *nup85-1* and *nup133-1* cells. B) Single calcium transients of different shapes could be detected in a number of *nup85-1* and *nup133-1* nuclei after both NF and CO4 addition. These signals could be clearly distinguished from the background noise by an increase of cpVenus(YFP) intensity correlated with a simultaneous decrease of ECFP signal. C) In one *nup133-1* mutant, a calcium spiking like response of four transients could be detected after CO4 treatment. However, individual peaks were broader and frequency was reduced compared to spiking in the wild type. Calcium signatures are shown as cpVenus/ECFP ratios. Nuclei were imaged every 1.5 seconds for 15-30 minutes following treatment with NF and CO4

9.1.3. CASTOR, POLLUX, NUP85 and NUP133 peptide antibodies

Polyclonal peptide antibodies against CASTOR, POLLUX, NUP85 and NUP133 were raised to corroborate protein localization and determine potential effect of mutations in *L. japonicus* NUPs on the NPC and on CASTOR and POLLUX. For immunization, peptides were selected that had no or low homology to other known proteins and contained predicted exposed epitopes, preferentially with several positive or negatively charged aa (R,H,K,D,E) to increase the potential binding avidity of the antibody. For CASTOR and POLLUX the homologous region as well as the predicted plastid transit domains (CASTOR to aa 69, POLLUX to aa 57) were omitted as targets. Among the suitable sequences one peptide per protein was selected that contained few or no predicted phosphorylation and N-glycosylation sites (Table 2). At least two rabbits (R) and two guinea-pigs (G) were immunized with each synthesized peptide.

Table 2: Target peptide sequences for antibody production

Target	Peptide aa sequence
NUP85	CLHKYRDFKKSLLQVSGGK
NUP133	CMHLPPEGGDSGQLEGNGYPR
CASTOR	CMVRRGSLPKDFVYPK
POLLUX	CFLRRTHNNKEDVPLKKR

Affinity purified antisera were tested in various concentrations by denaturing SDS page. C-terminal GFP fusions of CASTOR, POLLUX, NUP85 and NUP133 were expressed in *N. benthamiana* leaves under the control of the CaMV 35S promoter. Extracted protein was probed with both the target antibody as well as with an α -GFP antibody. In the native *L. japonicus* system, antibody specificity was determined by comparison of wild type root extract and protein extracted from mutants carrying early stop codons (*castor-12*, *pollux-5*, *nup85-1*) or frame shifts (*nup133-1*). Antibodies that could unambiguously detect protein from *L. japonicus* whole root extract were obtained for NUP85 (α -NUP85 G1 and G2) and NUP133 (α -NUP133 R1) (Figure 7). The band corresponding to NUP85 in *L. japonicus* showed an apparent molecular weight of 60 kDa, which is lower than the expected 80 kDa. This discrepancy could be due to altered running behavior by atypical binding to SDS or, alternatively, indicate an unpredicted cleavage of the native protein resulting in a smaller product. α -CASTOR antibodies R1 and G2 were able to detect overexpressed CASTOR-GFP fusion protein extracted from *N. benthamiana*, however neither antibody was usable for protein extracts from *L. japonicus*. While α -CASTOR G2 did not detect CASTOR protein at all, α -CASTOR R1 showed a strong signal that was partially obscured by an unspecific band of almost the same size (95 kDa), which was also present in the extract of the null mutant allele *castor-12* (Figure 7).

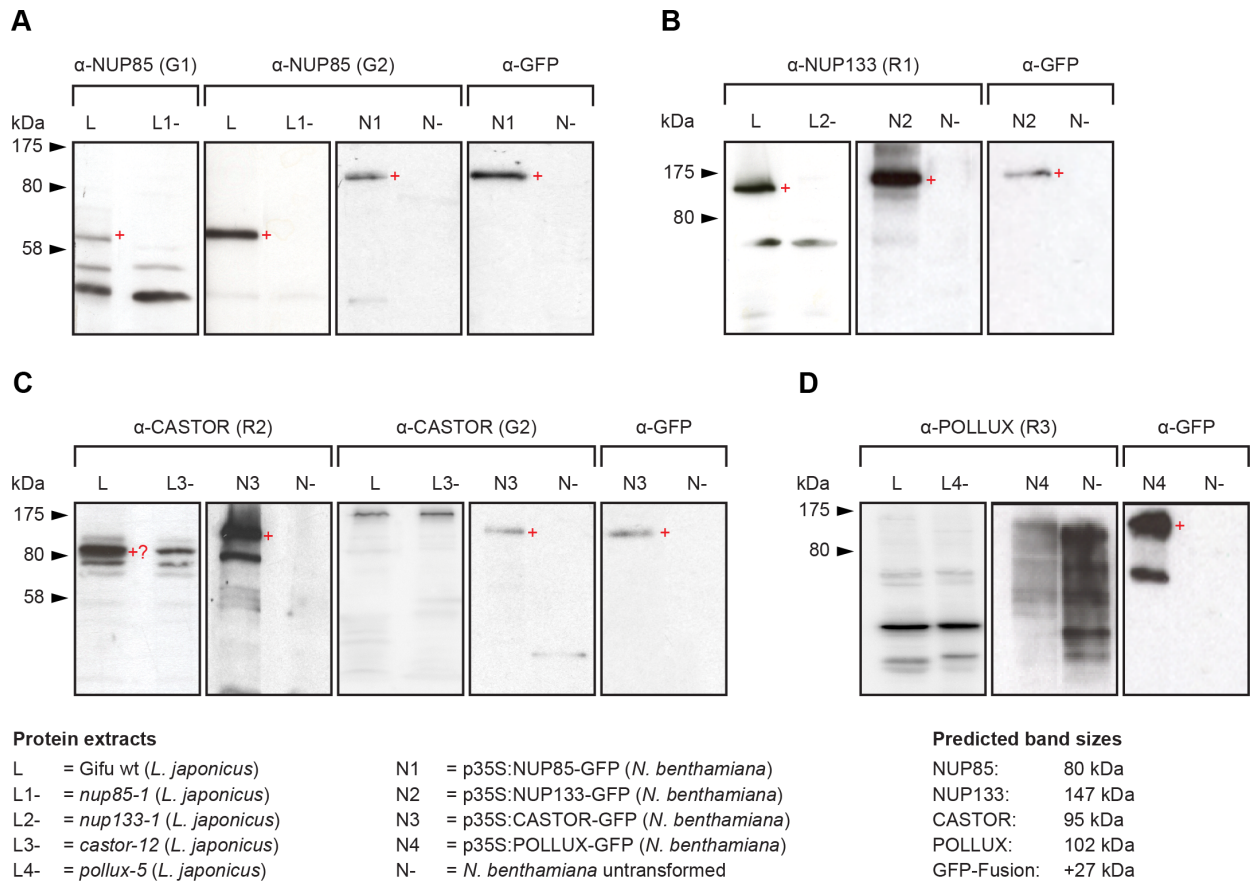


Figure 7: SDS page analysis of α -NUP85, α -NUP133, α -CASTOR and α -POLLUX antibodies. (A) α -NUP85 (G1 & G2) and (B) α -NUP133 (R1) antibodies were able to detect endogenous protein in *L. japonicus*. (C) Both α -CASTOR R2 and G2 antibodies failed to give a clear specific band in *L. japonicus* root extract, however they were able to detect overexpressed CASTOR-GFP fusion protein extracted from *N. benthamiana*. (D) α -POLLUX antibodies were unable to detect endogenous *L. japonicus* protein as well as overexpressed POLLUX-GFP (a representative negative example is shown for α -POLLUX R3). A red “+” indicates specific detection of the target protein.

Table 3: Custom antibodies and working dilutions

Antibody	Application	Optimal working dilution
α -NUP85 (G1)	SDS page	1:2000
α -NUP85 (G2)	SDS page	1:1000
α -NUP133 (R1)	SDS page	1:5000
α -NUP133 (R1)	Immunolocalization	1:500
α -CASTOR (R2)	SDS page	1:10000
α -CASTOR (G2)	SDS page	1:100

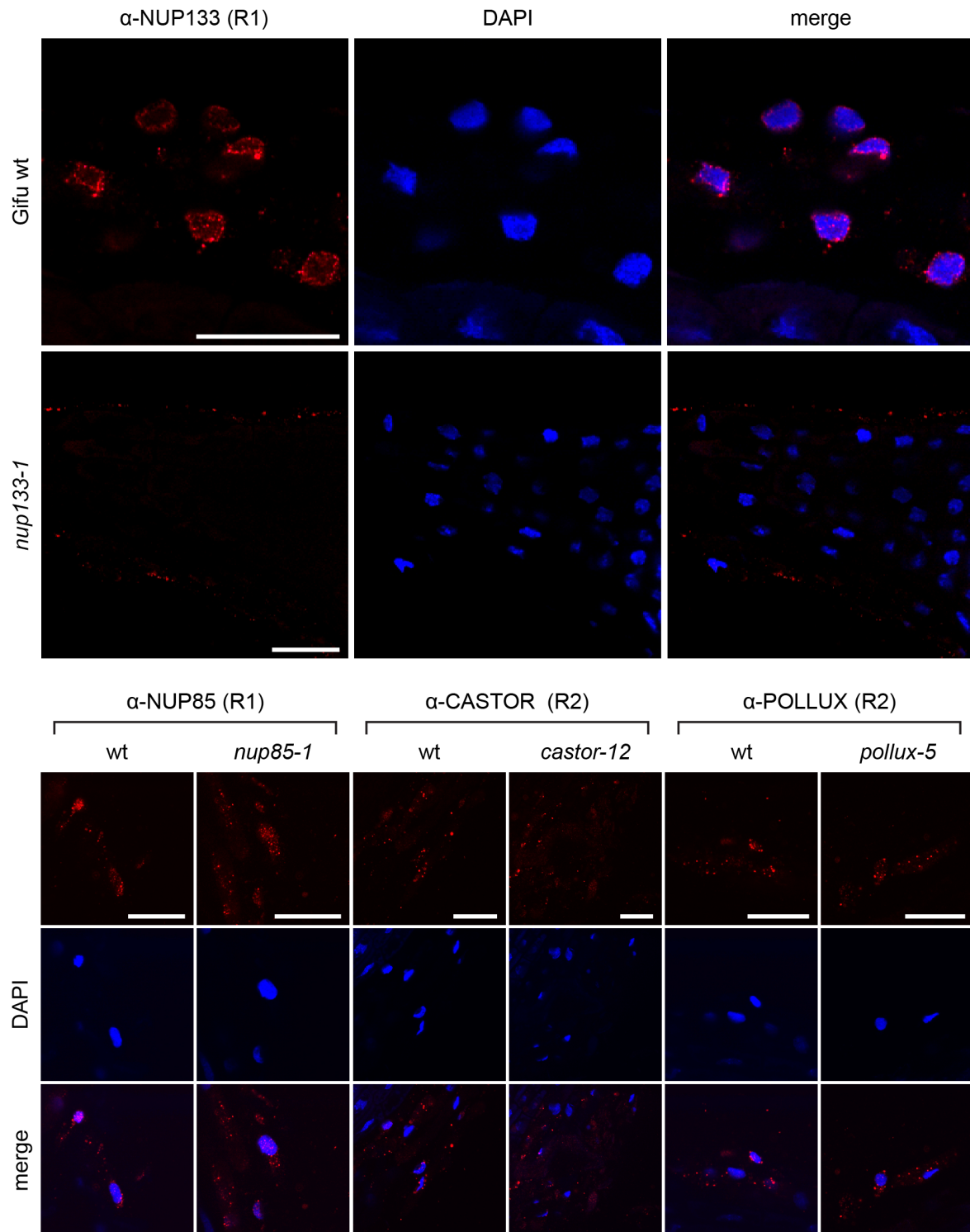


Figure 8: CLSM images of whole-mount immunostained *L. japonicus* roots. NUP133 was specifically detected by the α -NUP133 (R1) antibody in the nuclear envelope. The NUP133 signal was absent in the *nup133-1* mutant. Antibodies against NUP85, CASTOR and POLLUX failed to detect the native protein and only showed unspecific signal, which was also present in the mutant controls (a representative antibody is shown for each protein). Secondary antibodies were labeled with Alexa 647. Nuclear DNA was visualized by DAPI staining. Scale bars = 25

Unfortunately, all available POLLUX antibodies failed to detect both POLLUX protein extracted from *L. japonicus* as well as overexpressed POLLUX-GFP from *N. benthamiana* extracts. The determined optimal dilutions for the functional antibodies are listed in Table 3.

α -NUP85, α -NUP133, α -CASTOR and α -POLLUX antisera were analyzed for their ability to detect native protein by whole-mount immunostaining in *L. japonicus* roots using CLSM. Antibodies that failed to give a specific signal in Western blotting were again tested, as denaturing SDS page does not give a good indication of an antibody's ability to bind native protein. α -NUP133 (R1) was able to specifically detect NUP133, showing a clear signal in the nuclear envelope that was absent in the *nup133-1* mutant (Figure 8). Antibodies against NUP85, CASTOR and POLLUX did not show specific binding to the native protein, as the observed signal was identical in wild type and mutant control roots. While it is possible that *nup85-1*, *castor-12* and *pollux-5* mutants still express truncated protein that is not fully degraded, neither α -NUP85 nor α -CASTOR antibodies should detect it, as their target epitope would not be expressed in the early stop codon mutants. α -POLLUX could potentially still bind to truncated POLLUX protein expressed in the *pollux-5* mutant, however, the visible signals were not correlated with any clear subcellular localization and are likely due to unspecific binding.

9.1.4. *nup107* LORE1 insertion mutants are deficient in nodulation

LORE1 retrotransposon (Fukai et al., 2012; Urbański et al., 2012) lines of *L. japonicus* were screened for insertions in putative components of the NUP107-160 subcomplex, in order to investigate a potential role of other nucleoporins besides NUP85, NUP133 and NENA in plant-microbe symbiosis. A blast search against the *L. japonicus* genome (www.kazusa.or.jp/lotus/blast.html) identified candidate genes coding for predicted proteins homologous to mammalian nucleoporins SEC13 (2 hits), NUP96, NUP107 and NUP160. Based on gene structure prediction, insertion lines targeting putative coding regions were selected. The following R3 (third generation of tissue regenerated plants) lines were obtained from the *LORE1* insertion mutant collection: *nup96-1* (Plant ID: 30053096), *nup107-1* (Plant ID: 30054066), *nup160-1* (Plant ID: 30051932) and *nup160-2* (Plant ID: 30054781). The segregating R3 generations were genotyped using flanking and *LORE1* transposon specific primers. All plants of lines designated as *nup96-1* (27 individuals) and *nup160-2* (20 individuals) were homozygous wild type for the respective mutations, suggesting a mislabeling of the seeds. For line *nup160-1* individuals were either homozygous wild type or heterozygous, however, no homozygous mutant plants could be obtained in either the R3 or R4 generation. Only for line *nup107-1* unambiguous homozygous mutants could be identified in the R4 generation, which were further investigated.

The *NUP107* gene is located on *L. japonicus* chromosome 3 and has a predicted size of 18273 bases containing 23 exons with a coding sequence of 3228 bases. In line *nup107-1* the *LORE1* retrotransposon is inserted into the first predicted exon between bases 12 and 13 of the gene. Besides the insertion into *NUP107* two other *LORE1* insertions are present in

the plant line (ID 30054066; <http://users-mb.au.dk/pmgrp/>). The second insert is located in a predicted intergenic region on chromosome 2 (chr2_23555564_F), while the third targets the 5'UTR (815 bp upstream of the ATG) region of a putative protein phosphatase 2C on chromosome 4 (chr4.CM0182.350.r2.m). Among 37 available plants of a segregating R3 population grown at 24°C no homozygous *nup107-1* mutants could be identified; 21 individuals were heterozygous and 16 homozygous wild type. To prevent or minimize the loss of mutant plants caused by putative developmental defects similar to those observed in *nup85* and *nup133* double mutants (Binder and Parniske, 2014), *nup107-1* R4 individuals (offspring of heterozygous *nup107-1* plants) were grown at 18°C instead of 24°C. A segregating R4 *nup107-1* population of 83 plants was genotyped, revealing 31 homozygous wild type, 41 heterozygous and 11 homozygous *nup107-1* individuals. These values were significantly different from the expected segregation ratio of 1:2:1 ($p < 0.01$; χ^2 test), suggesting that gametophyte (pollen/embryo sac) viability could be affected in *nup107-1*. The plants were grown for 6 weeks, then inoculated with *M. loti* dsRED MAFF rhizobia and assayed for nodulation 4 weeks after inoculation. The wild type plants harbored an average of 10.04 nodules, while *nup107-1* mutants did not produce any nodules or nodule primordia (Figure 9C/D). All heterozygous individuals were carrying nodules (not quantified). Inoculated *nup107-1* plants were slightly smaller than wild type plants, likely due to the lack of active nitrogen fixation, however, they did not show obvious growth defects (Figure 9B) as those observed in *nup85/nup133* double mutants.

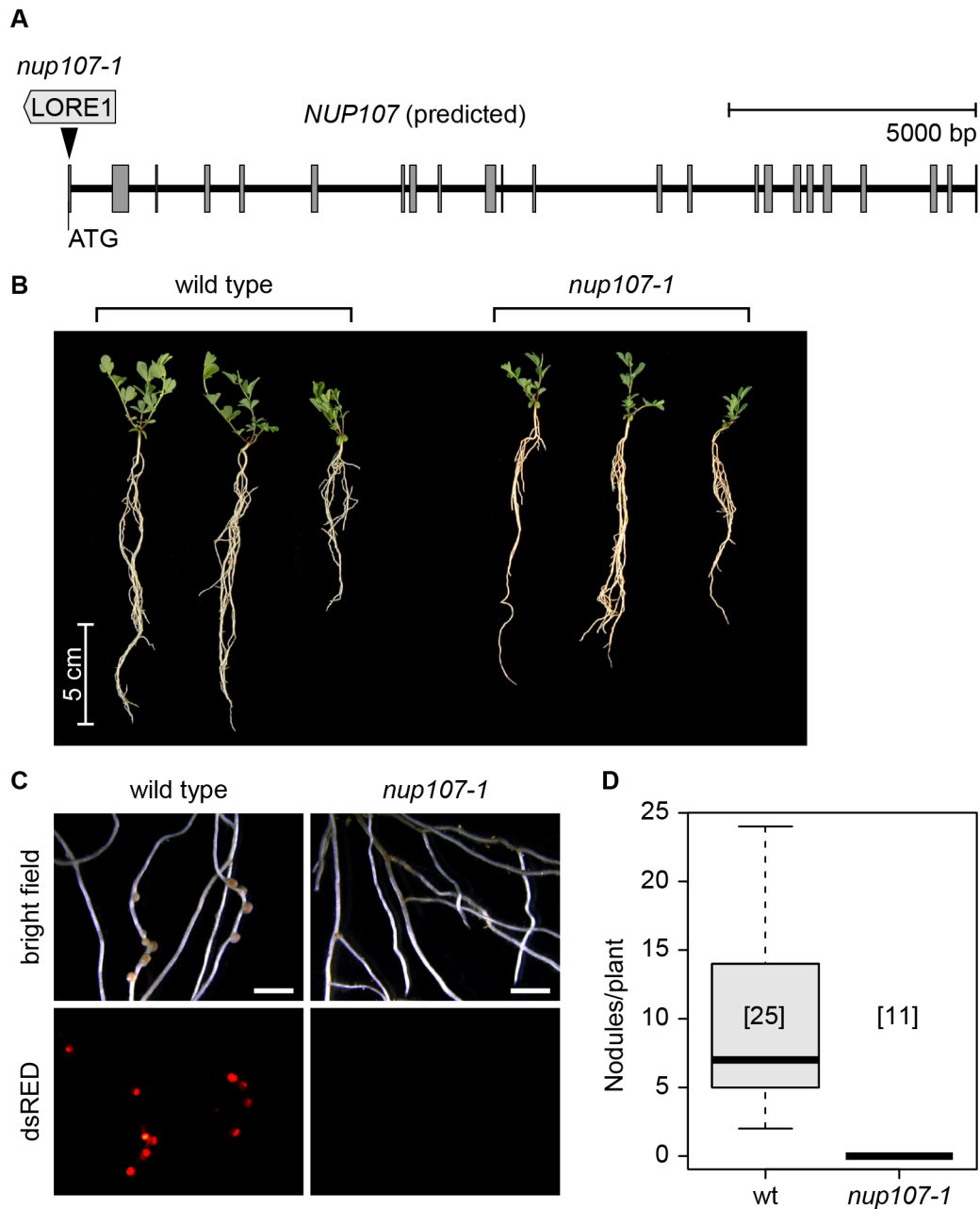


Figure 9: Nodulation defects in *nup107-1* LORE1 insertion mutants. A) Gene structure prediction of *NUP107* depicting exons (grey bars) and introns (black line). Line *nup107-1* contains a LORE1 insertion into the first predicted exon of the gene. B) Photographs of wild type and homozygous *nup107-1* plants grown for 10 weeks at 18°C and inoculated after 6 weeks with *M. loti* MAFF 303099 (dsRED). C) Stereomicroscopic images of wild type and *nup107-1* roots. Colonized nodules are visualized by the red fluorescence of *M. loti* expressing dsRED (scale bar = 3 mm). D) Box plot showing nodulation 4 weeks after inoculation with *M. loti* at 18°C. Number of analyzed plants is indicated in brackets.

9.1.5. CASTOR and POLLUX localize to the inner nuclear membrane in *N. benthamiana*

CASTOR and POLLUX localization was investigated using a bimolecular fluorescence complementation (BiFC) system based on dimerization of the *A. thaliana* bZIP63 transcription factor (Walter et al., 2004). Two N-terminal truncated versions of bZIP63 (Δ 1-165 aa) were generated (NLS-ZIP, NES-ZIP), both retaining the basic leucine zipper domain required for dimerization (ZIP). For NLS-ZIP the native NLS (RRSRRRKQ) was preserved, while for NES-ZIP the NLS was replaced with a NES of the rabbit heat stable protein kinase inhibitor PKI (Wen et al., 1995), in order to confer cytosolic localization. The proteins were fused to the N-terminal and C-terminal fragments of YFP (YFP-N/YFP-C) respectively, which are able to reconstitute active YFP upon dimerization (Walter et al., 2004). Co-expression of NLS-ZIP-YFP-N and NLS-ZIP-YFP-C under the strong dual CaMV 35S (2x35S) promoter in *N. benthamiana* leaves showed an exclusive nuclear YFP signal. Dimerization of NES-ZIP-YFP-N and NES-ZIP-YFP-N resulted in the expected cytosolic signal. However, additional nuclear signal was observed in some cells (Figure 10A). CASTOR and POLLUX were fused to the ZIP dimerization domain (without NLS or NES), which was in turn fused to YFP-N and YFP-C. As a control, CASTOR-ZIP-YFP-N and POLLUX-ZIP-YFP-N were co-expressed with CASTOR-ZIP-YFP-C and POLLUX-ZIP-YFP-C respectively. In both cases a clear signal in the nuclear envelope confirmed the previously observed localization of CASTOR and POLLUX homocomplexes (Charpentier et al., 2008) and suggested that fusion to the bZIP63 dimerization domain did not change the localization of the proteins (Figure 10A).

To study nuclear membrane localization, CASTOR-ZIP-YFP-N and POLLUX-ZIP-YFP-N were co-expressed in combination with NLS-ZIP-YFP-C and NES-ZIP-YFP-C under the control of 2x35S promoters. In all cases a YFP signal in the nuclear envelope could be observed (Figure 10B). For POLLUX, the signal was visible after 1 day following *N. benthamiana* infiltration. However, for CASTOR at least 2 days were required, indicating that CASTOR expression was weaker or that the protein was preferentially degraded. The positive interaction of CASTOR-ZIP-YFP-N and POLLUX-ZIP-YFP-N with NLS-ZIP-YFP-C suggested that both proteins are located in the INM and that their C termini face the nucleoplasm. Considering that NES-ZIP dimers were not exclusively cytosolic, but partially nuclear localized, the interaction of CASTOR-ZIP-YFP-N and POLLUX-ZIP-YFP-N with NES-ZIP did not conclusively indicate ONM localization, as the signal could partly be caused by interaction with nuclear NES-ZIP. Co-expression of CASTOR-ZIP-YFP-N with NES-ZIP or NLS-ZIP resulted in additional signal inside the nucleus, which was not observed for the interaction of CASTOR-ZIP-YFP-N with CASTOR-ZIP-YFP-C. Similar nuclear signals could also be detected for POLLUX-ZIP-YFP-N after two or more days of co-expression with NES-ZIP or NLS-ZIP.

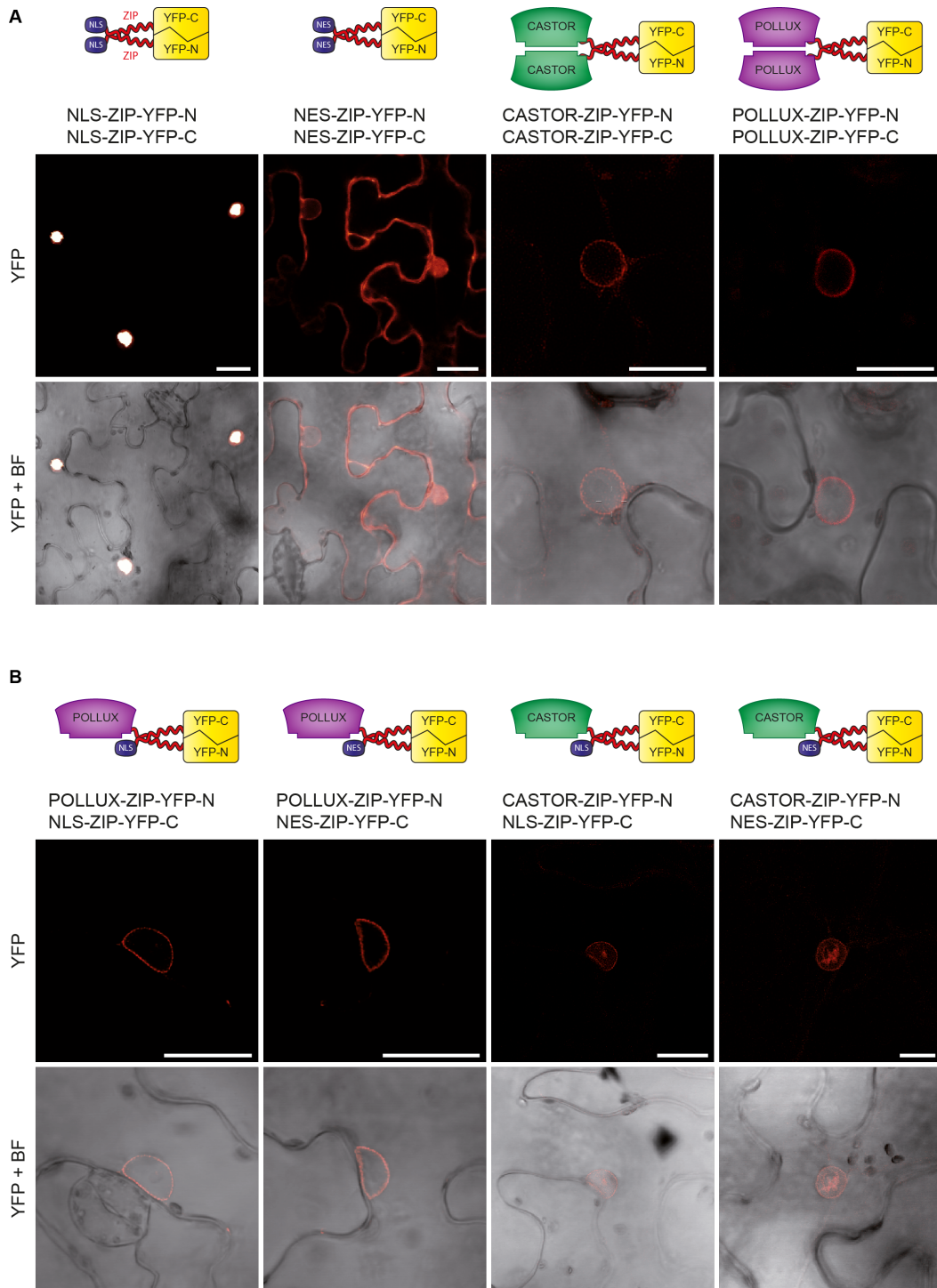


Figure 10: CLSM analysis of CASTOR and POLLUX localization in *N. benthamiana* by BiFC. Dimerization of the ZIP domain of bZIP63 fused to YFP-N and YFP-C reconstitutes active YFP. A) NLS-ZIP dimers localize exclusively to the nucleus, while NES-ZIP dimers show mostly cytosolic localization, with nuclear signal visible in some cells. Both CASTOR-ZIP and POLLUX-ZIP homocomplexes reconstitute a YFP signal in the nuclear envelope. B) Co-expression of either POLLUX-ZIP-YFP-N or CASTOR-ZIP-YFP-N together with NLS-ZIP-YFP-C suggests that both POLLUX and CASTOR are localized in the INM. In contrast, co-expression of the fusion proteins together with NES-ZIP-YFP-C does not exclusively indicate ONM localization, as NES-ZIP showed residual nuclear signal. BF = bright field; Scale bars = 25 μ m;

9.1.6. Differential nuclear and cytosolic protein localization by complementation of superfolder GFP

In order to analyze potential nuclear import defects of CASTOR and POLLUX in the *L. japonicus nup* mutants, the abundance of the proteins in INM compared to ONM needed to be determined. The bZIP63 based BiFC assay (chapter 9.1.5) was able to detect CASTOR and POLLUX in the INM, however, a ratiometric measurement of the protein levels was prevented by the fact that the ZIP dimerization domain of bZIP63 could not be targeted exclusively to the cytosol. As an alternative to the bZIP63 BiFC system, a localization assay based on the reconstitution of superfolder GFP was developed. The small 11th β -barrel domain of superfolder GFP (GFP11) is able to complement an inactive 1-10 β -barrel superfolder GFP domain (GFP1-10) to form functional GFP (Cabantous et al., 2005) and can therefore be used as a small unintrusive tag. NLS-GFP1-10 and NES-GFP1-10 fusions were constructed in order to differentially localize co-expressed proteins tagged with GFP11 to nucleus/INM and cytosol/ONM respectively. To account for differences in expression levels between cells, mCherry was fused N-terminally to GFP1-10 as a normalization marker. Expression of NLS-mCherry-GFP1-10 and NES-mCherry-GFP1-10 in *N. benthamiana* showed exclusive nuclear and cytosolic localization of mCherry. Co-expression of GFP11 together with NLS-mCherry-GFP1-10 constituted GFP signal in nucleus and cytosol respectively, indicating that GFP11 can be differentially detected in either compartment (Figure 11). Constructs for co-expression of CASTOR-GFP11 and POLLUX-GFP11 together with NLS-mCherry-GFP1-10 and NES-mCherry-GFP1-10 were generated, but have so far not been tested in *L. japonicus*.

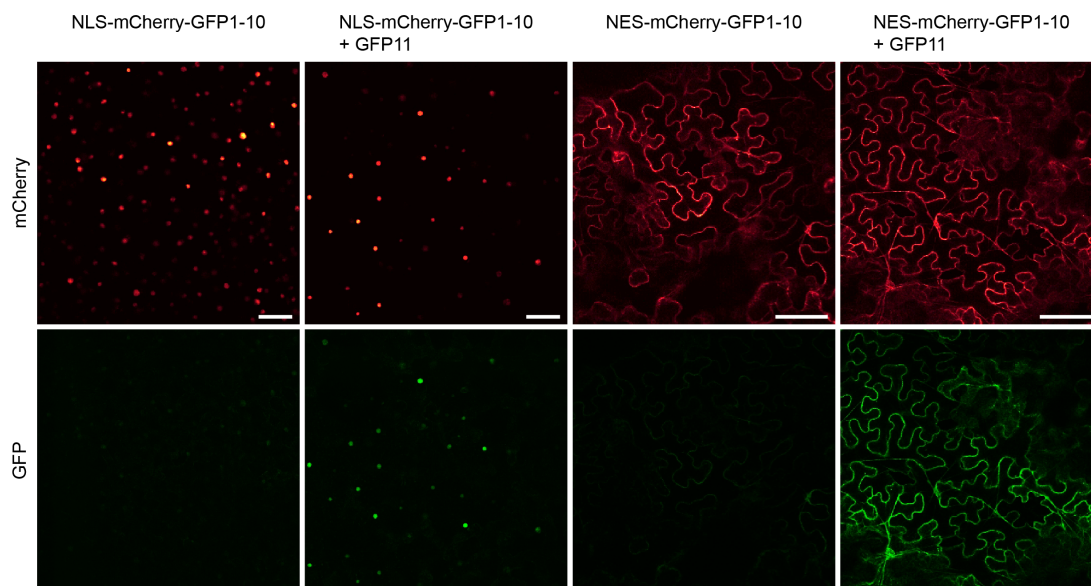


Figure 11: Superfolder GFP based complementation for detection of nuclear and cytosolic protein levels. Detection of mCherry revealed exclusive nuclear and cytosolic localization of NLS-mCherry-GFP1-10 and NES-mCherry-GFP1-10 respectively. Co-expression of NLS-mCherry-GFP1-10 together with GFP11 allowed for the detection of the nuclear fraction of GFP11, while co-expression of NES-mCherry-GFP1-10 and GFP11 reconstituted cytosolic GFP signal. Scale bars represent 100 μ m.

9.1.7. Simultaneous overexpression of CASTOR and POLLUX complements the nodulation phenotype in *L. japonicus nup* mutants

CASTOR and POLLUX were overexpressed in the *nup* mutant background to test for complementation of the symbiotic phenotype. With the Golden Gate cloning toolkit (Binder et al., 2014), LIII binary plasmids were generated containing a p35S:*GFP* transformation marker together with the full length genomic sequence of either *CASTOR* or *POLLUX* under the control of a polyubiquitin promoter (pUB:CASTOR and pUB:POLLUX). Additionally a plasmid with both *CASTOR* fused to *mCherry* and *POLLUX* fused to *YFP* was constructed (pUB:CASTOR+POLLUX). The constructs and an empty vector control (EV), containing only p35S:*GFP*, were transferred into *L. japonicus* mutants *nena-1*, *nup85-1* and *nup133-1* and in case of EV additionally into wild type plants. Transformed plants were inoculated with *M. loti* MAFF 303099 (expressing dsRED) and nodulation was analyzed four weeks later. No nodules were observed on mutant plants transformed with either EV, pUB:CASTOR or pUB:POLLUX (Figure 12; Figure 15). However, expression of pUB:CASTOR+POLLUX could restore nodulation in all three *nup* mutants (Figure 13; Figure 15). Since pUB:CASTOR+POLLUX did not contain a *GFP* transformation marker, successfully transformed roots were identified by the POLLUX-YFP signal, which could be detected on all mutant roots harboring nodules. On average, transformed plants contained 6.1 nodules per transformed root system in *nena-1*, 4.8 nodules in *nup85-1* and 4.5 nodules in *nup133-1*, while wild type plants transformed with EV harbored 6.2 nodules per transformed root system (Figure 15). The nodules formed on the *nup* mutants were colonized and appeared wild-type like (Figure 13). Unlike mutant plants transformed with EV, complemented roots did not display characteristic nitrogen starvation symptoms, indicating that the nodules were fixing nitrogen (data not shown). Both CASTOR-*mCherry* and POLLUX-*YFP* were expressed and showed a clear localization around the nuclear envelope, as well as additional clusters throughout the cell, likely caused by the strong overexpression (Figure 14). As previously observed in the BiFC dimerization assay (Figure 10), the CASTOR signal in the nuclear envelope was weaker than that of POLLUX, suggesting that this effect is neither dependent on the promoter nor on differences in expression between cDNA and genomic constructs. The transformation of *L. japonicus* wild type roots with pUB:CASTOR+POLLUX did not induce spontaneous nodule formation in the absence of rhizobia (data not shown), indicating that overexpression of CASTOR and POLLUX does not lead to auto-activation of downstream symbiotic signaling.

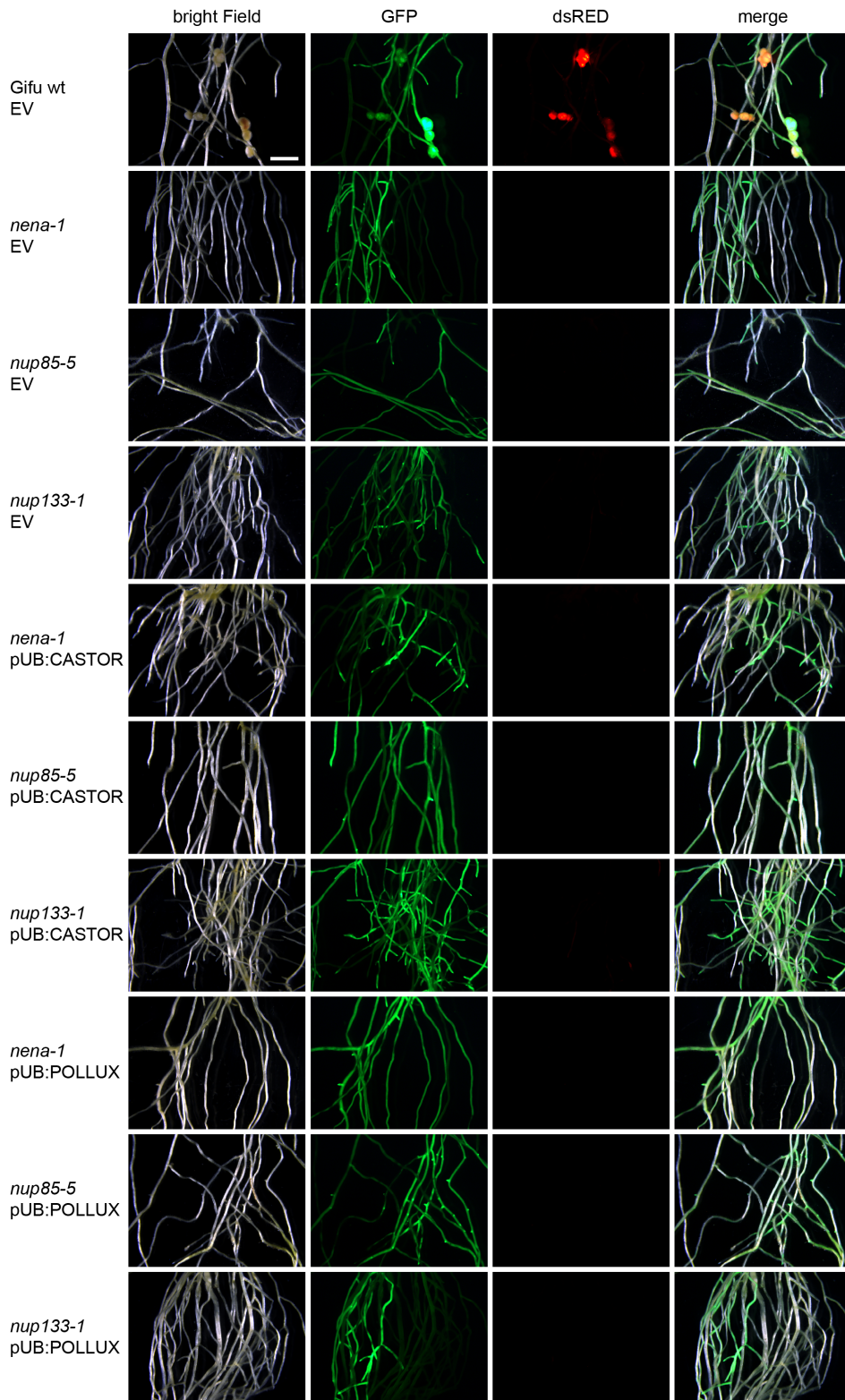


Figure 12: Individual overexpression of CASTOR or POLLUX in the *nup* mutant background does not restore nodulation. Roots of *nena*, *nup85* or *nup133* mutants were transformed with either empty vector control (EV), pUB:CASTOR or pUB:POLLUX and assayed 4 weeks after inoculation with *M. loti* MAFF (dsRED). Transformed parts of the root system express GFP as a visual marker. Scale bar = 3 mm.

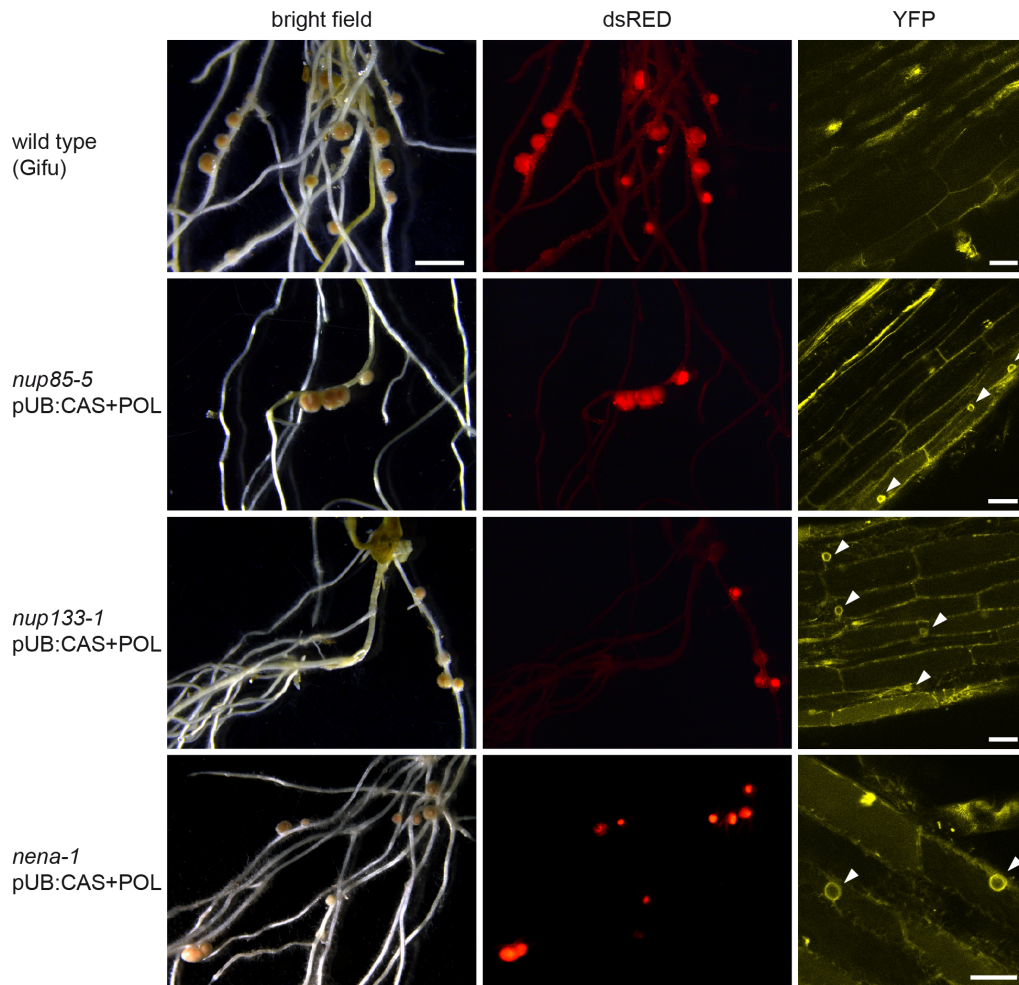


Figure 13: Overexpression of both CASTOR and POLLUX restores nodulation in *nena*, *nup85* and *nup133* plants. Roots transformed with pUB:CASTOR+POLLUX (pUB:CAS+POL) were assayed four weeks after inoculation with dsRED expressing *M. loti* MAFF rhizobia. Transformed roots were identified by expression of POLLUX-YFP (white arrowheads). Inoculated non-transformed wild type roots are shown in comparison. Scale bars= 3 mm (bright field) and 25 μ m (YFP).

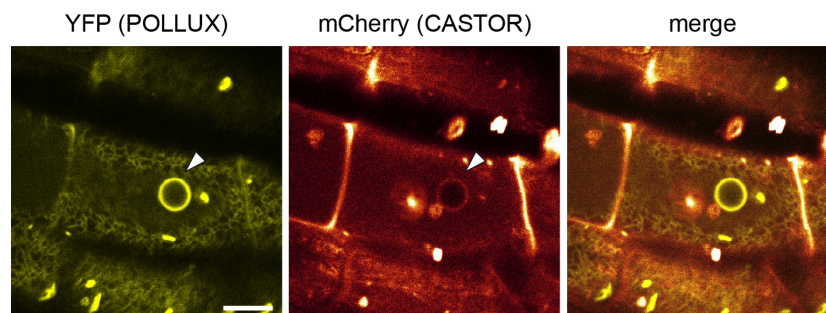


Figure 14: Localization of POLLUX-YFP and CASTOR-mCherry in *L. japonicus* roots. A weak mCherry and a stronger YFP signal, corresponding to CASTOR and POLLUX respectively, are visible in the nuclear periphery (white arrowheads) of roots transformed with pUB:CASTOR+POLLUX. Fluorescent clusters outside of the nuclear envelope partly correspond to overexpression artifacts and to *M. loti* MAFF rhizobia expressing dsRED. High background signals throughout the cells are due to the strong auto-fluorescence of *L. japonicus* hairy roots. Scale bar = 10 μ m.

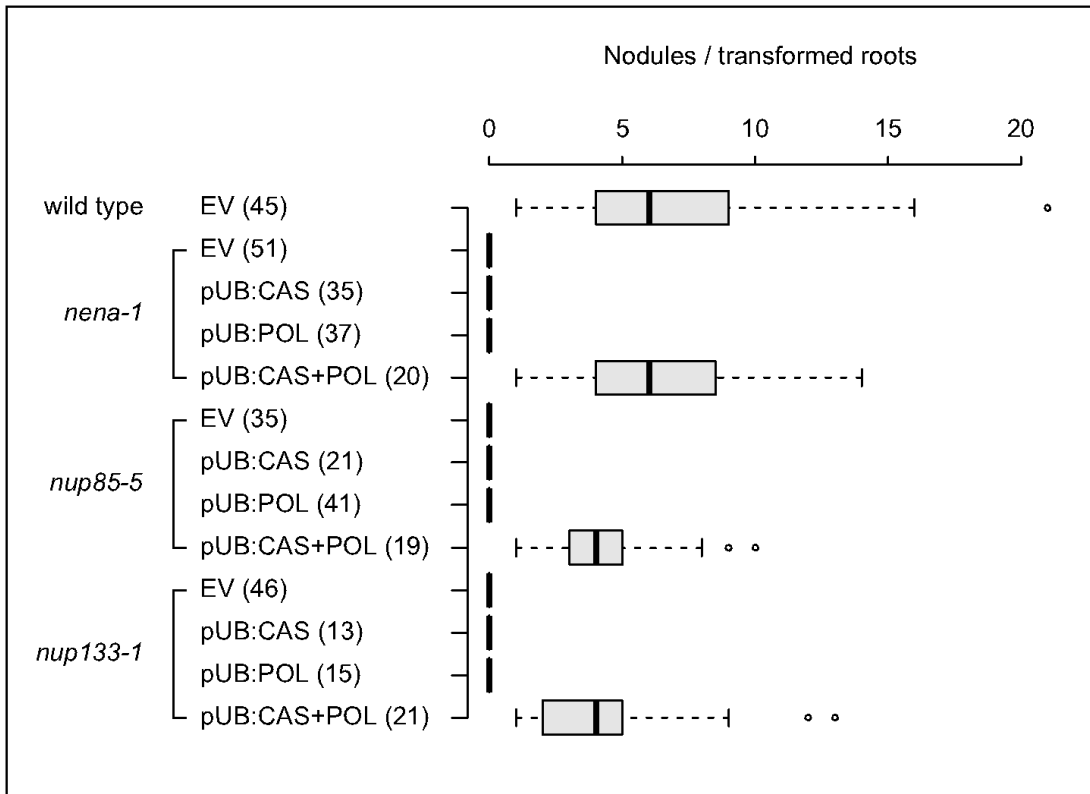


Figure 15: Boxplot showing number of nodules per plant on transformed roots 4 weeks after inoculation. The numbers of transformed plants for each construct are indicated in parentheses. EV = empty vector (p35S:GFP); CAS = CASTOR; POL = POLLUX.

9.2. Discussion

9.2.1. Transgenic *L. japonicus* calcium reporter lines for analysis of symbiotic calcium responses

Calcium ions are important secondary messengers in a multitude of signaling processes both in animals and plants. During establishment of plant-microbe symbiosis, calcium spiking is induced in response to fungal and bacterial signals and presumably directly decoded by CCaMK, which in turn leads to downstream expression of symbiosis associated genes (Ehrhardt et al., 1996; Shaw and Long, 2003; Miwa et al., 2006b; Kosuta et al., 2008; Sieberer et al., 2009; Chabaud et al., 2011; Sieberer et al., 2012; Genre et al., 2013). The generation of *L. japonicus* lines stably expressing the calcium sensor yellow cameleon 3.6 (YC3.6) enables the analysis of calcium dynamics with a high spatial resolution and specificity. In contrast to microinjection of individual root hairs with calcium sensitive dyes (Ehrhardt et al., 1996; Miwa et al., 2006a), the use of transgenic cameleon plants facilitates the screening of a larger number of cells and the study of cell types, which are not easily amenable for microinjection (e.g. cortex). By employing targeted cameleon versions (NES and NLS signals), it is also possible to study cytosolic and nuclear calcium signatures in isolation. In agreement with previous measurements in *M. truncatula* (Sieberer et al., 2009), cell autonomous NF induced nuclear calcium spiking could be detected in the majority of root hair nuclei in *L. japonicus*. The initial upward phase of individual spikes is most likely caused by the opening of calcium channels, allowing calcium to flow from its stores down its concentration gradient. The longer downward

phase corresponds to a slower active calcium re-uptake into the internal stores by calcium pumps (Oldroyd and Downie, 2006). The comparison of calcium oscillations in NLS-YC3.6 and NES-YC3.6 lines demonstrated that cytosolic calcium spikes in the tip region of root hairs are more symmetrical than those recorded in the nucleus, without a pronounced steep initial phase (Figure 5). This difference could be explained under the assumption that the calcium spiking machinery is primarily associated with the nucleus (in the nuclear envelope and in the nucleus-associated endoplasmic reticulum) (Capoen et al., 2011). Opening of nuclear and perinuclear calcium channels would therefore directly translate to the observed fast increase of calcium concentration in the nucleus, whereas in the root tip, calcium ions first would have to diffuse from the nucleus to the cytosolic region, resulting in a slower upward phase. Given the position of the CCaMK/CYCLOPS complex in the nucleus (Singh et al., 2014), nuclear spiking is presumably the primary signal carrier, which is transduced into the activation of *NIN* expression. Mathematical modelling predicted that continued nuclear spiking can likely not be explained by passive diffusion of calcium ions through the NPC, suggesting that calcium is instead released from calcium channels located in the INM (Capoen et al., 2011). Studies in both animals and plant cells also demonstrated the capacity of the nucleus to autonomously regulate calcium signaling (Pauly et al., 2000; Pauly et al., 2001; Xiong et al., 2004; Rodrigues et al., 2009). The interplay of nuclear and cytosolic calcium elevations and the relevance of cytosolic spiking in symbiotic signaling in particular are not clearly understood. Calcium oscillations are presumably initiated by the activation of both calcium channels and CASTOR/POLLUX (DMI in *M. truncatula*) through symbiotic secondary messengers (Charpentier et al., 2013). However, whether spiking originates in the cytosol, nucleus or on both sides in parallel could so far not be resolved (Capoen et al., 2011). It would be interesting to determine, if nuclear calcium spiking can be initiated and maintained, while blocking cytosolic calcium oscillations at the same time.

Recently short-chain chitin oligomers (primarily CO4 and CO5), were identified as fungal signaling molecules, which are able to induce nuclear calcium spiking in *M. truncatula* dependent on *DMI1* (*L. japonicus* POLLUX) and *DMI2* (*L. japonicus* SYMRK), but independent of the putative NF receptor NFP (Genre et al., 2013). In agreement with these results CO4 addition also triggered nuclear calcium spiking in *L. japonicus* NLS-YC3.6 plants, but was unable to induce wild type like spiking in *nup85* and *nup133* mutants (Figure 6), thereby confirming that activation of symbiotic signaling by CO4 is dependent on the common symbiosis pathway. Whereas in *M. truncatula* a CO4 concentration of 10^{-8} M was sufficient to induce spiking in the majority of epidermal cells (Genre et al., 2013), in *L. japonicus* 10^{-6} M CO4 was required to give a similar response. Whether this discrepancy is due to batch to batch variability in the CO4 samples or reflects actual physiological differences between the legumes will have to be determined. Based on the identification of both short-chain chitin oligomers (Genre et al., 2013) as well as mycorrhiza LCOs (Maillet et al., 2011), it was suggested that AM fungi could use different chitin based signaling molecules to trigger host responses, instead of a single LCO type as in rhizobial

species (Genre et al., 2013). It is therefore conceivable that different plant species can detect different MFs with varying specificity.

9.2.2. Nuclear calcium signaling in *nup85* and *nup133* mutants

In *L. japonicus*, components of the nuclear pore complex act upstream of calcium spiking (Kanamori et al., 2006; Saito et al., 2007; Groth et al., 2010), however, neither their exact position nor their function in symbiotic signal transduction is fully elucidated. An extended analysis of nuclear calcium responses in *nup85-1* and *nup133-1* plants expressing NLS-YC3.6 confirmed that fungal and bacterial signaling molecules are unable to induce continuous wild type like nuclear calcium spiking in the mutants (chapter 9.1.2). Nevertheless, single transients could still be observed both in response to NF and CO₄ and in a single case a calcium spiking like oscillation was activated in *nup85* following CO₄ treatment. Previously, a similar insular calcium spiking response was also recorded in a *vena-1* mutant in response to NF (in 1 of 90 analyzed root hairs) (Groth et al., 2010). These residual signals suggest that calcium spiking is still triggered, however, regular and continuous oscillations cannot be fully initiated and maintained. The transients recorded in the mutants do not exhibit the typical biphasic shape corresponding to the fast opening of calcium channels and slower reuptake of the calcium ions (Oldroyd and Downie, 2006), but are instead more irregular without a steep upward phase. This could be due to a delay in or incomplete opening of calcium channels. Alternatively, the recorded signals might not initiate in the nucleus, but originate from the cytosol and then diffuse into the nucleus. Either case suggests a disturbance in the calcium spiking machinery of the INM. Previously, it was demonstrated that a certain minimum number of calcium spikes (about 36) is required for the induction of the early nodulation gene ENOD11 (Miwa et al., 2006b). Moreover, a switch from low to high frequency calcium oscillations in the initial stages of RNS and AM establishment suggests that modulation of the spiking frequency itself could be important during symbiotic infection (Sieberer et al., 2012). Neither the residual calcium transients nor the low frequency short oscillations in the *nup* mutants will therefore likely be sufficient to activate the symbiotic program. Limited residual nodulation in the *nup* mutants could theoretically be initiated by rare wild type like calcium spiking, however, it might also depend on alternative infection modes, such as crack entry, which can bypass the requirements for normal root hair infection as observed in the *vena-1* mutant (Groth et al., 2010). In agreement with this, cortical expression of genes required for the induction of calcium spiking was shown not to be required during rhizobial infection (Hayashi et al., 2014).

9.2.3. A *LORE1* line with an insertion in *L. japonicus* *NUP107* is defective in nodulation

The investigation of *L. japonicus* *LORE1* retrotransposon lines targeting NUP107-160 members, revealed a symbiotic defect in a line containing a *LORE1* insertion in *NUP107* (chapter 9.1.4). As no progeny of homozygous *nup107-1* mutants were available for analysis, a segregating R4 population derived from heterozygous parents was genotyped

and phenotyped in parallel. The nodulation defect co-segregated with homozygous *nup107-1* plants, whereas both wild type and heterozygous individuals formed nodules. The other two LORE1 insertions present in the plant line are unlikely responsible for the phenotype, as they both target predicted non-coding regions on different chromosomes and should therefore not co-segregate with homozygous *nup107-1* individuals. In principle, an unidentified spontaneous mutation in a second gene in close proximity to the *NUP107* locus (which would co-segregate with it) could also cause the observed nodulation defect. To rule out this possibility, *nup107-1* plants will have to be complemented with a *NUP107* transgene once homozygous progeny is available. Moreover, the AM phenotype of the mutants should also be screened to test whether *NUP107* acts as a common symbiosis gene.

The insertion of the LORE1 transposon into the beginning of the first exon (between bases 12 and 13 from the ATG) of *L. japonicus* *NUP107* suggests that no functional protein or truncated protein can be produced in *nup107-1* plants. Under the assumption that this insertion is the cause of the nodulation defects, *NUP107* would be the fourth member of the *NUP107-160* subcomplex, (among *NUP85*, *NUP133* and *NENA*) with a function in plant-microbe symbiosis. This suggests that a fully functional *NUP107-160* subcomplex is required in symbiotic signaling. Several studies demonstrated that the loss of single *NUP107-160* members does not prevent the assembly of the subcomplex, however, multiple scaffold NUPs as well as peripheral NUPs are co-depleted in *nup85*, *nup133*, *seh1* and other *nup* mutants (Boehmer et al., 2003; Harel et al., 2003; Walther et al., 2003; Loïdice et al., 2004; Rasala et al., 2006; Ródenas et al., 2012). The localization of *NUP107* in the NE is also dependent on the presence of multiple other *NUP107-160* NUPs, including *NUP85* and *NUP160* (Ródenas et al., 2012). Many of the phenotypes associated with *NUP107-160* mutants are therefore likely due to defects in general functions of the subcomplex. Loss of the *NUP107* yeast homolog *NUP84* also results in similar phenotypes as those observed in yeast *nup85* and *nup133* mutants, including clustering of NPCs, severe growth defects at non-permissive temperature and accumulation of poly-(A)+ RNA in the nucleus (Li et al., 1995; Pemberton et al., 1995; Siniosoglou et al., 1996; Fernandez-Martinez et al., 2012).

Crystal structure analysis of the human proteins showed that *NUP107* connects *NUP133* to the NPC via direct binding and isothermal titration calorimetry demonstrated a very strong interaction between the two NUPs with a K_D of 4 nM (Boehmer et al., 2008). In agreement with this, depletion of *NUP107* in HeLa cells lead to a reduction of *NUP133* protein levels (Boehmer et al., 2003), suggesting that *NUP133* is anchored to the NPC via *NUP107*. Based on this observation, the nodulation defect in *L. japonicus* *nup107-1* could be primarily caused by a loss of *NUP133*. However, more recent data in *Caenorhabditis elegans* demonstrated that *NUP133* is still present in the NPC during interphase in *nup107*, suggesting that *NUP133* can form interactions with other NUPs than *NUP107* (Ródenas et al., 2012). This is also supported by yeast NPC models, which propose a head to tail orientation of multiple *NUP84* subcomplexes, whereby *NUP133* interacts with *NUP120*

(yeast homolog of NUP160) of a neighboring NUP84 subcomplex (Alber et al., 2007; Debler et al., 2008).

Unlike in strong *nup85*, *nup133* and *nena* alleles, which showed residual, nodulation at lower temperatures (Kanamori et al., 2006; Saito et al., 2007; Groth et al., 2010) the analyzed *nup107-1* mutants did not form any nodules even when grown at 18°C, indicating a more severe impact on the NUP107-160 complex compared to the other *nup* mutants. These results should be confirmed in a larger population side by side with the other mutants under identical conditions. The number of homozygous *L. japonicus nup107-1* offspring from heterozygous parents was lower than expected for a typical monogenic distribution, an effect that was previously also observed in segregating *nup85* and *nup133* mutant populations (Binder and Parniske, 2014). Moreover, *L. japonicus nup85* and *nup133* mutants as well as *A. thaliana nup160* single mutants and to a larger extent *nup160/nup133* double mutants produce fewer seeds than wild type plants (Kanamori et al., 2006; Saito et al., 2007; Wiermer et al., 2012). This could indicate that defects in the NUP107-160 subcomplex also have a detrimental effect on the germline, possibly by affecting gamete or embryo viability. Similar effects were also observed in animals. In *C. elegans* offspring of *nup107* mutants showed an increase in embryo lethality as well as impaired larval development, which was more severe at higher temperature (25°C vs 20°C) (Ródenas et al., 2012). Embryonic development was also disturbed in NUP107 transposon insertion lines of Zebrafish (Zheng et al., 2012).

It is probable that mutations in other NUP107-160 subcomplex members besides NUP107, NUP85, NUP133 and SEH1 would also affect plant-microbe symbiosis. Unfortunately, the three other available *L. japonicus LORE1* NUP107-160 lines could not be analyzed for symbiotic defects. The lines “*nup160-2*” and “*nup96-1*” were likely mislabeled as they did not contain the designated insertions, whereas for the fourth line “*nup160-1*” only heterozygous mutants could be identified both in R3 and R4 generations. The complete loss of *L. japonicus NUP160* might be lethal, however, multiple *A. thaliana nup160* SALK lines were previously reported to be viable (Dong et al., 2006; Parry et al., 2006; Wiermer et al., 2012).

9.2.4. Are CASTOR and POLLUX the targets that affect symbiotic signaling in *L. japonicus nup* mutants?

CASTOR and POLLUX are ion channels required for symbiotic calcium spiking (Miwa et al., 2006a; Charpentier et al., 2008). The proteins were originally localized to plastids in heterologous systems (Imaizumi-Anraku et al., 2005), however, immunogold labeling of native CASTOR in *L. japonicus* and fluorescence complementation of CASTOR and POLLUX homocomplexes in *N. benthamiana* demonstrated a localization in the nuclear envelope (Charpentier et al., 2008), consistent with the localization of the POLLUX homolog of *M. truncatula* DMI1 (Riely et al., 2007; Capoen et al., 2011). Based on similar mutant phenotypes and their localization in the nuclear rim, CASTOR and POLLUX were considered as potential targets for the symbiotic defects in the *nup* mutants. INM localization in *N. benthamiana* and complementation data are consistent with the idea of a

defect in INM import of both CASTOR and POLLUX caused by mutations in the NUP107-160 subcomplex.

Custom peptide antibodies against CASTOR and POLLUX were unsuitable for immunogold labeling of the native proteins (chapter 9.1.3), therefore alternative strategies using bimolecular fluorescence complementation were devised to corroborate the subcellular localization to ONM and INM (chapters 9.1.5 and 9.1.6). Fluorescence complementation in *N. benthamiana* using protein fusions to the dimerization domain of the bZIP63 transcription factor (ZIP) suggested that both CASTOR and POLLUX can be targeted to the INM, which is in agreement with their proposed function in nuclear calcium spiking and with the localization of DMI1 both to ONM and INM (Capoen et al., 2011). The unintended nuclear localization of the NES-ZIP construct could be caused by an unidentified cryptic NLS signal or might be due to interaction with other nuclear factors. For instance, bZIP63 strongly interacts with a variety of other bZIP proteins (Ehlert et al., 2006). Prolonged (two days or more) co-expression of CASTOR-ZIP-YFP-N or POLLUX-ZIP-YFP-N in *N. benthamiana* together with NLS-ZIP-YFP-C or NES-ZIP-YFP-C resulted in the appearance of additional signals in the nucleoplasm. As this localization pattern was not observed in the controls co-expressing POLLUX-ZIP-YFP-N/POLLUX-ZIP-YFP-C or CASTOR-ZIP-YFP-N/CASTOR-ZIP-YFP-C, it was likely driven by the truncated bZIP63. The ZIP domain and remaining C-terminus of bZIP63 might translocate and tether excess (and potentially misfolded or truncated) CASTOR-ZIP-YFP-N or POLLUX-ZIP-YFP-N to the nucleus.

The complementation of nodulation in *nup85*, *nup133* and *nen1* by the simultaneous expression of CASTOR and POLLUX under the strong constitutive polyubiquitin promoter is the first direct evidence that symbiotic defects in the *nup* mutants are linked to the ion channels. That CASTOR and POLLUX overexpression can restore RNS suggests an overall or localized reduction of the protein levels in the NPC mutants. A local decrease could be caused by impaired transport of both proteins to the INM. In general, different mechanisms have been reported for trafficking of integral membrane proteins into the INM. According to the diffusion/retention model some proteins reach the INM by passive diffusion along the pore membrane and are retained there by tethering to nuclear components (Soullam and Worman, 1995; Ellenberg et al., 1997; Ostlund et al., 1999; Wu et al., 2002; Malik et al., 2010). Other membrane proteins that carry NLSs are actively transported via binding to the nuclear transport factors karyopherin- α and karyopherin- β 1 (importins) (King et al., 2006; Turgay et al., 2010). This is likely also the case for CASTOR and POLLUX, which contain one or three predicted NLS sequences respectively (Charpentier et al., 2008). INM accumulation of actively transported proteins does not require attachment to nuclear structures, but can be achieved by faster active import compared to slower passive export (Meinema et al., 2011; Meinema et al., 2013). During active import of transmembrane proteins, part of the protein has to pass both through the central NPC channel as well as through the NPC scaffold (Meinema et al., 2011). As this implies a remodeling of nucleoporin connections in order to create an opening, it is

conceivable that structural defects in *nup* mutants can impair localization of nuclear envelope membrane proteins by affecting active import or passive export (Figure 18). A resulting decrease in the levels of CASTOR and POLLUX in the INM could disturb nuclear calcium spiking and prevent symbiotic signal transduction. Elevated expression of CASTOR and POLLUX could allow for a sufficient amount of both proteins to be transported into the INM, thus countering a possible import defect. Overexpression is unlikely to restore wild type levels of the ion channels in either ONM or INM. In fact, visible expression artifacts of POLLUX-YFP and CASTOR-mCherry outside of the nuclear rim (Figure 14), indicated a saturation of the nuclear membrane or of the trafficking pathway. This implies that calcium spiking is not disturbed by an overabundance of CASTOR and POLLUX, but instead requires only a minimum threshold of both proteins in the nuclear membranes. In agreement with this, nodulation in *castor* and *pollux* mutants could previously be restored by expression of the proteins using strong constitutive 35S and polyubiquitin promoters (Charpentier et al., 2008; Venkateshwaran et al., 2012)

Despite the high sequence similarity of the proteins, CASTOR and POLLUX do not function redundantly in symbiosis (Charpentier et al., 2008; Venkateshwaran et al., 2012). As presented here, individual overexpression of CASTOR or POLLUX alone was also insufficient to restore nodulation in *nup85*, *nup133* or *nena*, indicating that both proteins are affected in the mutants. Considering previous complementation experiments, the particular requirements for CASTOR and POLLUX during symbiotic signaling are difficult to reconcile (Charpentier et al., 2008; Venkateshwaran et al., 2012). In *M. truncatula*, the POLLUX homolog DMI1 alone is sufficient for calcium spiking and symbiotic signaling, whereas *M. truncatula* CASTOR is not required. This difference between DMI1 and POLLUX was pinpointed to an amino acid exchange (serine 237 to alanine) in the predicted selectivity filter region, which affects the ion conductance of the channels (Venkateshwaran et al., 2012). By introducing the change to the filter region of POLLUX, the modified channel becomes solosufficient and its expression in *dmi1*, *castor* or *pollux* single as well as *castor/pollux* double mutants restores nodulation. In contrast, expression of modified CASTOR carrying the DMI1 filter region is still not able to complement *dmi1*, *pollux* or *castor/pollux* mutants (Venkateshwaran et al., 2012). This functional inequality of CASTOR and POLLUX could be due to a difference in their subcellular localization. DMI1-GFP immunogold localization indicated a higher abundance of the protein in the INM (Capoen et al., 2011). It is therefore conceivable that a larger fraction of POLLUX is present in the INM compared to CASTOR. However, this explanation alone is probably incomplete, as overexpression of CASTOR should still be able to provide a sufficient amount of the ion channel in the INM. Interestingly, CASTOR expression levels were reduced compared to POLLUX both in the BiFC bZIP assay (chapter 9.1.5) and when CASTOR and POLLUX were co-expressed in transformed roots of *L. japonicus* (chapter 9.1.7). This difference was independent of the promoter (35S or polyubiquitin) or construct (cDNA or genomic). The inability of overexpressed CASTOR

to complement POLLUX could therefore also be due to increased degradation of CASTOR protein.

Ratiometric measurements of ONM and INM levels of CASTOR and POLLUX in *L. japonicus* wild type and *nup* mutants would provide direct evidence for an import defect of the proteins. The determination of ONM levels using the bZIP63 system was obstructed by leaky nuclear localization in the NES-ZIP constructs. To circumvent potential problems and localization artifacts caused by the intrinsic nuclear targeting introduced by bZIP63/ZIP, an alternative BiFC system based on complementation of superfolder GFP1-10 (localized to either nucleus or cytosol) by a GFP11 fragment (Cabantous et al., 2005) was assembled via the Golden Gate Toolkit (Binder et al., 2014). Preliminary constructs for co-expression of GFP11 together with NLS-GFP1-10 or NES-GFP1-10 demonstrated successful complementation that was clearly restricted to nucleus or cytosol respectively. The system will be useful to measure the ratio of CASTOR and POLLUX in INM and ONM and compare these values in wild type and *nup* mutants. The addition of an N-terminal mCherry protein fusion to the GFP1-10 module allows for normalization of expression differences caused by cell to cell variability. Ideally, CASTOR- and POLLUX-GFP11 fusions will be analyzed under the control of their respective native promoters, however, should these be too weak for visualization, a potential import defect should also be detectable in constructs driven by a stronger promoter, such as polyubiquitin.

9.3. Material and methods

9.3.1. Media

All media were autoclaved prior to use. Antibiotics and vitamins were sterile filtered and added after autoclaving to media cooled to at least 60°C.

Bacterial media

LB medium

Bacto Tryptone	10 g
Bacto Yeast Extract	5 g
NaCl	10 g
Bacto Agar (for plates)	15 g
H ₂ O	ad 1 l

TY medium

Bacto Tryptone	5 g
Bacto Yeast Extract	3 g
Bacto Agar (for plates)	15 g
H ₂ O	Ad 1 l

Plant media and solutions

B5 medium

Gamborg's B5 basal salt mixture	3.3 g
Sucrose	20 g
Bacto Agar (for plates)	10 g
H ₂ O	ad 1 l

adjusted to pH 5.5 with HCl

1 ml of B5 vitamin mix (1000x) was added after autoclaving.

1000 x B5 vitamin mixture

m-inositol	100 mg
Pyridoxine HCl	1 g
Nicotinic acid	1 g
Thiamine	10 g
ddH ₂ O	ad 1 l

sterile filtered (0.2 µm filter)

Fahraeus (FP) Medium

CaCl ₂ (40 g/l)	2.5 ml
MgSO ₄ (40 g/l)	3 ml
KH ₂ PO ₄ (30 g/l)	3.33 ml
Na ₂ HPO ₄ (44 g/l)	3.33 ml
Ferric citrate (2.5 g/l)	2 ml
Gibson Trace	1 ml
H ₂ O	ad 1 l

Gibson Trace

MnSO ₄	2.03 g
H ₃ BO ₃	2.86 g
ZnSO ₄	220 mg
CuSO ₄	80 mg
H ₂ MoO ₄	80 mg
H ₂ O	ad 1 l

9.3.2. Bacterial strains

Strain	Abbreviation	Reference
<i>Mesorhizobium loti</i> MAFF303099 dsRed	<i>M. loti</i> MAFF dsRed	Maekawa et al., 2009
<i>Agrobacterium tumefaciens</i> AGL1	<i>A. tumefaciens</i> AGL1	Gerard et al., 1991
<i>Agrobacterium rhizogenes</i> AR1193	<i>A. rhizogenes</i> AR1193	Stougaard et al., 1987
<i>Escherichia Coli</i> TOP10	<i>E. coli</i> TOP10	Invitrogen
<i>Escherichia Coli</i> DB3.1	<i>E. coli</i> DB3.1	Invitrogen

9.3.3. Plant lines

Plant species	Abbreviation
<i>Lotus japonicus</i> ecotype 'Miyakojima' MG-20	<i>L. japonicus</i> MG20 / MG20
<i>Lotus japonicus</i> ecotype "Gifu" B-129	<i>L. japonicus</i> Gifu / Gifu
<i>Nicotiana benthamiana</i>	<i>N. benthamiana</i>
<i>Arabidopsis thaliana</i>	<i>A. thaliana</i>

9.3.4. *Lotus japonicus* mutant alleles and transgenic lines

Allele	Mutation	Reference
<i>castor-12</i>	W ₉₃ to stop	Imaizumi-Anraku et al., 2005
<i>pollux-5</i>	W ₃₂₀ to stop	Imaizumi-Anraku et al., 2005
<i>nup133-1</i>	frame shift	Schauser et al., 1998; Kanamori et al., 2006
<i>nup85-1</i>	W ₃₀₆ to stop	Saito et al., 2007
<i>nen-1</i>	Q ₉₇ to stop	Groth et al., 2010
<i>nup107-1</i>	LORE1 insertion (between bases 12 and 13 from ATG)	this work
NLS-YC3.6	<i>L. japonicus</i> Gifu line expressing NLS-YC3.6 calcium sensor	Krebs et al., 2012
NES-YC3.6	<i>L. japonicus</i> MG20 line expressing NES-YC3.6 calcium sensor	Krebs et al., 2012

9.3.5. Oligonucleotides

Primers were designed using the Primer3Plus web interface (Untergasser et al., 2012; www.primer3plus.com). Typically primers were designed with a desired melting temperature from 57°C to 63°C, with an optimum of 60°C to the initial template (excluding possible overhang sequences).

Table 4: List of oligonucleotide primers.

Primer	Name	Sequence (5' → 3')
P003	bZIP_Z_Fw	Pho-CACTTGAGTGAGCTAGAGACACAA
P004	bZIP_noSTOP_Rw	Pho-CTGATCCCCAACGCTTCG
P006	SpyNC_RV	Pho-CCCGGGAGCGGTACC
P008	HA_Fw	Pho-GGCAGCATGTACCCATACGATGTTCCAG
P015	Cas_Start_Topo_FW	CACCATGTCCTTGGATTTCGGAGGT
P016	Pol_Start_Topo_FW	CACCATGATACCACTACCAGTAGCAGCA
P017	bzip_noStopII_RV	CTGATCCCCAACGCTTCG
P018	bzip_NZ_Start_Topo_FW	CACCATGAGACGGTCCAGAAGAAGAAAGC
P019	Nup133-1_CAPs_FW	TTCTGGCATTTCATCGAACAG
P020	Nup133-1_CAPs_RV	TTTGACCAGCCAGATCCTTC
P022	Nup85-1_dCAP_Rv	GAAAATGAGAAACATACTCAATCC
P023	Nup85-1_dCAP_II_FW	TAAGGTGTTGTTTGTCTTATTTTTATAGCCATG
P042	NES_BSA_FW	GGGGTCTCACACCATGCTGCAGAACGAGCTTGC
P043	NES_BSA_RV	GGGGTCTCATGGGTGGCGGCCGCACT
P044	Bzip_BSA_Fw	GGGGTCTCACCCACTTGAGTGAGCTAGAGACACAA
P045	Bzip_Mut1_RV	GGGGTCTCAAGCCCCTTCATGAGTTTTGAAT
P046	Bzip_Mut2_FW	GGGGTCTCAGGCTCACTGATGTAACTCAAACA
P047	Bzip_BSA_Rv	GGGGTCTCACCTTCTGATCCCCAACGCTTCG
P122	Cas 1+	ATGAAGACTTTACGGGTCTCACACCATGTCCTTGGATT CGGAGGT
P123	Cas 2-	ATGAAGACTTGCCAAATTGCGAGAGCCAGT
P132	Cas 2+ II	ATGAAGACTTTGGCCTCCAGTTTGCCCTTG
P151	Cas 2b-	TAGAAGACAATTCGGAGCTGGCATGATTAC
P152	Cas 2b+	TAGAAGACAACGAAGGTATTGGTCCAAGGT
P133	Cas 3- II	ATGAAGACTTTGTCTCTCTTAAGCAAAGGTGGAATATTC
P134	Cas 3+ II	ATGAAGACTTGACAATTTGGCTATTATGTTTTAAATAATC
P154	Cas 3b-	TAGAAGACAACCTCGACTTTGTTAGCTTTACTACTTTTTTC
P153	Cas 3b+	TAGAAGACAACGAGCATTATATTGAGGATGG
P135	Cas 4- II	ATGAAGACTTCTACCTTTCTCTTGGTGTAATCTGGATC
P128	Cas 4+	ATGAAGACTTGTAGACCATAATAGTGTTGACTTTTTGC
P129	Cas 5-	ATGAAGACTTTACACGAGCATCGCAAAGG
P130	Cas 5+	ATGAAGACTTTGTATTCACATTATATCTGAGGCATTG
P131	Cas 6-	ATGAAGACTTCAGAGGTCTCACCTTTTCCTTTTCAGTAA TCACCACAA
P093	Pol 1+	ATGAAGACTTTACGGGTCTCACACCATGATACCACTAC CAGTAGCAGCA
P094	Pol 2-	ATGAAGACTTAGTTTTCTTCAATGGTGGCTTG
P095	Pol 2+	ATGAAGACTTAACCTAAGACCCTACTTCCACCACC
P096	Pol 3-	ATGAAGACTTGGAGACAATAACACAAATCATAGATATAA GA
P097	Pol 3+	ATGAAGACTTAGGCCCTCCTCCGTCAAA
P098	Pol 4-	ATGAAGACTTGATACGACCCTCTGCCCG
P099	Pol 4+	ATGAAGACTTTATCTGTCTCAATTAGTTCAGGTGG
P100	Pol 5-	ATGAAGACTTCTGCAAGAGTGCAAAATTCAG
P101	Pol 5+	ATGAAGACTTGCAGACTGTATTTGAAATAGAATT
P102	Pol 6-	ATGAAGACTTGTAGACTCTCTAGGTGCCGCC
P103	Pol 6+	ATGAAGACTTCTACCATTGGAGACTTTTTGATTCC

P104	Pol 7-	ATGAAGACTTCAGAGGTCTCACCTTATCGCCTGAAGCA ATTACAA
P221	Nup96-1 +	TTCAGCCGCCTTGTTAAGCCCCTC
P222	Nup96-1 -	ACCGATAGTGCTTCTGCTCCGCC
P223	Nup107-1 + b	CCACCACCATTCAATCGCCCATTT
P224	Nup107-1 - b	TGCAGTAAACCCAATACCCATGATGTGA
P225	Nup107-1 +	TTCACGGTAAACGCAAGATG
P226	Nup107-1 -	TGGGTAATGGAATGGAGGAG
P227	Nup160-1 +	TCGCGTTCATCTGCAAAAACGAGG
P228	Nup160-1 -	TCCAGCTTCATCTCTCAGCTCATGCAA
P229	Nup160-2 + b	TCAAGGGGTGAGGATTGCATGTGG
P230	Nup160-2 - b	TGCGTTGTTCTTGACACCAGTTATGGA
P231	Nup160-2 +	CCAGGGGTTTCATCTTAATGC
P232	Nup160-2 -	CCTTTTTTCAGTCCATCAGCAG
P252	P2 (LORE1)	CCATGGCGGTTCCGTGAATCTTAGG

pho = 5' phosphorylation

9.3.6. Bacterial growth conditions

E. coli was grown at constant 37 °C in LB medium overnight unless stated otherwise. *Agrobacterium* strains were grown at 28 °C for 1-2 days in LB medium, *Mesorhizobium loti* strains were grown at 28 °C for 2 to 4 days in TY medium. Liquid cultures were shaken at 200 rpm.

9.3.7. Plant germination and growth

L. japonicus seeds were scarified with sandpaper, sterilized with 2% NaOCl containing 0.1% sodium dodecylsulfate, washed and incubated for at least 6 hours or overnight in sterile water. If not specified otherwise the plants were grown at 24°C in a 16 h light / 8 h dark cycle.

9.3.8. Transformation of *E. coli* cells

Chemically competent *E. coli* TOP10 or DB3.1 cells frozen at -80°C in 15% glycerol were provided by Karl Heinz Braun or Petra Winterholler. Cells were thawed on ice for 2 minutes and 20-50 µl of the suspension was added to a 1.5 ml microliter tube. 1-5 µl of plasmid DNA or ligation reaction were added and mixed by gentle pipetting. The reaction was incubated on ice for 5 minutes, and then a heat shock of 42°C was applied for 30 seconds. The tubes were immediately returned to ice and 200 µl of LB medium was added. After incubation at 37°C on a shaker (200 rpm) for 30 min to 1 h, 50-200 µl of the suspension was plated on LB plates containing the appropriate antibiotics and incubated overnight at 37°C. Successful transformations were screened by colony PCR and/or following plasmid extraction by restriction digestions and sequencing.

9.3.9. Transformation of *Agrobacterium* cells

Electrocompetent *A. rhizogenes* AR1193 or *A. tumefaciens* AGL1 cells frozen at -80°C in 10% glycerol were provided by Karl Heinz Braun, Petra Winterholler or Jessica Folgmann. The cells were thawed on ice for 2 minutes and mixed together in chilled 1.5 ml microliter tubes with 1-2 µl of plasmid DNA (10-50 ng) by gentle pipetting. The mixed suspension

was pipetted into chilled electroporation cuvettes. For electroporation the following settings were used: Voltage 1.2 kV, conductance = 25/25/125 Fd; resistance = 200 Ω . After triggering the pulse, the cells were immediately transferred to 1.5 ml microliter tubes containing 500 μ l of LB medium. Cells were incubated at 28°C for 1 hour and 20-100 μ l were plated on LB plates containing the appropriate antibiotics. Successful transformations were screened by colony PCR.

9.3.10. *N. benthamiana* transformation

Transformation of *N. benthamiana* leaves was done as previously described (Voinnet et al., 2003) with *A. tumefaciens* strain AGL1 carrying the respective constructs.

9.3.11. Hairy root transformation

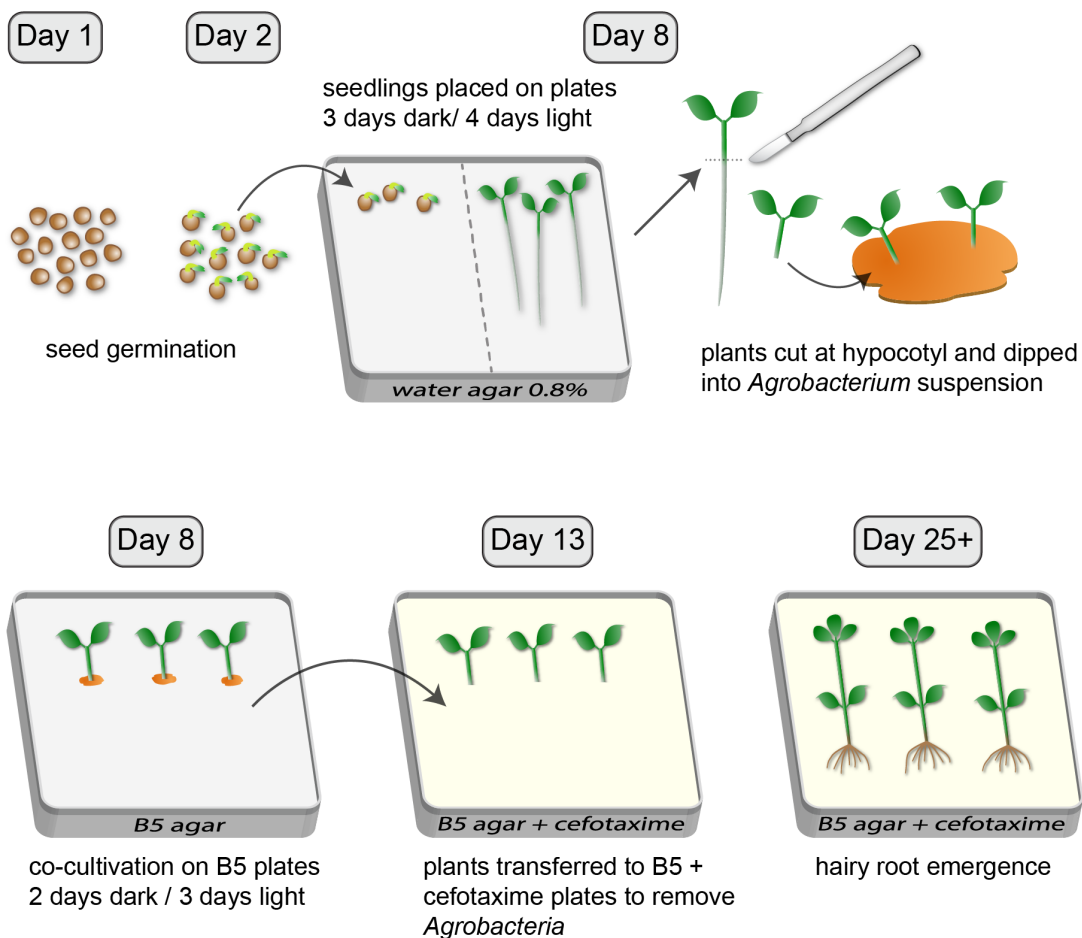


Figure 16: Hairy root transformation

Following germination *L. japonicus* seedlings were grown on 0.8% bacto agar plates for 3 days in the dark and 4 days in the light at 24 °C prior to transformation. *A. rhizogenes* AR1193 carrying the LIII plasmids were precultivated on agar plates containing the appropriate antibiotics for 2-3 days until densely grown. Bacteria from a single plate were scraped off and dissolved in 1 ml of LB medium of which 200 μ l each was plated on fresh LB plates (with appropriate antibiotics) and grown for 1 to 1.5 days more.

For hairy root transformation the bacteria were scraped off the LB plates onto a Petri dish and diluted in 500 µl of sterile water. The roots were cut at the hypocotyls with a scalpel that was covered with bacterial suspension (Figure 16). The wound was shortly dipped into the bacteria and the plants were placed on agar plates containing B5 medium. The plates were covered with aluminum foil and co-cultivated in a dark room at approximately 20 °C. After 2 days the aluminum foil was partly removed (two thirds of the bottom of the plates was still covered to limit light exposure of the roots) and the plants were incubated for 3 days in 16 h light/8 h dark condition at 24°C in a growth chamber. The plants were transferred to B5 plates containing Cefotaxime (333 µg/ml) in order to halt the growth of the *Agrobacteria*. The plants were then cultivated at 24 °C in 16 h light/8 h dark conditions until emergence of hairy roots (2 to 3 weeks).

9.3.12. Nodulation assay

L. japonicus plants were inoculated with *Mesorhizobium loti* MAFF303099 expressing dsRed (Maekawa et al., 2009). The bacteria were inoculated from a preculture plate and grown in 50 ml liquid TY medium containing 10 µg/ml gentamycin for 3 to 4 days. The liquid cultures were centrifuged for 10 minutes at 3000 g, washed with 30 ml H₂O, centrifuged again for 10 minutes at 3000 g, then suspended in 10 ml FP medium. OD₆₀₀ was measured and the suspension was diluted in FP medium to an OD₆₀₀ of 0.02.

For nodulation tests of *L. japonicus* LORE1 insertion lines (segregating R3 and R4 generation), plants were germinated and grown on 0.8% H₂O agar plates for 1 week at 18°C then transferred to “96 well pots”, watered with 10 ml FP medium each and grown for five weeks at 18°C (during which time genomic DNA was extracted from 3 small leaves each). Each plant was inoculated with 5 ml of *M. loti* MAFF303099 dsRED diluted in FP medium (OD₆₀₀ of 0.02) and grown again at 18°C. Nodulation was quantified four weeks after inoculation.

For nodulation of transformed *L. japonicus* hairy roots, plants were transferred the B5 agar plates into closed sterile glass jars (WECK) containing 300 g of sand/vermiculite (1:1) supplemented with 60 ml FP medium (15-20 plants per jar). The plants were grown in the jars for two weeks at 24°C, and then inoculated evenly with 30 ml of *M. loti* MAFF303099 dsRED (OD₆₀₀ of 0.02). Nodulation was assayed four weeks later.

9.3.13. Crossing

L. japonicus flowers in the right stage (contain ripe anthers with unreleased pollen and a straight style) were selected and carefully emasculated by removing petals and anthers with forceps, without releasing the pollen. Pollen was harvested from the donor plant and released onto the thumb nail. The stigma of the emasculated flower was gently pressed into the pollen. The flower was covered with a plastic tube, which was stuffed with slightly moist cotton at the bottom for protection and to prevent cross-pollination.

9.3.14. Extraction of genomic plant DNA

From each *L. japonicus* plant young leaves (5-20 mg) were collected in a 96 well plate containing tungsten beads. 300 µl of 65 °C preheated DNA extraction buffer (200 mM Tris

base, 250 mM NaCl, 25 mM Na₂-EDTA, 0.5% SDS, pH to 7.4 with HCl) was added to each well. The samples were homogenized using a Qiagen TissueLyser (2 x 2 min at 30 Hz, plates were inverted after 2 min). The plates were centrifuged shortly, placed between metal binders (to prevent the lids from opening) and incubated at 65 °C for 30 minutes in a water bath. Following incubation the samples were chilled on ice for 5 minutes. 140 µl of potassium acetate solution was added. After mixing, the plates were incubated for 15 minutes on ice and then centrifuged at 5650 rpm (Sorvall 75006444, HIGHplate rotor) for 15 minutes at 4 °C. 320 µl of the supernatant from each sample was added to a new 96 well plate containing 255 µl isopropanol per well. The plates were inverted several times and stored at -20 °C for at least 2 hours to permit precipitation of the DNA. After defrosting for 5 minutes, the plates were centrifuged at 5650 rpm for 1 h at 4 °C. The supernatant was discarded. To remove salt 400 µl 70% ethanol was added. The plates were gently vortexed and centrifuged for 30 minutes at 5650 rpm. The supernatant was discarded and the samples were air dried to permit the evaporation of the remaining ethanol. The DNA was suspended in 50 µl TE buffer overnight at 4 °C.

9.3.15. Plant genotyping

Following DNA extraction, *L. japonicus nup85* and *nup133* crosses and their progeny were genotyped either by CAPs/dCAPs analysis or via the KASP system (LGC genomics). CAPs/dCAPs PCR was performed using 10-50 ng of genomic *L. japonicus* DNA as a template, with primers P22/P23 (NUP85) and P19/P20 (NUP133). PCR products were digested with restriction enzymes NcoI-HF (NUP85) and RsaI (NUP133) and the products were separated on a 3% agarose gel. In case of NUP85, the wild type allele resulted in two bands of 30 bp and 177 bp and the *nup85-1* allele in a single band of 207 bp. In case of NUP133, the wild type allele showed two bands at 92 bp and 198 bp and the *nup133-1* a single band at 290 bp. KASP genotyping PCR was performed according to the manufacturer's instructions in a CFX96™ Real-Time PCR Detection System (Bio-Rad) with specific primer sets for discrimination of wild type and *nup85/nup133* mutant alleles. Data were analyzed and visualized with the allelic discrimination option of the CFX96 software (Bio-Rad). KASP primers were designed by LGC genomics. Successful crosses and identified double mutants were confirmed by sequencing.

Genomic DNA extracts of segregating *nup96-1*, *nup107-1*, *nup160-1* and *nup160-2* LORE1 individuals were genotyped by PCR using flanking forward and reverse primers that bind to the respective genomic sequence as well as a LORE1 specific reverse primer (P252). One PCR with the flanking primers identified the wild type allele, while a second PCR using the forward flanking primer together with the reverse LORE1 specific primer identified the presence of the mutant allele containing the retrotransposon (Figure 17). Flanking primer pairs used for genotyping of *nup96-1* were P221/P222, for *nup107-1* P223/P224 or P225/P226, for *nup160-1* P227/P228, and for *nup160-2* P229/P230 or P231/P232.

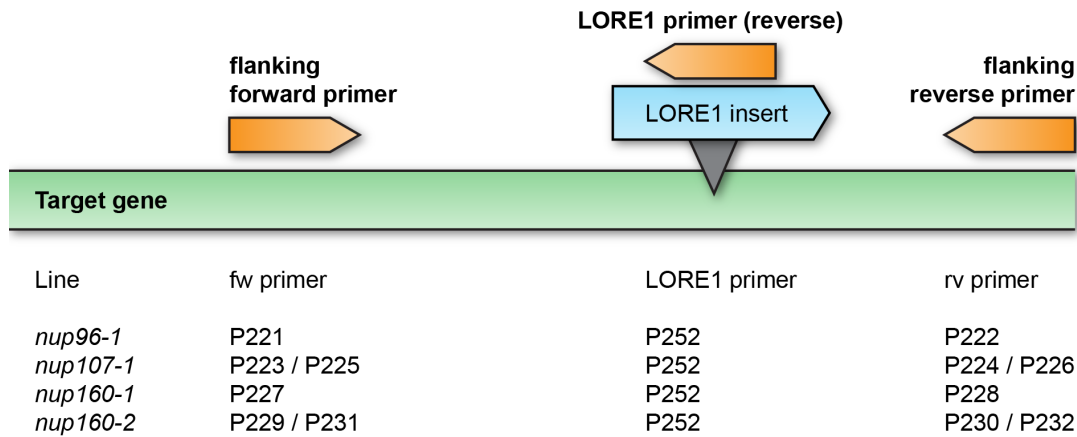


Figure 17: Primers for genotyping of LORE1 insertion lines. Wild type alleles were identified by a PCR using the flanking forward (fw) and reverse (rv) primers. LORE1 alleles were identified by using the fw flanking primer together with a rv LORE1 specific primer (P252).

9.3.16. Polymerase-chain reaction

Amplification of DNA fragments for cloning purposes was performed using Phusion high fidelity polymerase (NEB) in either HF or GC buffer. PCRs for genotyping and colony screening were performed using Taq polymerase in standard buffer (NEB).

9.3.17. Sequencing

DNA sequence analysis was performed by the “Sequencing Service of the Faculty of Biology” with an ABI3730 48 capillary sequencer (Applied Biosystems) using Big Dye Terminator 3.1. Sequencing runs were set up according to the “cycle, clean & run” protocol with 100 – 500 ng of plasmid DNA and 3.2 pmol of sequencing primer in a total volume of 7 µl.

9.3.18. Plasmid isolation

Plasmid DNA was isolated from 2 ml of overnight cultures of *E.coli* grown at 37°C using the GeneJET Plasmid Miniprep Kit (Thermo Scientific) according to the manufacturer’s instructions.

9.3.19. Molecular Cloning

CASTOR and POLLUX BiFC localization constructs

Plasmids *CASTOR*:YFPCE/:YFPNE and *POLLUX*:YFPCE/:YFPNE (Charpentier et al., 2008), which contained the cDNA sequence of *CASTOR* and *POLLUX* fused to sequences coding for C- and N-terminal parts of YFP, were amplified with primers P6 and P8 (whole vector amplification). The sequence of the C-terminal part of *bZIP63* coding for the dimerization domain (ZIP; aa 140-314 of bZIP63) was amplified from bZIP63-YFP^N (Walter et al., 2004) with primers P3 and P4. Both PCR fragments were fused by blunt end ligation using T4 ligase (NEB). Among the resulting plasmids, those that contained the *bZIP63* fragment fused to *CASTOR/POLLUX* in the correct orientation were selected. As initial tests did not show YFP complementation with either construct containing *CASTOR* or *POLLUX* (data not shown), new constructs under a stronger 2x35S promoter in a different plasmid background (pAM-PAT-35SS-YFPⁿ and pAM-PAT-35SS; Lefebvre et al.,

2010) were constructed. For that, the *CASTOR-ZIP* fusion construct was again amplified with P15 and P17 and the *POLLUX-ZIP* fusion construct with P16 and P17. Additionally, the sequence coding for the C-terminal part of *bZIP63* containing NLS and dimerization domain (NLS-ZIP; aa 131-314 of *bZIP63*) was amplified with primers P18 and P17 from template *bZIP63-YFP^N* (Walter et al., 2004). The PCR fragments were inserted into pENTR/D-TOPO via TOPO cloning (Life Technologies) according to the manufacturer's instructions, resulting in entry vectors pENTR-CASTOR-ZIP, pENTR-POLLUX-ZIP and pENTR-NLS-ZIP. Additionally, the entry vector pENTR-NES-ZIP, which contained the coding sequence of the *bZIP63* dimerization domain with an N-terminal NES fusion (and no more NLS), was constructed by *BsaI* cut-ligation from the following 3 PCR fragments into the vector pENTR-*BsaI* (Binder et al., 2014): 1) NES was amplified from template NES-YC3.6 (Krebs et al., 2012) with primers P42 and P43; 2) *ZIP-part1* was amplified from template *bZIP63-YFP^N* (Walter et al., 2004) with primers P44 and P45 and 3) *ZIP-part2* was also amplified from *bZIP63-YFP^N* (Walter et al., 2004) with primers P46 and P47. Each entry vector was cloned into pAM-PAT-35SS-YFPⁿ and pAM-PAT-35SS-YFP^c (Lefebvre et al., 2010) by LR reaction (Life Technologies) according to the manufacturer's instructions, resulting in the final vectors: CASTOR-ZIP-YFP-N, CASTOR-ZIP-YFP-C, POLLUX-ZIP-YFP-N, POLLUX-ZIP-YFP-C, NLS-ZIP-YFP-N, NLS-ZIP-YFP-C, NES-ZIP-YFP-N, NES-ZIP-YFP-C.

CASTOR and POLLUX genomic complementation constructs

CASTOR and *POLLUX* constructs for *nup* mutant complementation were assembled using the Golden Gate toolkit described in part II of the thesis (for general assembly method and constructs see there). The *CASTOR* and *POLLUX* genomic sequences were amplified from *L. japonicus* Gifu B-129 DNA as multiple fragments in order to remove *BsaI* and *BpiI* sites by introduction of silent mutations. Additionally fragments that could not be amplified were further subdivided into smaller pieces. In total, *CASTOR* was split into 7 fragments, which were amplified with the following primers: 1) P122/P123; 2) P132/P151; 3) P152/P133; 4) P134/P154; 5) P153/P135; 6) P128/P129; 7) P130/P131. *POLLUX* was split into 6 fragments and amplified with the following primers: 1) P93/P94; 2) P95/P96; 3) P97/P98; 4) P99/P100; 5) P101/P102; 6) P103/P104. The fragments were assembled by *BpiI* cut-ligation into the LI+*BpiI* backbone, resulting in the LI constructs LI C-D *CASTOR* and LI C-D *POLLUX*. For generation of expression constructs pUB:*CASTOR* and pUB:*POLLUX*, Level I modules LI C-D *CASTOR* and LI C-D *POLLUX* were first assembled individually into LII F 1-2 backbones by *BsaI* cut-ligation. The LII constructs combined sequences of *CASTOR* or *POLLUX* with the *L. japonicus* polyubiquitin promoter element (G7) and a nos terminator sequence (G6). The final LIII constructs pUB:*CASTOR* and pUB:*POLLUX* were assembled from *CASTOR* and *POLLUX* LII F 1-2 synthetic genes together with a LII R 3-4 element containing a GFP transformation marker under the control of a 35S promoter. For assembly of the binary plasmid pUB:*CASTOR*+*POLLUX*, LI C-D *POLLUX* was first combined with the polyubiquitin promoter (G7), C-terminal YFP tag (G12) and nos terminator (G6) into a LII F 1-2 construct, while *CASTOR* was combined with

polyubiquitin promoter (G7), C-terminal mCherry tag (G25) and HSP terminator (G45) into a LII R 3-4 construct. The resulting LII CASTOR and POLLUX plasmids were then assembled into the LIII binary plasmid pUB:CASTOR+POLLUX by BpiI cut-ligation.

Construction of superfolder GFP based nuclear and cytosolic localization constructs

Superfolder GFP based constructs for localization of INM and ONM proteins were assembled using the Golden Gate toolkit (Binder et al., 2014). Module LI C-D 11GFP (G42) was combined with a polyubiquitin promoter (G7) and a nos terminator (G6) by BsaI cut-ligation into a LII F 1-2 vector. The LII vector was assembled into a LIII binary plasmid using a LII 2-6 dy element by BpiI cut-ligation. NLS-mCherry-GFP1-10 and NES-mCherry-GFP1-10 were assembled by combination of a 35S promoter (G5), a N-terminal NLS (G60) or NES (G61) element, a LI C-D mCherry gene (G57), a C-terminal GFP1-10 element (G76) and a 35S terminator (G59) into a LII F 3-4 vector by BsaI cut-ligation. The LII synthetic gene was in turn assembled with a LII dy 1-3 and a LII dy 4-6 into a LIII binary plasmid by BpiI cut-ligation.

9.3.20. SDS page

For total protein extraction 2 week old *L. japonicus* roots were ground in liquid nitrogen and taken up (100mg/ 200µl) in denaturing extraction buffer (10 mM EDTA, 50 mM HEPES, 150 mM NaCl, 10% Sucrose, 5 M Urea, 2 M Thiourea, 1.5% Triton-X 100, 1% SDS, 2 mM DTT, 1 mM PMSF, Sigma protease inhibitor cocktail). The solution was incubated for 1 hour at 37°C. For extraction of protein from transformed *N. benthamiana* leaves, two leaf discs were frozen in liquid nitrogen in 2 ml microcentrifuge tubes and homogenized in a Quiagen TissueLyser (30 Hz, 2 min) with 2 added tungsten beads, then taken up in 250 µl of extraction & loading buffer (55 mM Tris-HCl pH 6.8, 2% SDS, 17% glycerol, 0.005% bromphenol blue, 3% DTT, 1 mM PMSF, Sigma protease inhibitor cocktail). Constructs used for *N. benthamiana* transformation were the following: Plasmids p35S:CASTOR and p35S:POLLUX were obtained from Myriam Charpentier (Charpentier et al., 2008), plasmids p35S:NUP85-GFP and p35S:NUP133-GFP from Martin Groth (Groth et al., 2010). Proteins were separated on a polyacrylamide SDS gel and transferred overnight at 4°C and 30V or for 3 h at 30 V and 1 h at 100 V onto a PVDF membrane. Membranes were blocked in 5% skim milk in TBS (+0.1% Tween 20) and incubated overnight at 4°C in the primary antibody diluted in TBS (+3% skim milk and 0.1% Tween 20). Optimal working conditions were determined for primary antibodies (Table 3; see results section). Secondary antibodies were used in the dilutions specified in Table 5. Signals of HRP coupled antibodies were analyzed in a PEQlap Fusion-SL chemiluminescence imaging system. Image acquisition of secondary antibodies coupled to infrared dyes was performed with a LI-COR Odyssey infrared imager using the Odyssey software.

Table 5: Secondary antibodies for SDS page analysis

Secondary Antibody	Conjugate	Dilution
α -guineapig 680 LT (Li-COR)	IRDye 680	1:20000
α -rabbit 680 LT (Li-COR)	IRDye 680	1:20000
α -rabbit HRP	horse radish peroxidase (HRP)	1:20000
α -guineapig HRP	horse radish peroxidase (HRP)	1:25000

9.3.21. Whole-mount immunolocalization

Immunolocalization of *L. japonicus* root tissue was performed as described in Binder and Parniske, 2014.

9.3.22. Microscopy

Confocal laser scanning microscopy was performed with a Leica SP5 microscope. *N. benthamiana* leaves were vacuum infiltrated prior to imaging and imaged with a HCX PL Fluotar 20x/0.5 PM2 objective. *L. japonicus* whole-mount root samples prepared for immunolocalization were covered with a coverslip and imaged with a Leica HCX PL APO 63x/1.4 oil immersion objective. For image acquisition the resolution was set to 512 x 512 or 1024 x 1024 pixels and the frame average to 4. Using the argon laser at 20% power, GFP was excited with the 488 nm laser line and detected at 500-530 nm, CFP was excited with the 458 nm spectral line and detected at 465-505 nm, YFP with the 514 nm spectral line and detected at 530-550 nm. mCherry was excited with a diode-pumped solid state (DPSS) Laser at 561 nm and detected at 580-620 nm. For multi-color imaging the frame sequential scan mode was used. Images of *L. japonicus* root systems were taken using a Leica M165 FC epifluorescence stereomicroscope equipped with a GFP and RFP filter

9.3.23. Calcium imaging

L. japonicus plants stably expressing NES-YC3.6 and NLS-YC3.6 constructs were generated by *Agrobacterium* mediated transformation as described in Kato et al. (2005) with the following minor modifications: Plates were made with 0.6% Gelrite (Carl, Roth) instead of phytagel and the antibiotic claforan was replaced by cefotaxime (Hexal AG). NLS-YC3.6 *L. japonicus* plants were crossed to *nup85-1* and *nup133-1* mutants. From among the segregating F2 individuals, homozygous mutants that showed NLS-YC3.6 reporter expression were selected and propagated. For calcium measurements wild type NLS-YC3.6 and NES-YC3.6 plants as well as *nup85-1* and *nup133-1* plants expressing NLS-YC3.6 were grown on filter paper on 0.8% bacto agar plates for six days (24°C, 16h light / 8 h dark). The plants were transferred to 0.8% Gelrite (Carl Roth) plates with ½ strength B&D medium (Broughton and Dilworth, 1971) supplemented with 2 mM MgSO₄ and 0.1 µg AVG [l- α -(2-aminoethoxyvinyl)-glycine; Sigma-Aldrich]. The roots were covered with a gas permeable plastic membrane (lumox® Film 25; Sarstedt) and the plants were grown for a minimum of 4 more days. FRET-based calcium imaging was performed with an upright Leica SP5 confocal laser scanning microscope using either a Leica HCX APO L40/0.80 W U-V-1 or a Leica HCX IRAPO L 25x/0.95 W objective. During culturing and microscopy the seedlings were constantly kept under a gas permeable plastic film (lumox® Film). Either 10⁻⁸ M - 10⁻⁷ M NF or 10⁻⁷ M - 10⁻⁶ M chitin tetramer, both diluted in

water, were applied directly onto the roots below the plastic film. For measuring calcium oscillations, resolution was set to 512 x 512 pixels, pinhole to a Z volume corresponding to 10 μm , scanning speed to 700 Hz, line average to 2 and an image was collected every 1.5 sec. FRET-based cpVenus/ECFP ratio shifts were measured by exciting the cameleon sensor with the 458 line of the Argon laser at 10% - 15% laser power and measuring the emission simultaneously at around 470–500 nm for ECFP and 530–580 nm for cpVenus. cpVenus and ECFP intensity values were measured for a defined ROI and the background fluorescence in a region outside of the root was subtracted. Calcium spiking traces were calculated and generated in Microsoft Excel.

10. General Discussion

10.1. Analysis of symbiotic signaling and flexible construct adaptation via Golden Gate cloning

Golden Gate (GG) assembly provides an efficient and reliable way to ligate multiple DNA fragments in one single reaction (Engler et al., 2008). The GG toolkit presented here serves as a flexible framework for the generation of modular synthetic gene constructs. With the available modules, such as promoters, fluorescent markers, peptide tags and localization signals, constructs for many routine applications can be assembled out of the box. The primary goal of the toolkit was to simplify the creation of binary plasmids for co-expression analysis in plants. Proof of principle experiments demonstrated the successful construction and expression of multigene constructs in different plant systems as well as efficient gene silencing and complementation (Binder et al., 2014).

As a practical application, the GG system was used to study the function of the NPC in symbiotic signaling, by creating genomic *CASTOR* and *POLLUX* constructs (chapter 9.1.7) as well as a custom superfolder GFP based localization system for nuclear/INM and cytosolic/ONM proteins (chapter 9.1.6). Genomic DNA constructs containing both exon and intron sequences are generally preferable over cDNA constructs, as these can fail to reproduce native gene function, due to a lowered expression rate, altered gene regulation or the absence of alternative splice forms (Morello et al., 2011; Parra et al., 2011; Kalyna et al., 2012; Syed et al., 2012). In the past, alternative splicing (AS) was assumed to be fairly rare in plants, but recent estimates suggest that at least 60% of the genes in *A. thaliana* are subject to AS (Syed et al., 2012). Assembly of constructs containing multiple large genomic sequences can be difficult with classical and recombination based cloning techniques. Even cloning of single genomic constructs is often challenging, as regions spanning several large introns can be problematic to amplify in a single PCR reaction. GG cloning of genomic *CASTOR* and *POLLUX* sequences was facilitated by amplification of smaller sub-parts of the genes (L0 fragments), which could be efficiently assembled via BpiI cut-ligation without introducing additional sequences. The use of sub-fragments facilitates the removal of type IIS restriction sites and also circumvents amplification problems of larger sequences. Once individual LI modules were created, GG assembly of binary plasmids containing either the single genes or both *CASTOR* and *POLLUX* was straightforward. Additionally, other potential target genes (for instance the sequence of the calcium pump *MCA8*) could have been included into a binary plasmid without much effort.

The modular nature of the GG system allows for easy optimization of constructs. This is illustrated in the cloning of the two BiFC based system for the determination of INM and ONM protein levels (chapters 9.1.5 and 9.1.6). The assay based on bZIP63 was constructed by classical and GATEWAY based cloning, and required laborious and time consuming re-amplification and re-cloning into different vector backbones in order to exchange an initial weaker promoter for a 2x35S promoter. In contrast, construction of the superfolder GFP based localization assay was purely based on GG assembly using standard toolkit

modules. The constructs could therefore be easily adapted to include an additional mCherry as a normalization control, requiring only one additional cloning step. Future alterations, such as an exchange of the promoters will also be straightforward to perform. One disadvantage of the GG construction method is the requirement to remove type IIS restriction sites, as these diminish the assembly efficiency. Genes with a very high number of type IIS restriction sites can therefore be more difficult to integrate into the system. However, by using mutagenesis PCR in combination with partial gene synthesis, even unfavorable target sequences can be freed of type IIS sites with reasonable effort and cost. A long term goal in symbiosis research has been the creation of non-legume nitrogen fixing crop plants, such as cereals (Rogers and Oldroyd, 2014). Challenges like these require co-expression of multiple genes and frequent construct adaptations and will therefore greatly benefit from modular multigene assembly.

10.2. A window into the NPC - Study of *L. japonicus* NUP107-160 subcomplex mutants

Phenotypes correlated with the loss or knock-down of NUP107-160 components are surprisingly diverse depending on the organism and respective NUP (González-Aguilera and Askjaer, 2012; Binder and Parniske, 2013) and the mechanisms underlying many of the defects are not clearly understood. The analysis of *L. japonicus* NUP107-160 subcomplex mutants was conducted to decipher their role in symbiosis and to better understand how the mutations affect the plant NPC.

Unlike highly redundant FG-nucleoporins of the central channel (Strawn et al., 2004; Frey and Gorlich, 2007), structural NUPs of the NUP107-160 complex are considered to be non-interchangeable and have been linked with specific functions (Boehmer et al., 2008; González-Aguilera and Askjaer, 2012). In light of the phenotypes in *L. japonicus*, this view has to be somewhat relativized. The study of *nup85*, *nup133*, *nen/seh1* and *nup107* mutants indicates inherent redundancy also in the composition of the NUP107-160 subcomplex. The *nup* mutants share very similar phenotypes primarily related to symbiosis, suggesting that the NUP107-160 complex is in part functionally compromised. Quantitative immunoblots indicated that the loss of single NUP107-160 members leads to a reduction of other subcomplex constituents (Binder and Parniske, 2014), which was previously also observed in human cells (Boehmer et al., 2003; Harel et al., 2003; Walther et al., 2003; Loiodice et al., 2004; Rasala et al., 2006). Despite these effects, NUP133 localization was not changed in the *nup85-1* mutant background (Binder and Parniske, 2014) and the subcomplex appeared to remain largely functional, as evident by the lack of obvious developmental defects and NPC structural aberrations in the single mutants. Many NUP107-160/NUP84 subcomplex NUPs share similar structural motives, particularly α -solenoid domains and β -propellers, which are involved in protein-protein interactions (Berke et al., 2004; Brohawn et al., 2009; Kampmann and Blobel, 2009). Redundancy in the NUP107-160 assembly could therefore be achieved via alternate NUP-NUP interactions in the absence of a particular subcomplex member. Alternatively or in

parallel, the NUP107-160 complex could be stabilized by connections to the remaining NPC. Higher order interactions with other parts of the NPC are assumed to be primarily mediated by β -propeller domains, which are exposed towards the NUP107-160 subcomplex border (Kampmann and Blobel, 2009). Copurification of a set of core NUPs (NUP192, NUP188, NUP170, NIC96, NUP159) together with the NUP84 subcomplex in different NUP84 truncation mutants previously suggested that the NUP84 subcomplex is associated with the NPC by multiple relatively weak cooperative interactions (Fernandez-Martinez et al., 2012). These connections occur mostly between the hub and the short arms of the Y-shaped NUP84 complex, but do not map to a single NUP. The sum of the interactions might retain the bulk of the NUP84/NUP107-160 structure, even when single subcomplex components and internal connections are lost. At the same time the structure would be more susceptible to stresses, which could explain the temperature sensitivity of many NUP107-160 mutants. A loose analogy for the NPC might be that of a large sturdy warehouse building constructed from copies of different bricks. If one type of scaffold brick is removed, the walls sag a little and a few other bricks, which do not fit properly anymore, might fall out as well, but otherwise the house remains standing. Nevertheless, too much stress, like an earthquake, could bring it crashing down. Moreover, the skewed walls prevents one of the doors from opening properly, so on busy days the delivered cargo starts to pile up in front of the warehouse.

The reduced seed number in *nup85* and *nup133* mutants (Kanamori et al., 2006; Saito et al., 2007) and decreased amount of homozygous *nup85/nup133* (Binder and Parniske, 2014) and *nup107* individuals (chapter 9.1.4) indicated defects in the germline or in seed development. These phenotypes could be related to the role of the NUP107-160 subcomplex outside of the NPC during cell division. In animals the whole subcomplex localizes to kinetochores and spindles during mitosis and mediates kinetochore function and centrosome attachment (Chatel and Fahrenkrog, 2011; Nakano et al., 2011). Early developmental stages leading to seed production appear to be more susceptible than later time points, as single *nup85*, *nup133* and *nena* mutants develop normally once seeds are produced, unlike the *nup85/nup133* double mutants which are also severely affected in growth after germination (Binder and Parniske, 2014).

10.3. Proposed function of the NUP107-160 subcomplex in symbiotic signaling

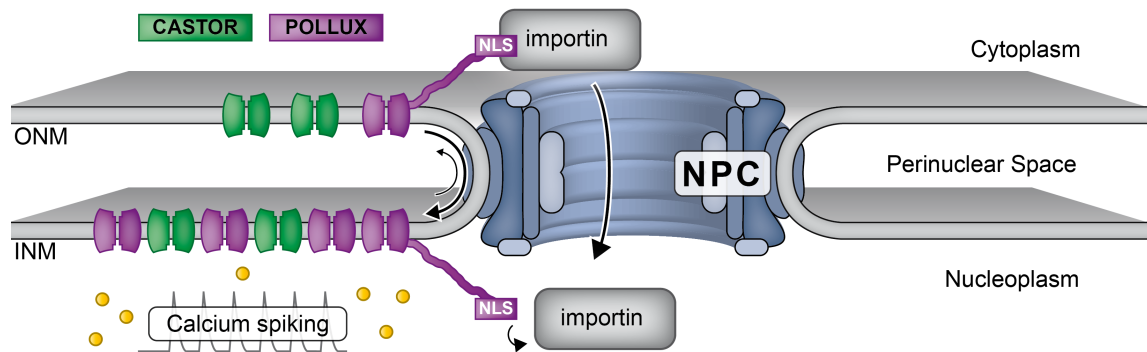
Successful complementation of *nup85*, *nup133* and *nena* mutants (chapter 9.1.7) and INM localization of CASTOR and POLLUX (chapter 9.1.5) provided a strong indication that the symbiotic defects of the NPC scaffold mutants are the result of impaired INM import of CASTOR and POLLUX. In yeast, active transport of transmembrane proteins into the INM depends on long unfolded linker domains (Meinema et al., 2011). Bioinformatic analysis of CASTOR and POLLUX also predicted long highly disordered regions in the N-terminus of both ion channels (Supplementary Figure 1), suggesting that the N-terminal part of the protein is translocated through the NPC scaffold during import. Unstructured

regions between paralogs often show a higher sequence evolution than ordered regions (Siltberg-Liberles et al., 2011) and the N-terminal regions of CASTOR and POLLUX are also the most divergent between the proteins (Imaizumi-Anraku et al., 2005). The predicted unstructured domain of POLLUX is larger (159 aa) than that of CASTOR (87 aa), which might reflect a more efficient INM import of POLLUX. The observed aberrant residual nuclear calcium transients in *nup85* and *nup133* (chapter 9.1.2) are consistent with a disturbance in the calcium spiking machinery caused by a lack of CASTOR and POLLUX in the INM. CASTOR/POLLUX and *M. truncatula* DMI1 are assumed to conduct primarily potassium to balance the calcium release during symbiotic calcium spiking (Charpentier et al., 2008; Venkateshwaran et al., 2012). Mathematical modeling suggested that calcium oscillations require the simultaneous activation of DMI1 and of the calcium channels (Charpentier et al., 2013). According to the model, the potassium current driven by DMI1 is needed to facilitate a stepwise activation of the calcium channels and to sustain calcium oscillations via a positive feedback loop. In the *nup* mutants, both calcium channels and CASTOR/POLLUX are likely still activated via secondary messengers following addition of NF and CO₄. However, an insufficient potassium conductance due to reduced amounts of CASTOR and POLLUX in the INM would prevent sustained nuclear calcium oscillations and only induce the rare single transients or short irregular oscillations, which were observed in *nup85* and *nup133* (chapter 9.1.2).

To date there is no direct evidence that mutations in scaffold NUPs of the NUP107-160 subcomplex can interfere with transport of transmembrane proteins into the INM. Nevertheless, NPC structural data and microscopic analysis are consistent with this scenario. Cryo-electron tomography demonstrated an overall flexible structure of the NPC, which allows for conformational changes during transport of cargo (Beck et al., 2004; Beck et al., 2007). There is also evidence of peripheral channels within the NPC (Hinshaw et al., 1992; Stoffler et al., 2003), which could be involved in the import of INM proteins (Zuleger et al., 2008) and the extended Y shape of the NUP107-160/NUP84 subcomplex suggests a porous rather than dense structure of the scaffold (Boehmer et al., 2008). Moreover, different arrangements of certain NUPs in various crystal forms indicated the potential for dynamic NUP-NUP interaction within the NPC (Melčák et al., 2007; Boehmer et al., 2008; Debler et al., 2008). Active transport of INM proteins by importins implies that part of the transmembrane protein (the unfolded domain) has to pass through the NPC scaffold (Meinema et al., 2011; Figure 18).

Internal connections between NUP107-160 NUPs are largely formed by interaction of α -solenoid folds, which are assumed to provide conformational flexibility for the subcomplex (Kampmann and Blobel, 2009), as demonstrated for α -solenoid domains in COPII coatamers and clathrin triskelia (Fath et al., 2007; Ferguson et al., 2008). In agreement with this, different crystal structures of the NUP85/SEH1 dimer revealed a hinge motion of 35° (Debler et al., 2008). This flexibility might be required to create additional openings to allow unstructured protein domains to pass by during import.

A) *L. japonicus* wt



B) *nup* mutants

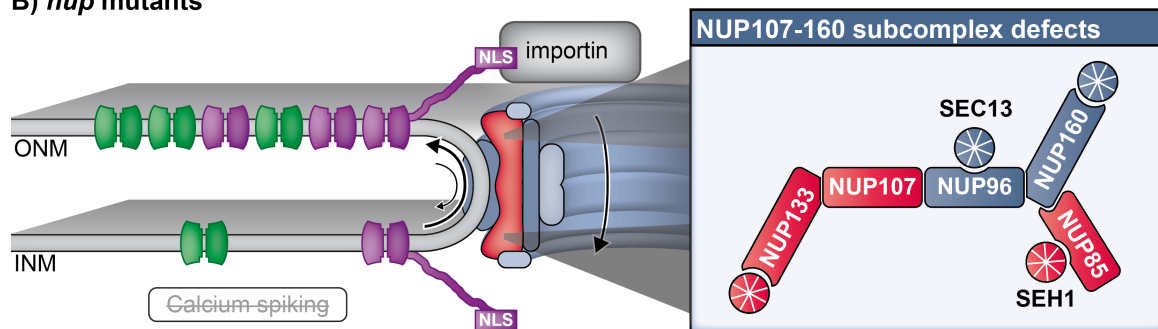


Figure 18: Hypothetical model for the impact of mutations in the NUP107-160 subcomplex on symbiotic signaling. A) Transmembrane ion channels CASTOR and POLLUX are present in the INM and required for nuclear calcium spiking. CASTOR and POLLUX are likely actively transported to the INM via recognition of NLS sequences by importins. During import the predicted disordered N terminal region of CASTOR and POLLUX would be able to pass through the NPC scaffold. B) Mutations in NUP107-160 subcomplex components (NUP133, NUP107, NUP85 or NENA/SEH1) could lead to structural changes in the NPC, which affect active import of membrane proteins into the INM. As a consequence both CASTOR and POLLUX protein levels in the INM would be reduced, thereby preventing symbiotic calcium spiking.

Accordingly, the loss of individual NUP107-160 members, while not preventing assembly of the subcomplex into the NPC, could lower the plasticity of the subcomplex and thus hinder the import of proteins from ONM to INM (Figure 18). Other transmembrane proteins are likely similarly affected in INM import as CASTOR and POLLUX. The symbiotic phenotypes and lack of obvious pleiotropic defects in the mutants would therefore suggest that symbiotic signaling and in particular calcium spiking are more susceptible to changes in INM protein levels compared to other signaling pathways. Alternatively, other phenotypes might be more subtle or dependent on external stimuli or stresses. As both symbiosis and defense signaling are impaired as a result of mutations in the NPC scaffold (Binder and Parniske, 2013), it is tempting to propose a common function of the NUP107-160 complex in plant-microbe signaling. Further work will be necessary to conclude if these defects are mechanistically related. Calcium also acts as an important secondary messenger in plant defense responses (Lecourieux et al., 2006; Poovaiah et al., 2013) and while nuclear calcium signaling in plant immunity is not well understood, defense related elicitors such as flg22, harpin, and cryptogein were shown to

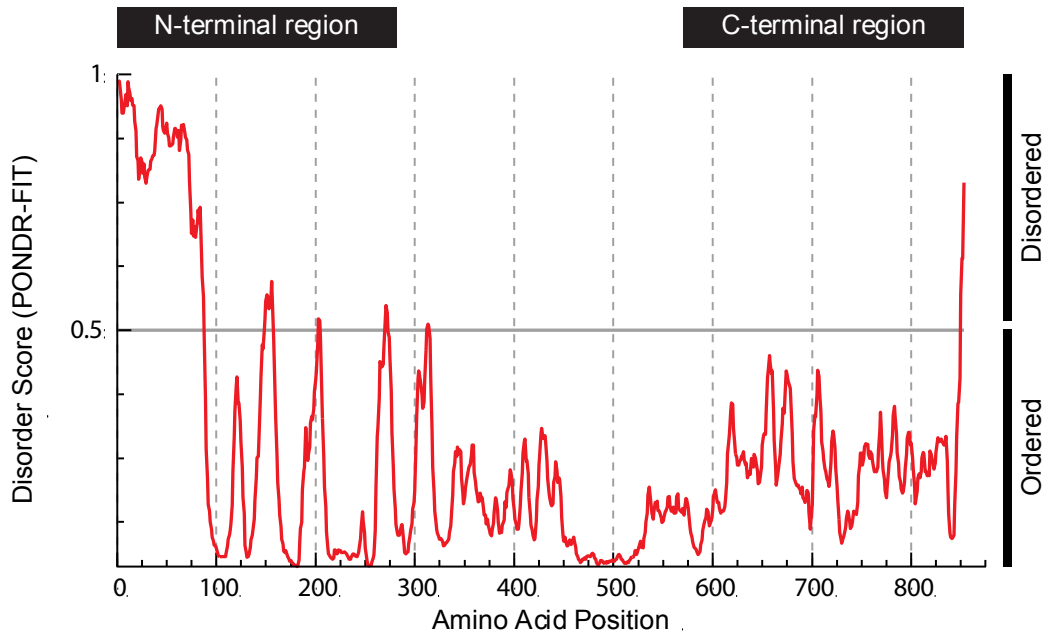
trigger an increase in nuclear calcium levels (Lecourieux et al., 2005). It is therefore conceivable that impaired immunity in *NUP107-160* mutants is also related to nuclear calcium signaling.

Future analyses will be required to confirm that CASTOR and POLLUX protein levels are indeed reduced in the INM. Other nuclear transmembrane proteins of different sizes should be tested to determine the specificity of the proposed import defect. Potential candidates are the calcium ATPase MCA8 (115 kDa), which was previously localized to both ONM and INM (Capoen et al., 2011) as well as the large INM protein (237 kDa) NUA (Xu et al., 2007) and the smaller (50 kDa) INM SUN domain proteins (Graumann et al., 2010).

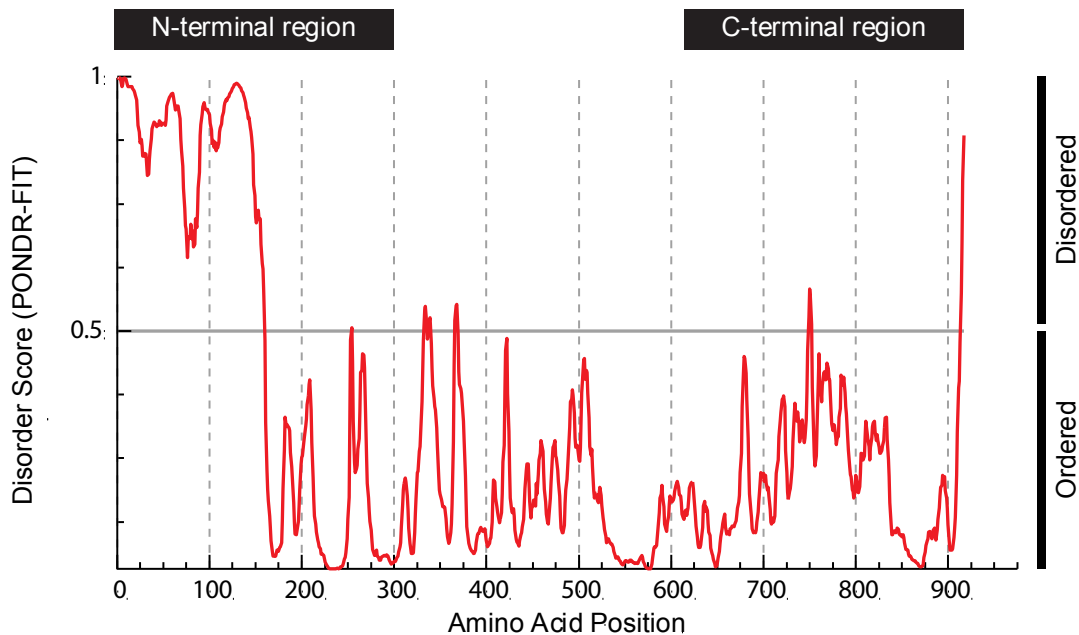
11. Appendix

11.1. Supplementary Figure

A) CASTOR



B) POLLUX



Supplementary Figure 1: Prediction of unstructured regions in CASTOR and POLLUX. The N-terminal part of both CASTOR (aa 1-87) and POLLUX (aa 1-159) is predicted to be highly disordered. Disorder Score was determined using PONDR-FIT (Xue et al., 2010; www.disprot.org/pondr-fit.php)

11.2. List of Figures

Figure 1: Arbuscule development and nutrient provision	10
Figure 2: Establishment of root nodule endosymbiosis.....	12
Figure 3: Symbiotic signal transduction.....	17
Figure 4: The nuclear pore complex in plant-microbe interactions	23
Figure 5: Nod factor induced calcium spiking in <i>L. japonicus</i>	51
Figure 6: Residual calcium signatures in <i>nup85</i> and <i>nup133</i> nuclei	53
Figure 7: SDS page analysis of α -NUP85, α -NUP133, α -CASTOR and α -POLLUX antibodies.....	55
Figure 8: CLSM images of whole-mount immunostained <i>L. japonicus</i> roots	56
Figure 9: Nodulation defects in <i>nup107-1</i> LORE1 insertion mutants	59
Figure 10: CLSM analysis of CASTOR and POLLUX localization in <i>N. benthamiana</i> by BiFC.....	61
Figure 11: Superfolder GFP based complementation for detection of nuclear and cytosolic protein levels	62
Figure 12: Individual overexpression of CASTOR or POLLUX in the <i>nup</i> mutant background does not restore nodulation.....	64
Figure 13: Overexpression of both CASTOR and POLLUX restores nodulation in <i>nup</i> mutant plants.....	65
Figure 14: Localization of POLLUX-YFP and CASTOR-mCherry in <i>L. japonicus</i> roots.....	65
Figure 15: Boxplot showing number of nodules per plant on transformed roots 4 weeks after inoculation	66
Figure 16: Hairy root transformation.....	78
Figure 17: Primers for genotyping of LORE1 insertion lines	81
Figure 18: Hypothetical model for the impact of mutations in the NUP107-160 subcomplex on symbiotic signaling	90

11.3. List of Tables

Table 1: Analysis of calcium oscillations in wild type and nucleoporin mutant nuclei	52
Table 2: Target peptide sequences for antibody production	54
Table 3: Custom antibodies and working dilutions	55
Table 4: List of oligonucleotide primers.....	76
Table 5: Secondary antibodies for SDS page analysis	84

12. Acknowledgements

I am very grateful to my supervisor Martin Parniske for giving me the opportunity to work in his lab. Due to his valuable advice, general support and by providing challenging tasks I was able to learn and profit a lot during the course of my dissertation.

I would also like to thank the reviewers of my thesis for their time and effort to evaluate this work.

I am thankful to all present and former people of the “3rd floor genetics” for providing a generally helpful, cooperative and fun work environment. In particular I want to acknowledge Matthias Ellerbeck, for valuable insights and discussions and his help in unravelling several puzzling cloning problems. Special thanks go to the “Golden Gate team”, Jayne Lambert, Robert Morbitzer and Claudia Popp for their efforts in construction of the cloning toolkit and to Thomas Lahaye and Thomas Ott for their input and feedback. Additionally I want to thank Thomas Lahaye for his support during the end of my thesis. Many thanks go to my “office bench neighbour” Sylvia Singh for always taking the time to discuss problems and help out with advice. I am also grateful to Aline Banhara and Ana Cosme for the help they provided with the *Arabidopsis* plants. Additionally I want to thank Melanie Paul for her diligent and dedicated support during her time as a student helper.

Thanks go to Andreas Brachmann who was my mentor during my diploma thesis and who later could always be relied upon for advice. I am also thankful to Arthur Schüßler for his support with all microcopy related issues and for keeping the confocal microscope running.

Additionally I also want to thank Axel Strauß for his help with statistical analysis, Prof. Gerhard Wanner and Sylvia Dobler for their support with electron microscopy and Dr. Lothar Schermelleh for his help with super resolution microscopy.

Finally I am most grateful to my fiancée Christina for her love and support.

13. Curriculum Vitae

ANDREAS BINDER

Personal Data:

Date of birth: 22nd of March 1982
Place of birth: Ebersberg

Primary and Secondary Education

1988-1992 Grundschole Ebersberg (Primary School)
1992-2001 Gymnasium Grafing (Secondary School)
Degree: Abitur

Civillian Service

Aug. 2001 – Mai 2002 Red Cross Ebersberg

Higher Education

Sep. 2002 – Feb. 2008 Ludwig-Maximilians-University Munich
Study of Biology
Major: Genetics; Minors: Microbiology, Biochemistry
Diploma thesis at the Institute of Genetics under Prof. Dr. Martin Parniske (Grade 1.3)

Apr. 2008 – Nov. 2014 Dissertation at Ludwig-Maximilians-University Munich
at the Institute of Genetics under Prof. Dr. Martin Parniske
(End of practical work in November 2013)
Titel: "Characterization of the *Lotus japonicus* nuclear pore NUP107-160 subcomplex in plant-microbe symbiosis"

14. References

- Akiyama, K., Matsuzaki, K.-I., and Hayashi, H. (2005). Plant sesquiterpenes induce hyphal branching in arbuscular mycorrhizal fungi. *Nature* 435, 824-827.
- Alber, F., Dokudovskaya, S., Veenhoff, L.M., Zhang, W., Kipper, J., Devos, D., Suprpto, A., Karni-Schmidt, O., Williams, R., Chait, B.T., Sali, A., and Rout, M.P. (2007). The molecular architecture of the nuclear pore complex. *Nature* 450, 695-701.
- Andriankaja, A., Boisson-Dernier, A., Frances, L., Sauviac, L., Jauneau, A., Barker, D.G., and De Carvalho-Niebel, F. (2007). AP2-ERF transcription factors mediate Nod factor dependent *Mt ENOD11* activation in root hairs via a novel cis-regulatory motif. *Plant Cell* 19, 2866-2885.
- Ané, J.-M., Kiss, G.B., Riely, B.K., Penmetsa, R.V., Oldroyd, G.E.D., Ayax, C., Lévy, J., Debelle, F., Baek, J.-M., Kalo, P., Rosenberg, C., Roe, B.A., Long, S.R., Dénarié, J., and Cook, D.R. (2004). *Medicago truncatula* *DMI1* required for bacterial and fungal symbioses in legumes. *Science* 303, 1364-1367.
- Antolín-Llovera, M., Ried, M.K., Binder, A., and Parniske, M. (2012). Receptor kinase signaling pathways in plant-microbe interactions. *Annual Review of Phytopathology* 50, 451-473.
- Antolín-Llovera, M., Ried, Martina k., and Parniske, M. (2014). Cleavage of the SYMBIOSIS RECEPTOR-LIKE KINASE ectodomain promotes complex formation with Nod factor receptor 5. *Current Biology* 24, 422-427.
- Balzergue, C., Puech-Pagès, V., Bécard, G., and Rochange, S.F. (2010). The regulation of arbuscular mycorrhizal symbiosis by phosphate in pea involves early and systemic signalling events. *Journal of Experimental Botany*.
- Baptiste, E., Charlebois, R., Macleod, D., and Brochier, C. (2005). The two tempos of nuclear pore complex evolution: highly adapting proteins in an ancient frozen structure. *Genome Biology* 6, R85.
- Bayle, V., Nussaume, L., and Bhat, R.A. (2008). Combination of novel green fluorescent protein mutant TSapphire and DsRed variant mOrange to set up a versatile in planta FRET-FLIM assay. *Plant Physiology* 148, 51-60.
- Beck, M., Förster, F., Ecke, M., Plitzko, J.M., Melchior, F., Gerisch, G., Baumeister, W., and Medalia, O. (2004). Nuclear pore complex structure and dynamics revealed by cryoelectron tomography. *Science* 306, 1387-1390.
- Beck, M., Lucic, V., Forster, F., Baumeister, W., and Medalia, O. (2007). Snapshots of nuclear pore complexes in action captured by cryo-electron tomography. *Nature* 449, 611-615.
- Belgareh, N., Rabut, G., Băi, S.W., Van Overbeek, M., Beaudouin, J., Daigle, N., Zatsepina, O.V., Pasteau, F., Labas, V., Fromont-Racine, M., Ellenberg, J., and Doye, V. (2001). An evolutionarily conserved NPC subcomplex, which redistributes in part to kinetochores in mammalian cells. *The Journal of Cell Biology* 154, 1147-1160.
- Berke, I.C., Boehmer, T., Blobel, G., and Schwartz, T.U. (2004). Structural and functional analysis of Nup133 domains reveals modular building blocks of the nuclear pore complex. *The Journal of Cell Biology* 167, 591-597.
- Besserer, A., Puech-Pagès, V., Kiefer, P., Gomez-Roldan, V., Jauneau, A., Roy, S., Portais, J.-C., Roux, C., Bécard, G., and Séjalon-Delmas, N. (2006). Strigolactones stimulate arbuscular mycorrhizal fungi by activating mitochondria. *PLoS Biology* 4, e226.
- Binder, A., Lambert, J., Morbitzer, R., Popp, C., Ott, T., Lahaye, T., and Parniske, M. (2014). A modular plasmid assembly kit for multigene expression, gene silencing and silencing rescue in plants. *PLoS ONE* 9, e88218.
- Binder, A., and Parniske, M. (2013). "The nuclear pore complex in symbiosis and pathogen defence," in *Annual Plant Reviews*. John Wiley & Sons Ltd), 229-254.
- Binder, A., and Parniske, M. (2014). Analysis of the *Lotus japonicus* nuclear pore NUP107-160 subcomplex reveals pronounced structural plasticity and functional redundancy. *Frontiers in Plant Science* 4.

- Boehmer, T., Enninga, J., Dales, S., Blobel, G., and Zhong, H. (2003). Depletion of a single nucleoporin, Nup107, prevents the assembly of a subset of nucleoporins into the nuclear pore complex. *Proceedings of the National Academy of Sciences, USA* 100, 981-985.
- Boehmer, T., Jeudy, S., Berke, I.C., and Schwartz, T.U. (2008). Structural and functional studies of Nup107/Nup133 interaction and its implications for the architecture of the nuclear pore complex. *Molecular Cell* 30, 721-731.
- Bootman, M.D., Fearnley, C., Smyrnias, I., Macdonald, F., and Roderick, H.L. (2009). An update on nuclear calcium signalling. *Journal of Cell Science* 122, 2337-2350.
- Breullin, F., Schramm, J., Hajirezaei, M., Ahkami, A., Favre, P., Druge, U., Hause, B., Bucher, M., Kretschmar, T., Bossolini, E., Kuhlemeier, C., Martinoia, E., Franken, P., Scholz, U., and Reinhardt, D. (2010). Phosphate systemically inhibits development of arbuscular mycorrhiza in *Petunia hybrida* and represses genes involved in mycorrhizal functioning. *The Plant Journal* 64, 1002-1017.
- Broghammer, A., Krusell, L., Blaise, M., Sauer, J., Sullivan, J.T., Maolanon, N., Vinther, M., Lorentzen, A., Madsen, E.B., Jensen, K.J., Roepstorff, P., Thirup, S., Ronson, C.W., Thygesen, M.B., and Stougaard, J. (2012). Legume receptors perceive the rhizobial lipochitin oligosaccharide signal molecules by direct binding. *Proceedings of the National Academy of Sciences* 109, 13859-13864.
- Brohawn, S.G., Partridge, J.R., Whittle, J.R.R., and Schwartz, T.U. (2009). The nuclear pore complex has entered the atomic age. *Structure* 17, 1156-1168.
- Broughton, W.J., and Dilworth, M.J. (1971). Control of leghaemoglobin synthesis in snake beans. *Biochemical Journal* 125, 1075-1080.
- Bukata, L., Parker, S.L., and D'angelo, M.A. (2013). Nuclear pore complexes in the maintenance of genome integrity. *Current Opinion in Cell Biology* 25, 378-386.
- Bultmann, S., Morbitzer, R., Schmidt, C.S., Thanisch, K., Spada, F., Elsaesser, J., Lahaye, T., and Leonhardt, H. (2012). Targeted transcriptional activation of silent oct4 pluripotency gene by combining designer TALEs and inhibition of epigenetic modifiers. *Nucleic Acids Research*.
- Cabantous, S., Terwilliger, T.C., and Waldo, G.S. (2005). Protein tagging and detection with engineered self-assembling fragments of green fluorescent protein. *Nature Biotechnology* 23, 102-107.
- Capelson, M., Doucet, C., and Hetzer, M.W. (2010). Nuclear pore complexes: guardians of the nuclear genome. *Cold Spring Harbor Symposia on Quantitative Biology* 75, 585-597.
- Capelson, M., and Hetzer, M.W. (2009). The role of nuclear pores in gene regulation, development and disease. *EMBO Rep* 10, 934-934.
- Capoen, W., Sun, J., Wysham, D., Otegui, M.S., Venkateshwaran, M., Hirsch, S., Miwa, H., Downie, J.A., Morris, R.J., Ané, J.-M., and Oldroyd, G.E.D. (2011). Nuclear membranes control symbiotic calcium signaling of legumes. *Proceedings of the National Academy of Sciences, USA* 108, 14348-14353.
- Catoira, R., Galera, C., De Billy, F., Penmetsa, R.V., Journet, E.-P., Maillet, F., Rosenberg, C., Cook, D., Gough, C., and Dénarié, J. (2000). Four genes of *Medicago truncatula* controlling components of a Nod factor transduction pathway. *Plant Cell* 12, 1647-1666.
- Cerri, M.R., Frances, L., Laloum, T., Auriac, M.-C., Niebel, A., Oldroyd, G.E.D., Barker, D.G., Fournier, J., and De Carvalho-Niebel, F. (2012). *Medicago truncatula* ERN transcription factors: regulatory interplay with NSP1/NSP2 GRAS factors and expression dynamics throughout rhizobial infection. *Plant Physiology* 160, 2155-2172.
- Chabaud, M., Genre, A., Sieberer, B.J., Faccio, A., Fournier, J., Novero, M., Barker, D.G., and Bonfante, P. (2011). Arbuscular mycorrhizal hyphopodia and germinated spore exudates trigger Ca²⁺ spiking in the legume and nonlegume root epidermis. *New Phytologist* 189, 347-355.

- Charpentier, M., Bredemeier, R., Wanner, G., Takeda, N., Schleiff, E., and Parniske, M. (2008). *Lotus japonicus* CASTOR and POLLUX are ion channels essential for perinuclear calcium spiking in legume root endosymbiosis. *Plant Cell* 20, 3467-3479.
- Charpentier, M., Vaz Martins, T., Granqvist, E., Oldroyd, G.E.D., and Morris, R.J. (2013). The role of DMI1 in establishing Ca²⁺ oscillations in legume symbioses. *Plant Signaling & Behavior* 8, e22894.
- Chatel, G., and Fahrenkrog, B. (2011). Nucleoporins: Leaving the nuclear pore complex for a successful mitosis. *Cellular Signalling* 23, 1555-1562.
- Chen, P.-Y., Wang, C.-K., Soong, S.-C., and To, K.-Y. (2003). Complete sequence of the binary vector pBI121 and its application in cloning T-DNA insertion from transgenic plants. *Molecular Breeding* 11, 287-293.
- Chen, T., Zhu, H., Ke, D., Cai, K., Wang, C., Gou, H., Hong, Z., and Zhang, Z. (2012). A MAP kinase kinase interacts with SymRK and regulates nodule organogenesis in *Lotus japonicus*. *Plant Cell* 24, 823-838.
- Cheng, Y.T., Germain, H., Wiermer, M., Bi, D., Xu, F., García, A.V., Wirthmueller, L., Després, C., Parker, J.E., Zhang, Y., and Li, X. (2009). Nuclear pore complex component MOS7/Nup88 is required for innate immunity and nuclear accumulation of defense regulators in *Arabidopsis*. *Plant Cell* 21, 2503-2516.
- Chiu, W.-L., Niwa, Y., Zeng, W., Hirano, T., Kobayashi, H., and Sheen, J. (1996). Engineered GFP as a vital reporter in plants. *Current Biology* 6, 325-330.
- Combier, J.-P., Frugier, F., De Billy, F., Boualem, A., El-Yahyaoui, F., Moreau, S., Vernié, T., Ott, T., Gamas, P., Crespi, M., and Niebel, A. (2006). MtHAP2-1 is a key transcriptional regulator of symbiotic nodule development regulated by microRNA169 in *Medicago truncatula*. *Genes & Development* 20, 3084-3088.
- Day, R.B., Mcalvin, C.B., Loh, J.T., Denny, R.L., Wood, T.C., Young, N.D., and Stacey, G. (2000). Differential expression of two soybean apyrases, one of which is an early nodulin. *Molecular Plant-Microbe Interactions* 13, 1053-1070.
- Debler, E.W., Ma, Y., Seo, H.-S., Hsia, K.-C., Noriega, T.R., Blobel, G., and Hoelz, A. (2008). A fence-like coat for the nuclear pore membrane. *Molecular Cell* 32, 815-826.
- Delaux, P.-M., Bécard, G., and Combier, J.-P. (2013). NSP1 is a component of the Myc signaling pathway. *New Phytologist* 199, 59-65.
- Demchenko, K., Winzer, T., Stougaard, J., Parniske, M., and Pawlowski, K. (2004). Distinct roles of *Lotus japonicus* SYMRK and SYM15 in root colonization and arbuscule formation. *New Phytologist* 163, 381-392.
- Den Herder, G., Yoshida, S., Antolin-Llovera, M., Ried, M., and Parniske, M. (2012). *Lotus japonicus* E3 ligase SEVEN IN ABSENTIA 4 destabilizes the Symbiosis Receptor-like kinase SYMRK and negatively regulates rhizobial infection. *Plant Cell* 24, 1691-1707.
- Dénarié, J., Debelle, F., and Promé, J.-C. (1996). Rhizobium lipo-chitoooligosaccharide nodulation factors: signaling molecules mediating recognition and morphogenesis. *Annual Review of Biochemistry* 65, 503-535.
- Depicker, A., Stachel, S., Dhaese, P., Zambryski, P., and Goodman, H.M. (1982). Nopaline synthase: transcript mapping and DNA sequence. *Journal of molecular and applied genetics* 1, 561-573.
- Dong, C.-H., Hu, X., Tang, W., Zheng, X., Kim, Y.S., Lee, B.-H., and Zhu, J.-K. (2006). A putative *Arabidopsis* nucleoporin, AtNUP160, is critical for RNA export and required for plant tolerance to cold stress. *Molecular and Cellular Biology* 26, 9533-9543.
- Doucet, C.M., Talamas, J.A., and Hetzer, M.W. (2010). Cell cycle-dependent differences in nuclear pore complex assembly in metazoa. *Cell* 141, 1030-1041.
- Downie, J.A., and Walker, S.A. (1999). Plant responses to nodulation factors. *Current Opinion in Plant Biology* 2, 483-489.
- Doyle, J.J. (2011). Phylogenetic perspectives on the origins of nodulation. *Molecular Plant-Microbe Interactions* 24, 1289-1295.

- Ehlert, A., Weltmeier, F., Wang, X., Mayer, C.S., Smeekens, S., Vicente-Carbajosa, J., and Dröge-Laser, W. (2006). Two-hybrid protein-protein interaction analysis in *Arabidopsis* protoplasts: establishment of a heterodimerization map of group C and group S bZIP transcription factors. *Plant Journal* 46, 890-900.
- Ehrhardt, D.W., Atkinson, S.R., and Long, C. (1992). Depolarisation of alfalfa root hair membrane potential by *Rhizobium meliloti* Nod factors. *Science* 256, 998-1000.
- Ehrhardt, D.W., Wais, R., and Long, S.R. (1996). Calcium spiking in plant root hairs responding to rhizobium nodulation signals. *Cell* 85, 673-681.
- Ellenberg, J., Siggia, E.D., Moreira, J.E., Smith, C.L., Presley, J.F., Worman, H.J., and Lippincott-Schwartz, J. (1997). Nuclear membrane dynamics and reassembly in living cells: targeting of an inner nuclear membrane protein in interphase and mitosis. *The Journal of Cell Biology* 138, 1193-1206.
- Endre, G., Kereszt, A., Kevei, Z., Mihacea, S., Kalo, P., and Kiss, G.B. (2002). A receptor kinase gene regulating symbiotic nodule development. *Nature* 417, 962-966.
- Engler, C., Kandzia, R., and Marillonnet, S. (2008). A one pot, one step, precision cloning method with high throughput capability. *PLoS ONE* 3, e3647.
- Esseling, J.J., Lhuissier, F.G.P., and Emons, A.M.C. (2003). Nod factor-induced root hair curling: continuous polar growth towards the point of nod factor application. *Plant Physiology* 132, 1982-1988.
- Etzler, M.E., Kalsi, G., Ewing, N.N., Roberts, N.J., Day, R.B., and Murphy, J.B. (1999). A nod factor binding lectin with apyrase activity from legume roots. *Proceedings of the National Academy of Sciences* 96, 5856-5861.
- Fath, S., Mancias, J.D., Bi, X., and Goldberg, J. (2007). Structure and organization of coat proteins in the COPII cage. *Cell* 129, 1325-1336.
- Feddermann, N., Duvvuru Muni, R.R., Zeier, T., Stuurman, J., Ercolin, F., Schorderet, M., and Reinhardt, D. (2010). The *PAM1* gene of petunia, required for intracellular accommodation and morphogenesis of arbuscular mycorrhizal fungi, encodes a homologue of VAPYRIN. *Plant Journal* 64, 470-481.
- Felle, H.H., Kondorosi, É., Kondorosi, A., and Schultze, M. (1996). Rapid alkalinization in alfalfa root hairs in response to rhizobial lipochitooligosaccharide signals. *Plant Journal* 10, 295-301.
- Felle, H.H., Kondorosi, É., Kondorosi, Á., and Schultze, M. (1995). Nod signal-induced plasma membrane potential changes in alfalfa root hairs are differentially sensitive to structural modifications of the lipochitooligosaccharide. *Plant Journal* 7, 939-947.
- Felle, H.H., Kondorosi, É., Kondorosi, Á., and Schultze, M. (1998). The role of ion fluxes in Nod factor signalling in *Medicago sativa*. *Plant Journal* 13, 455-463.
- Ferguson, M.L., Prasad, K., Boukari, H., Sackett, D.L., Krueger, S., Lafer, E.M., and Nossal, R. (2008). Clathrin triskelia show evidence of molecular flexibility. *Biophysical Journal* 95, 1945-1955.
- Fernandez-Martinez, J., Phillips, J., Sekedat, M.D., Diaz-Avalos, R., Velazquez-Muriel, J., Franke, J.D., Williams, R., Stokes, D.L., Chait, B.T., Sali, A., and Rout, M.P. (2012). Structure-function mapping of a heptameric module in the nuclear pore complex. *The Journal of Cell Biology* 196, 419-434.
- Fitter, A.H. (2005). Darkness visible: reflections on underground ecology. *Journal of Ecology* 93, 231-243.
- Floss, D.S., Levy, J.G., Lévesque-Tremblay, V., Pumplin, N., and Harrison, M.J. (2013). DELLA proteins regulate arbuscule formation in arbuscular mycorrhizal symbiosis. *Proceedings of the National Academy of Sciences* 110, E5025-5034.
- Foo, E., Ross, J.J., Jones, W.T., and Reid, J.B. (2013). Plant hormones in arbuscular mycorrhizal symbioses: an emerging role for gibberellins. *Annals of Botany* 111, 769-779.

- Fournier, J., Timmers, A.C.J., Sieberer, B.J., Jauneau, A., Chabaud, M., and Barker, D.G. (2008). Mechanism of infection thread elongation in root hairs of *Medicago truncatula* and dynamic interplay with associated rhizobial colonization. *Plant Physiology* 148, 1985-1995.
- Frey, S., and Gorlich, D. (2007). A saturated FG-repeat hydrogel can reproduce the permeability properties of nuclear pore complexes. *Cell* 130, 512-523.
- Fukai, E., Soyano, T., Umehara, Y., Nakayama, S., Hirakawa, H., Tabata, S., Sato, S., and Hayashi, M. (2012). Establishment of a *Lotus japonicus* gene tagging population using the exon-targeting endogenous retrotransposon *LORE1*. *Plant Journal* 69, 720-730.
- Genre, A., Chabaud, M., Balzergue, C., Puech-Pagès, V., Novero, M., Rey, T., Fournier, J., Rochange, S., Bécard, G., Bonfante, P., and Barker, D.G. (2013). Short-chain chitin oligomers from arbuscular mycorrhizal fungi trigger nuclear Ca²⁺ spiking in *Medicago truncatula* roots and their production is enhanced by strigolactone. *New Phytologist* 198, 190-202.
- Genre, A., Chabaud, M., Faccio, A., Barker, D.G., and Bonfante, P. (2008). Prepenetration apparatus assembly precedes and predicts the colonization patterns of arbuscular mycorrhizal fungi within the root cortex of both *Medicago truncatula* and *Daucus carota*. *Plant Cell* 20, 1407-1420.
- Genre, A., Chabaud, M., Timmers, T., Bonfante, P., and Barker, D.G. (2005). Arbuscular mycorrhizal fungi elicit a novel intracellular apparatus in *Medicago truncatula* root epidermal cells before infection. *Plant Cell* 17, 3489-3499.
- Gerard, R.L., Pascal, A.S., and Robert, A.L. (1991). A DNA transformation-competent *Arabidopsis* genomic library in *Agrobacterium*. *Nature Biotechnology* 9, 963-967.
- Gleason, C., Chaudhuri, S., Yang, T., Munoz, A., Poovaiah, B.W., and Oldroyd, G.E.D. (2006). Nodulation independent of rhizobia induced by a calcium-activated kinase lacking autoinhibition. *Nature* 441, 1149-1152.
- Gobbato, E., Marsh, John f., Vernié, T., Wang, E., Maillet, F., Kim, J., Miller, J.B., Sun, J., Bano, S.A., Ratet, P., Mysore, Kirankumar s., Dénarié, J., Schultze, M., and Oldroyd, Giles e.D. (2012). A GRAS-type transcription factor with a specific function in mycorrhizal signaling. *Current Biology* 22, 2236-2241.
- González-Aguilera, C., and Askjaer, P. (2012). Dissecting the NUP107 complex: multiple components and even more functions. *Nucleus* 3, 340-348.
- Goormachtig, S., Capoen, W., James, E.K., and Holsters, M. (2004). Switch from intracellular to intercellular invasion during water stress-tolerant legume nodulation. *Proceedings of the National Academy of Sciences of the United States of America* 101, 6303-6308.
- Granqvist, E., Wysham, D., Hazledine, S., Kozłowski, W., Sun, J., Charpentier, M., Martins, T.V., Haleux, P., Tsaneva-Atanasova, K., Downie, J.A., Oldroyd, G.E.D., and Morris, R.J. (2012). Buffering capacity explains signal variation in symbiotic calcium oscillations. *Plant Physiology* 160, 2300-2310.
- Graumann, K., Runions, J., and Evans, D.E. (2010). Characterization of SUN-domain proteins at the higher plant nuclear envelope. *The Plant Journal* 61, 134-144.
- Grefen, C., Donald, N., Hashimoto, K., Kudla, J., Schumacher, K., and Blatt, M.R. (2010). A ubiquitin-10 promoter-based vector set for fluorescent protein tagging facilitates temporal stability and native protein distribution in transient and stable expression studies. *The Plant Journal* 64, 355-365.
- Grossman, E., Medalia, O., and Zwerger, M. (2012). Functional architecture of the nuclear pore complex. *Annual Review of Biophysics* 41, 557-584.
- Groth, M., Takeda, N., Perry, J., Uchida, H., Dräxl, S., Brachmann, A., Sato, S., Tabata, S., Kawaguchi, M., Wang, T.L., and Parniske, M. (2010). *NENA*, a *Lotus japonicus* homolog of *Sec13*, is required for rhizodermal infection by arbuscular mycorrhizal fungi and rhizobia but dispensable for cortical endosymbiotic development. *Plant Cell* 22, 2509-2526.
- Grünwald, D., and Singer, R.H. (2012). Multiscale dynamics in nucleocytoplasmic transport. *Current Opinion in Cell Biology* 24, 100-106.

- Grünwald, D., Singer, R.H., and Rout, M. (2011). Nuclear export dynamics of RNA-protein complexes. *Nature* 475, 333-341.
- Guilley, H., Dudley, R.K., Jonard, G., Balázs, E., and Richards, K.E. (1982). Transcription of cauliflower mosaic virus DNA: detection of promoter sequences, and characterization of transcripts. *Cell* 30, 763-773.
- Gust, A.A., Willmann, R., Desaki, Y., Grabherr, H.M., and Nürnberger, T. (2012). Plant LysM proteins: modules mediating symbiosis and immunity. *Trends in Plant Science* 17, 495-502.
- Gutjahr, C., Novero, M., Guether, M., Montanari, O., Udvardi, M., and Bonfante, P. (2009). Presymbiotic factors released by the arbuscular mycorrhizal fungus *Gigaspora margarita* induce starch accumulation in *Lotus japonicus* roots. *New Phytologist* 183, 53-61.
- Gutjahr, C., and Parniske, M. (2013). Cell and developmental biology of arbuscular mycorrhiza symbiosis. *Annual Review of Cell and Developmental Biology* 29, 593-617.
- Harberd, N.P., Belfield, E., and Yasumura, Y. (2009). The angiosperm gibberellin-GID1-DELLA growth regulatory mechanism: how an “inhibitor of an inhibitor” enables flexible response to fluctuating environments. *Plant Cell* 21, 1328-1339.
- Harel, A., Orjalo, A.V., Vincent, T., Lachish-Zalait, A., Vasu, S., Shah, S., Zimmerman, E., Elbaum, M., and Forbes, D.J. (2003). Removal of a single pore subcomplex results in vertebrate nuclei devoid of nuclear pores. *Molecular Cell* 11, 853-864.
- Harris, J.M., Wais, R., and Long, S.R. (2003). Rhizobium-induced calcium spiking in *Lotus japonicus*. *Molecular Plant-Microbe Interactions* 16, 335-341.
- Harrison, M.J. (2012). Cellular programs for arbuscular mycorrhizal symbiosis. *Current Opinion in Plant Biology* 15, 691-698.
- Hayashi, T., Banba, M., Shimoda, Y., Kouchi, H., Hayashi, M., and Imaizumi-Anraku, H. (2010). A dominant function of CCaMK in intracellular accommodation of bacterial and fungal endosymbionts. *Plant Journal* 63, 141-154.
- Hayashi, T., Shimoda, Y., Sato, S., Tabata, S., Imaizumi-Anraku, H., and Hayashi, M. (2014). Rhizobial infection does not require cortical expression of upstream common symbiosis genes responsible for the induction of Ca²⁺ spiking. *The Plant Journal* 77, 146-159.
- Heckmann, A.B., Lombardo, F., Miwa, H., Perry, J.A., Bunnnewell, S., Parniske, M., Wang, T.L., and Downie, J.A. (2006). *Lotus japonicus* nodulation requires two GRAS domain regulators, one of which is functionally conserved in a non-legume. *Plant Physiology* 142, 1739-1750.
- Heckmann, A.B., Sandal, N., Bek, A.S., Madsen, L.H., Jurkiewicz, A., Nielsen, M.W., Tirichine, L., and Stougaard, J. (2011). Cytokinin induction of root nodule primordia in *Lotus japonicus* is regulated by a mechanism operating in the root cortex. *Molecular Plant-Microbe Interactions* 24, 1385-1395.
- Held, M., Hossain, M.S., Yokota, K., Bonfante, P., Stougaard, J., and Szczygłowski, K. (2010). Common and not so common symbiotic entry. *Trends in Plant Science* 15, 540-545.
- Hiei, Y., Ohta, S., Komari, T., and Kumashiro, T. (1994). Efficient transformation of rice (*Oryza sativa* L.) mediated by *Agrobacterium* and sequence analysis of the boundaries of the T-DNA. *Plant Journal* 6, 271-282.
- Hinshaw, J.E., Carragher, B.O., and Milligan, R.A. (1992). Architecture and design of the nuclear pore complex. *Cell* 69, 1133-1141.
- Hirsch, S., Kim, J., Muñoz, A., Heckmann, A.B., Downie, J.A., and Oldroyd, G.E.D. (2009). GRAS proteins form a DNA binding complex to induce gene expression during nodulation signaling in *Medicago truncatula*. *Plant Cell* 21, 545-557.
- Hochuli, E., Bannwarth, W., Dobeli, H., Gentz, R., and Stuber, D. (1988). Genetic approach to facilitate purification of recombinant proteins with a novel metal chelate adsorbent. *Nature Biotechnology* 6, 1321-1325.
- Hoelz, A., Debler, E.W., and Blobel, G. (2011). The structure of the nuclear pore complex. *Annual Review of Biochemistry* 80, 613-643.
- Hogekamp, C., Arndt, D., Pereira, P., Becker, J.D., Hohnjec, N., and Küster, H. (2011). Laser-microdissection unravels cell-type specific transcription in arbuscular mycorrhizal roots,

- including CAAT-box TF gene expression correlating with fungal contact and spread. *Plant Physiology*.
- Horváth, B., Yeun, L.H., Domonkos, Á., Halász, G., Gobbato, E., Ayaydin, F., Miró, K., Hirsch, S., Sun, J., Tadege, M., Ratet, P., Mysore, K.S., Ané, J.-M., Oldroyd, G.E.D., and Kaló, P. (2011). *Medicago truncatula* IPD3 Is a member of the common symbiotic signaling pathway required for rhizobial and mycorrhizal symbioses. *Molecular Plant-Microbe Interactions* 24, 1345-1358.
- Imaizumi-Anraku, H., Takeda, N., Charpentier, M., Perry, J., Miwa, H., Umehara, Y., Kouchi, H., Murakami, Y., Mulder, L., Vickers, K., Pike, J., Allan Downie, J., Wang, T., Sato, S., Asamizu, E., Tabata, S., Yoshikawa, M., Murooka, Y., Wu, G.-J., Kawaguchi, M., Kawasaki, S., Parniske, M., and Hayashi, M. (2005). Plastid proteins crucial for symbiotic fungal and bacterial entry into plant roots. *Nature* 433, 527-531.
- Ivanov, S., Fedorova, E.E., Limpens, E., De Mita, S., Genre, A., Bonfante, P., and Bisseling, T. (2012). Rhizobium-legume symbiosis shares an exocytotic pathway required for arbuscule formation. *Proceedings of the National Academy of Sciences, USA* 109, 8316-8321.
- James, E.K., and Sprent, J.I. (1999). Development of N₂-fixing nodules on the wetland legume *Lotus uliginosus* exposed to conditions of flooding. *New Phytologist* 142, 219-231.
- Jarsch, I.K., and Ott, T. (2011). Perspectives on remorin proteins, membrane rafts, and their role during plant-microbe interactions. *Molecular Plant-Microbe Interactions* 24, 7-12.
- Kalderon, D., Roberts, B.L., Richardson, W.D., and Smith, A.E. (1984). A short amino acid sequence able to specify nuclear location. *Cell* 39, 499-509.
- Kaló, P., Gleason, C., Edwards, A., Marsh, J., Mitra, R.M., Hirsch, S., Jakab, J., Sims, S., Long, S.R., Rogers, J., Kiss, G.B., Downie, J.A., and Oldroyd, G.E.D. (2005). Nodulation signaling in legumes requires NSP2, a member of the GRAS family of transcriptional regulators. *Science* 308, 1786-1789.
- Kalsi, G., and Etzler, M.E. (2000). Localization of a Nod Factor-binding protein in legume roots and factors influencing its distribution and expression. *Plant Physiology* 124, 1039-1048.
- Kalyna, M., Simpson, C.G., Syed, N.H., Lewandowska, D., Marquez, Y., Kusenda, B., Marshall, J., Fuller, J., Cardle, L., Mcnicol, J., Dinh, H.Q., Barta, A., and Brown, J.W.S. (2012). Alternative splicing and nonsense-mediated decay modulate expression of important regulatory genes in Arabidopsis. *Nucleic Acids Research* 40, 2454-2469.
- Kampmann, M., and Blobel, G. (2009). Three-dimensional structure and flexibility of a membrane-coating module of the nuclear pore complex. *Nat Struct Mol Biol* 16, 782-788.
- Kanamori, N., Madsen, L.H., Radutoiu, S., Frantescu, M., Quistgaard, E.M., Miwa, H., Downie, J.A., James, E.K., Felle, H.H., Haaning, L.L., Jensen, T.H., Sato, S., Nakamura, Y., Tabata, S., Sandal, N., and Stougaard, J. (2006). A nucleoporin is required for induction of Ca²⁺ spiking in legume nodule development and essential for rhizobial and fungal symbiosis. *Proceedings of the National Academy of Sciences, USA* 103, 359-364.
- Karas, B., Murray, J., Gorzelak, M., Smith, A., Sato, S., Tabata, S., and Szczyglowski, K. (2005). Invasion of *Lotus japonicus* root hairless 1 by *Mesorhizobium loti* involves the nodulation factor-dependent induction of root hairs. *Plant Physiology* 137, 1331-1344.
- Karimi, M., Inzé, D., and Depicker, A. (2002). GATEWAY vectors for *Agrobacterium*-mediated plant transformation. *Trends in Plant Science* 7, 193-195.
- Kato, T., Goto, Y., Ono, K., Hayashi, M., and Murooka, Y. (2005). Expression of a major house dust mite allergen gene from *Dermatophagoides farinae* in *Lotus japonicus* accession miyakojima MG-20. *Journal of Bioscience and Bioengineering* 99, 165-168.
- Ke, D., Fang, Q., Chen, C., Zhu, H., Chen, T., Chang, X., Yuan, S., Kang, H., Ma, L., Hong, Z., and Zhang, Z. (2012). The small GTPase ROP6 interacts with NFR5 and is involved in nodule formation in *Lotus japonicus*. *Plant Physiology* 159, 131-143.
- Kereszt, A., Mergaert, P., and Kondorosi, E. (2011). Bacteroid development in legume nodules: evolution of mutual benefit or of sacrificial victims? *Molecular Plant-Microbe Interactions* 24, 1300-1309.

- Kevei, Z., Lougnon, G., Mergaert, P., Horvath, G.V., Kereszt, A., Jayaraman, D., Zaman, N., Marcel, F., Regulski, K., Kiss, G.B., Kondorosi, A., Endre, G., Kondorosi, E., and Ane, J.M. (2007). 3-hydroxy-3-methylglutaryl coenzyme a reductase 1 interacts with NOR1 and is crucial for nodulation in *Medicago truncatula*. *Plant Cell* 19, 3974-3989.
- King, M.C., Lusk, C., and Blobel, G. (2006). Karyopherin-mediated import of integral inner nuclear membrane proteins. *Nature* 442, 1003-1007.
- Kistner, C., and Parniske, M. (2002). Evolution of signal transduction in intracellular symbiosis. *Trends in Plant Science* 7, 511-518.
- Kistner, C., Winzer, T., Pitzschke, A., Mulder, L., Sato, S., Kaneko, T., Tabata, S., Sandal, N., Stougaard, J., Webb, K.J., Szczyglowski, K., and Parniske, M. (2005). Seven *Lotus japonicus* genes required for transcriptional reprogramming of the root during fungal and bacterial symbiosis. *Plant Cell* 17, 2217-2229.
- Kosuta, S., Chabaud, M., Lougnon, G., Gough, C., Dénarié, J., Barker, D.G., and Bécard, G. (2003). A diffusible factor from arbuscular mycorrhizal fungi induces symbiosis-specific *MtENOD11* expression in roots of *Medicago truncatula*. *Plant Physiology* 131, 952-962.
- Kosuta, S., Hazledine, S., Sun, J., Miwa, H., Morris, R.J., Downie, J.A., and Oldroyd, G.E.D. (2008). Differential and chaotic calcium signatures in the symbiosis signaling pathway of legumes. *Proceedings of the National Academy of Sciences, USA* 105, 9823-9828.
- Kosuta, S., Held, M., Hossain, M.S., Morieri, G., Macgillivray, A., Johansen, C., Antolín-Llovera, M., Parniske, M., Oldroyd, G.E.D., Downie, A.J., Karas, B., and Szczyglowski, K. (2011). *Lotus japonicus* symRK-14 uncouples the cortical and epidermal symbiotic program. *Plant Journal* 67, 929-940.
- Kovach, M.E., Elzer, P.H., Steven Hill, D., Robertson, G.T., Farris, M.A., Roop II, R.M., and Peterson, K.M. (1995). Four new derivatives of the broad-host-range cloning vector pBBR1MCS, carrying different antibiotic-resistance cassettes. *Gene* 166, 175-176.
- Krebs, M., Held, K., Binder, A., Hashimoto, K., Den Herder, G., Parniske, M., Kudla, J., and Schumacher, K. (2012). FRET-based genetically encoded sensors allow high-resolution live cell imaging of Ca²⁺ dynamics. *Plant Journal* 69, 181-192.
- Kudla, J., Batistič, O., and Hashimoto, K. (2010). Calcium signals: the lead currency of plant information processing. *Plant Cell* 22, 541-563.
- Kuhn, H., Küster, H., and Requena, N. (2010). Membrane steroid-binding protein 1 induced by a diffusible fungal signal is critical for mycorrhization in *Medicago truncatula*. *New Phytologist* 185, 716-733.
- Kwon, C., Neu, C., Pajonk, S., Yun, H.S., Lipka, U., Humphry, M., Bau, S., Straus, M., Kwaaitaal, M., Rampelt, H., Kasmi, F.E., Jurgens, G., Parker, J., Panstruga, R., Lipka, V., and Schulze-Lefert, P. (2008). Co-option of a default secretory pathway for plant immune responses. *Nature* 451, 835-840.
- Lauressergues, D., Delaux, P.-M., Formey, D., Lelandais-Brière, C., Fort, S., Cottaz, S., Bécard, G., Niebel, A., Roux, C., and Combier, J.-P. (2012). The microRNA miR171h modulates arbuscular mycorrhizal colonization of *Medicago truncatula* by targeting *NSP2*. *Plant Journal* 72, 512-522.
- Lecourieux, D., Lamotte, O., Bourque, S., Wendehenne, D., Mazars, C., Ranjeva, R., and Pugin, A. (2005). Proteinaceous and oligosaccharidic elicitors induce different calcium signatures in the nucleus of tobacco cells. *Cell Calcium* 38, 527-538.
- Lecourieux, D., Ranjeva, R., and Pugin, A. (2006). Calcium in plant defence-signalling pathways. *New Phytologist* 171, 249-269.
- Lefebvre, B., Timmers, T., Mbengue, M., Moreau, S., Hervé, C., Tóth, K., Bittencourt-Silvestre, J., Klaus, D., Deslandes, L., Godiard, L., Murray, J.D., Udvardi, M.K., Raffaele, S., Mongrand, S., Cullimore, J., Gamas, P., Niebel, A., and Ott, T. (2010). A remorin protein interacts with symbiotic receptors and regulates bacterial infection. *Proceedings of the National Academy of Sciences, USA* 107, 2343-2348.

- Levy, J., Bres, C., Geurts, R., Chalhoub, B., Kulikova, O., Duc, G., Journet, E.P., Ane, J.M., Lauber, E., Bisseling, T., Denarie, J., Rosenberg, C., and Debelle, F. (2004). A putative Ca²⁺ and calmodulin-dependent protein kinase required for bacterial and fungal symbioses. *Science* 303, 1361-1364.
- Li, O., Heath, C.V., Amberg, D.C., Dockendorff, T.C., Copeland, C.S., Snyder, M., and Cole, C.N. (1995). Mutation or deletion of the *Saccharomyces cerevisiae* RAT3/NUP133 gene causes temperature-dependent nuclear accumulation of poly(A)⁺ RNA and constitutive clustering of nuclear pore complexes. *Molecular Biology of the Cell* 6, 401-417.
- Liao, J., Singh, S., Hossain, M.S., Andersen, S.U., Ross, L., Bonetta, D., Zhou, Y., Sato, S., Tabata, S., Stougaard, J., Szczyglowski, K., and Parniske, M. (2012). Negative regulation of CCaMK is essential for symbiotic infection. *Plant Journal* 72, 572-584.
- Liu, J., Blaylock, L.A., Endre, G., Cho, J., Town, C.D., Vandenbosch, K.A., and Harrison, M.J. (2003). Transcript profiling coupled with spatial expression analyses reveals genes involved in distinct developmental stages of an arbuscular mycorrhizal symbiosis. *Plant Cell* 15, 2106-2123.
- Liu, W., Kohlen, W., Lillo, A., Op Den Camp, R., Ivanov, S., Hartog, M., Limpens, E., Jamil, M., Smaczniak, C., Kaufmann, K., Yang, W.-C., Hooiveld, G.J.E.J., Charnikhova, T., Bouwmeester, H.J., Bisseling, T., and Geurts, R. (2011). Strigolactone biosynthesis in *Medicago truncatula* and rice requires the symbiotic GRAS-type transcription factors NSP1 and NSP2. *Plant Cell* 23, 3853-3865.
- Lohmann, G.V., Shimoda, Y., Nielsen, M.W., Jørgensen, F.G., Grossmann, C., Sandal, N., Sørensen, K., Thirup, S., Madsen, L.H., Tabata, S., Sato, S., Stougaard, J., and Radutoiu, S. (2010). Evolution and regulation of the *Lotus japonicus* LysM receptor gene family. *Molecular Plant-Microbe Interactions* 23, 510-521.
- Loiodice, I., Alves, A., Rabut, G., Van Overbeek, M., Ellenberg, J., Sibarita, J.-B., and Doye, V. (2004). The entire Nup107-160 Complex, including three new members, is targeted as one entity to kinetochores in mitosis. *Molecular Biology of the Cell* 15, 3333-3344.
- Lutzmann, M., Kunze, R., Buerer, A., Aebi, U., and Hurt, E. (2002). Modular self-assembly of a Y-shaped multiprotein complex from seven nucleoporins. *EMBO Journal* 21, 387-397.
- Madsen, E.B., Antolin-Llovera, M., Grossmann, C., Ye, J., Vieweg, S., Broghammer, A., Krusell, L., Radutoiu, S., Jensen, O.N., Stougaard, J., and Parniske, M. (2011). Autophosphorylation is essential for the in vivo function of the *Lotus japonicus* Nod factor receptor 1 and receptor-mediated signalling in cooperation with Nod factor receptor 5. *Plant Journal* 65, 404-417.
- Madsen, E.B., Madsen, L.H., Radutoiu, S., Olbryt, M., Rakwalska, M., Szczyglowski, K., Sato, S., Kaneko, T., Tabata, S., Sandal, N., and Stougaard, J. (2003). A receptor kinase gene of the LysM type is involved in legume perception of rhizobial signals. *Nature* 425, 637-640.
- Madsen, L.H., Tirichine, L., Jurkiewicz, A., Sullivan, J.T., Heckmann, A.B., Bek, A.S., Ronson, C.W., James, E.K., and Stougaard, J. (2010). The molecular network governing nodule organogenesis and infection in the model legume *Lotus japonicus*. *Nature Communications* 1, 1-12.
- Maekawa, T., Kusakabe, M., Shimoda, Y., Sato, S., Tabata, S., Murooka, Y., and Hayashi, M. (2008). Polyubiquitin promoter-based binary vectors for overexpression and gene silencing in *Lotus japonicus*. *Molecular Plant-Microbe Interactions* 21, 375-382.
- Maekawa, T., Maekawa-Yoshikawa, M., Takeda, N., Imaizumi-Anraku, H., Murooka, Y., and Hayashi, M. (2009). Gibberellin controls the nodulation signaling pathway in *Lotus japonicus*. *Plant Journal* 58, 183-194.
- Maillet, F., Poinot, V., Andre, O., Puech-Pages, V., Haouy, A., Gueunier, M., Cromer, L., Giraudet, D., Formey, D., Niebel, A., Martinez, E.A., Driguez, H., Becard, G., and Denarie, J. (2011). Fungal lipochitooligosaccharide symbiotic signals in arbuscular mycorrhiza. *Nature* 469, 58-63.
- Malik, P., Korfali, N., Srsen, V., Lazou, V., Batrakou, D., Zuleger, N., Kavanagh, D., Wilkie, G., Goldberg, M., and Schirmer, E. (2010). Cell-specific and lamin-dependent targeting of

- novel transmembrane proteins in the nuclear envelope. *Cellular and Molecular Life Sciences* 67, 1353-1369.
- Mantovani, R. (1999). The molecular biology of the CCAAT-binding factor NF-Y. *Gene* 239, 15-27.
- Markmann, K., Giczey, G., and Parniske, M. (2008). Functional adaptation of a plant receptor-kinase paved the way for the evolution of intracellular root symbioses with bacteria. *PLoS Biology* 6, e68.
- Markmann, K., and Parniske, M. (2009). Evolution of root endosymbiosis with bacteria: How novel are nodules? *Trends in Plant Science* 14, 77-86.
- Marsh, J.F., Rakocevic, A., Mitra, R.M., Brocard, L., Sun, J., Eschstruth, A., Long, S.R., Schultze, M., Ratet, P., and Oldroyd, G.E. (2007). *Medicago truncatula* NIN is essential for rhizobial-independent nodule organogenesis induced by autoactive calcium/calmodulin-dependent protein kinase. *Plant Physiology* 144, 324-335.
- Mbengue, M., Camut, S., De Carvalho-Niebel, F., Deslandes, L., Froidure, S., Klaus-Heisen, D., Moreau, S., Rivas, S., Timmers, T., Herve, C., Cullimore, J., and Lefebvre, B. (2010). The *Medicago truncatula* E3 ubiquitin ligase PUB1 interacts with the LYK3 symbiotic receptor and negatively regulates infection and nodulation. *Plant Cell* 22, 3474-3488.
- Mehlmer, N., Parvin, N., Hurst, C.H., Knight, M.R., Teige, M., and Vothknecht, U.C. (2012). A toolset of aequorin expression vectors for in planta studies of subcellular calcium concentrations in *Arabidopsis thaliana*. *Journal of Experimental Botany* 63, 1751-1761.
- Meinema, A.C., Laba, J.K., Hapsari, R.A., Otten, R., Mulder, F.a.A., Kralt, A., Van Den Bogaart, G., Lusk, C.P., Poolman, B., and Veenhoff, L.M. (2011). Long Unfolded Linkers Facilitate Membrane Protein Import Through the Nuclear Pore Complex. *Science* 333, 90-93.
- Meinema, A.C., Poolman, B., and Veenhoff, L.M. (2013). Quantitative analysis of membrane protein transport across the nuclear pore complex. *Traffic* 14, 487-501.
- Melčák, I., Hoelz, A., and Blobel, G. (2007). Structure of Nup58/45 suggests flexible nuclear pore diameter by intermolecular sliding. *Science* 315, 1729-1732.
- Menge, J.A., Steirle, D., Bagyaraj, D.J., Johnson, E.L.V., and Leonard, R.T. (1978). Phosphorus concentrations in plants responsible for inhibitor of mycorrhizal infection. *New Phytologist* 80, 575-578.
- Messinese, E., Mun, J.-H., Yeun, L.H., Jayaraman, D., Rougé, P., Barre, A., Lougnon, G., Schornack, S., Bono, J.-J., Cook, D.R., and Ané, J.-M. (2007). A novel nuclear protein interacts with the symbiotic DMI3 calcium- and calmodulin-dependent protein kinase of *Medicago truncatula*. *Molecular Plant-Microbe Interactions* 20, 912-921.
- Middleton, P.H., Jakab, J., Penmetsa, R.V., Starker, C.G., Doll, J., Kaló, P., Prabhu, R., Marsh, J.F., Mitra, R.M., Kereszt, A., Dudas, B., Vandenbosch, K., Long, S.R., Cook, D.R., Kiss, G.B., and Oldroyd, G.E.D. (2007). An ERF transcription factor in *Medicago truncatula* that is essential for nod factor signal transduction. *The Plant Cell Online* 19, 1221-1234.
- Miller, J.B., and Oldroyd, G.D. (2012). "The role of diffusible signals in the establishment of rhizobial and mycorrhizal symbioses," in *Signaling and Communication in Plant Symbiosis*, eds. S. Perotto & F. Baluška. Springer Berlin Heidelberg, 1-30.
- Mitra, R.M., Gleason, C.A., Edwards, A., Hadfield, J., Downie, J.A., Oldroyd, G.E.D., and Long, S.R. (2004). A Ca²⁺/calmodulin-dependent protein kinase required for symbiotic nodule development: Gene identification by transcript-based cloning. *Proceedings of the National Academy of Sciences, USA* 101, 4701-4705.
- Miwa, H., Sun, J., Oldroyd, G.E., and Downie, J.A. (2006a). Analysis of Nod-factor-induced calcium signaling in root hairs of symbiotically defective mutants of *Lotus japonicus*. *Molecular Plant-Microbe Interactions* 19, 914-923.
- Miwa, H., Sun, J., Oldroyd, G.E.D., and Allan Downie, J. (2006b). Analysis of calcium spiking using aameleon calcium sensor reveals that nodulation gene expression is regulated by calcium spike number and the developmental status of the cell. *Plant Journal* 48, 883-894.

- Morello, L., Gianì, S., Troina, F., and Breviario, D. (2011). Testing the IMETER on rice introns and other aspects of intron-mediated enhancement of gene expression. *Journal of Experimental Botany* 62, 533-544.
- Murakami, Y., Miwa, H., Imaizumi-Anraku, H., Kouchi, H., Downie, J.A., Kawaguchi, M., and Kawasaki, S. (2007). Positional cloning identifies *Lotus japonicus* NSP2, a putative transcription factor of the GRAS family, required for *NIN* and *ENOD40* gene expression in nodule initiation. *DNA Research* 13, 255-265.
- Murray, J.D., Muni, R.R.D., Torres-Jerez, I., Tang, Y., Allen, S., Andriankaja, M., Li, G., Laxmi, A., Cheng, X., Wen, J., Vaughan, D., Schultze, M., Sun, J., Charpentier, M., Oldroyd, G., Tadege, M., Ratet, P., Mysore, K.S., Chen, R., and Udvardi, M.K. (2011). Vapyrin, a gene essential for intracellular progression of arbuscular mycorrhizal symbiosis, is also essential for infection by rhizobia in the nodule symbiosis of *Medicago truncatula*. *Plant Journal* 65, 244-252.
- Mussolino, C., Morbitzer, R., Lütge, F., Dannemann, N., Lahaye, T., and Cathomen, T. (2011). A novel TALE nuclease scaffold enables high genome editing activity in combination with low toxicity. *Nucleic Acids Research* 39, 9283-9293.
- Nagai, T., Ibata, K., Park, E.S., Kubota, M., Mikoshiba, K., and Miyawaki, A. (2002). A variant of yellow fluorescent protein with fast and efficient maturation for cell-biological applications. *Nature Biotechnology* 20, 87-90.
- Nagaya, S., Kawamura, K., Shinmyo, A., and Kato, K. (2010). The *HSP* terminator of *Arabidopsis thaliana* increases gene expression in plant cells. *Plant and Cell Physiology* 51, 328-332.
- Nakagawa, T., Kurose, T., Hino, T., Tanaka, K., Kawamukai, M., Niwa, Y., Toyooka, K., Matsuoka, K., Jinbo, T., and Kimura, T. (2007). Development of series of gateway binary vectors, pGWBs, for realizing efficient construction of fusion genes for plant transformation. *Journal of Bioscience and Bioengineering* 104, 34-41.
- Nakano, H., Wang, W., Hashizume, C., Funasaka, T., Sato, H., and Wong, R.W. (2011). Unexpected role of nucleoporins in coordination of cell cycle progression. *Cell Cycle* 10, 425-433.
- Neumann, N., Lundin, D., and Poole, A.M. (2010). Comparative genomic evidence for a complete nuclear pore complex in the last eukaryotic common ancestor. *PLoS ONE* 5, e13241.
- Norris, S.R., Meyer, S.E., and Callis, J. (1993). The intron of *Arabidopsis thaliana* polyubiquitin genes is conserved in location and is a quantitative determinant of chimeric gene expression. *Plant Molecular Biology* 21, 895-906.
- Ohta, S., Mita, S., Hattori, T., and Nakamura, K. (1990). Construction and expression in tobacco of a β -glucuronidase (GUS) reporter gene containing an intron within the coding sequence. *Plant and Cell Physiology* 31, 805-813.
- Oláh, B., Brière, C., Bécard, G., Dénarié, J., and Gough, C. (2005). Nod factors and a diffusible factor from arbuscular mycorrhizal fungi stimulate lateral root formation in *Medicago truncatula* via the DMI1/DMI2 signalling pathway. *Plant Journal* 44, 195-207.
- Oldroyd, G.E.D., and Downie, J.A. (2006). Nuclear calcium changes at the core of symbiosis signalling. *Current Opinion in Plant Biology* 9, 351-357.
- Oldroyd, G.E.D., and Downie, J.A. (2008). Coordinating nodule morphogenesis with rhizobial infection in legumes. *Annual Review of Plant Biology* 59, 519-546.
- Oldroyd, G.E.D., and Long, S.R. (2003). Identification and characterization of *Nodulation-Signaling Pathway 2*, a gene of *Medicago truncatula* Involved in nod factor signaling. *Plant Physiology* 131, 1027-1032.
- Oldroyd, G.E.D., Murray, J.D., Poole, P.S., and Downie, J.A. (2011). The rules of engagement in the legume-rhizobial symbiosis. *Annual Review of Genetics* 45, 119-144.
- Op Den Camp, R.H.M., Polone, E., Fedorova, E., Roelofsen, W., Squartini, A., Op Den Camp, H.J.M., Bisseling, T., and Geurts, R. (2012). Nonlegume *Parasponia andersonii* deploys a broad Rhizobium host range strategy resulting in largely variable symbiotic effectiveness. *Molecular Plant-Microbe Interactions* 25, 954-963.

- Ortu, G., Balestrini, R., Pereira, P.A., Becker, J.D., Küster, H., and Bonfante, P. (2012). Plant genes related to gibberellin biosynthesis and signaling are differentially regulated during the early stages of AM fungal interactions. *Molecular Plant* 5, 951-954.
- Ostlund, C., Ellenberg, J., Hallberg, E., Lippincott-Schwartz, J., and Worman, H.J. (1999). Intracellular trafficking of emerin, the Emery-Dreifuss muscular dystrophy protein. *Journal of Cell Science* 112, 1709-1719.
- Ovchinnikova, E., Journet, E.-P., Chabaud, M., Cosson, V., Ratet, P., Duc, G., Fedorova, E., Liu, W., Den Camp, R.O., Zhukov, V., Tikhonovich, I., Borisov, A., Bisseling, T., and Limpens, E. (2011). IPD3 controls the formation of nitrogen-fixing symbiosomes in pea and *Medicago* spp. *Molecular Plant-Microbe Interactions* 24, 1333-1344.
- Palma, K., Zhang, Y., and Li, X. (2005). An importin alpha homolog, MOS6, plays an important role in plant innate immunity. *Current Biology* 15, 1129-1135.
- Parniske, M. (2008). Arbuscular mycorrhiza: The mother of plant root endosymbioses. *Nature Reviews: Microbiology* 6, 763-775.
- Parra, G., Bradnam, K., Rose, A.B., and Korf, I. (2011). Comparative and functional analysis of intron-mediated enhancement signals reveals conserved features among plants. *Nucleic Acids Research* 39, 5328-5337.
- Parry, G., Ward, S., Cernac, A., Dharmasiri, S., and Estelle, M. (2006). The *Arabidopsis* SUPPRESSOR OF AUXIN RESISTANCE proteins are nucleoporins with an important role in hormone signaling and development. *Plant Cell* 18, 1590-1603.
- Pauly, N., Knight, M.R., Thuleau, P., Graziana, A., Muto, S., Ranjeva, R., and Mazars, C. (2001). The nucleus together with the cytosol generates patterns of specific cellular calcium signatures in tobacco suspension culture cells. *Cell Calcium* 30, 413-421.
- Pauly, N., Knight, M.R., Thuleau, P., Van Der Luit, A.H., Moreau, M., Trewavas, A.J., Ranjeva, R., and Mazars, C. (2000). Cell signalling: Control of free calcium in plant cell nuclei. *Nature* 405, 754-755.
- Pawlowski, K., and Sprent, J.I. (2008). "Comparison between actinorhizal and legume symbiosis," in *Nitrogen-fixing Actinorhizal Symbioses*, eds. K. Pawlowski & W. Newton. Springer Netherlands), 261-288.
- Pemberton, L.F., Rout, M.P., and Blobel, G. (1995). Disruption of the nucleoporin gene NUP133 results in clustering of nuclear pore complexes. *Proceedings of the National Academy of Sciences, USA* 92, 1187-1191.
- Plet, J., Wasson, A., Ariel, F., Le Signor, C., Baker, D., Mathesius, U., Crespi, M., and Frugier, F. (2011). MtCRE1-dependent cytokinin signaling integrates bacterial and plant cues to coordinate symbiotic nodule organogenesis in *Medicago truncatula*. *Plant Journal* 65, 622-633.
- Poovaliah, B.W., Du, L., Wang, H., and Yang, T. (2013). Recent advances in calcium/calmodulin-mediated signaling with an emphasis on plant-microbe interactions. *Plant Physiology* 163, 531-542.
- Pumplin, N., and Harrison, M.J. (2009). Live-cell imaging reveals periarbuscular membrane domains and organelle location in *Medicago truncatula* roots during arbuscular mycorrhizal symbiosis. *Plant Physiology* 151, 809-819.
- Pumplin, N., Mondo, S.J., Topp, S., Starker, C.G., Gantt, J.S., and Harrison, M.J. (2010). *Medicago truncatula* Vapyrin is a novel protein required for arbuscular mycorrhizal symbiosis. *Plant Journal* 61, 482-494.
- Quinn, J.M., and Etzler, M.E. (1987). Isolation and characterization of a lectin from the roots of *Dolichos biflorus*. *Archives of Biochemistry and Biophysics* 258, 535-544.
- Radutoiu, S., Madsen, L.H., Madsen, E.B., Felle, H.H., Umehara, Y., Gronlund, M., Sato, S., Nakamura, Y., Tabata, S., Sandal, N., and Stougaard, J. (2003). Plant recognition of symbiotic bacteria requires two LysM receptor-like kinases. *Nature* 425, 585-592.
- Radutoiu, S., Madsen, L.H., Madsen, E.B., Jurkiewicz, A., Fukai, E., Quistgaard, E.M., Albrechtsen, A.S., James, E.K., Thirup, S., and Stougaard, J. (2007). LysM domains mediate lipochitin-

- oligosaccharide recognition and *Nfr* genes extend the symbiotic host range. *EMBO Journal* 26, 3923-3935.
- Rasala, B.A., Orjalo, A.V., Shen, Z., Briggs, S., and Forbes, D.J. (2006). ELYS is a dual nucleoporin/kinetochore protein required for nuclear pore assembly and proper cell division. *Proceedings of the National Academy of Sciences, USA* 103, 17801-17806.
- Reddy D. M. R., S., Schorderet, M., Feller, U., and Reinhardt, D. (2007). A petunia mutant affected in intracellular accommodation and morphogenesis of arbuscular mycorrhizal fungi. *Plant Journal* 51, 739-750.
- Remy, W., Taylor, T.N., Hass, H., and Kerp, H. (1994). Four hundred-million-year-old vesicular arbuscular mycorrhizae. *Proceedings of the National Academy of Sciences, USA* 91, 11841-11843.
- Riely, B.K., Lounnon, G., Ané, J.-M., and Cook, D.R. (2007). The symbiotic ion channel homolog DMI1 is localized in the nuclear membrane of *Medicago truncatula* roots. *Plant Journal* 49, 208-216.
- Rizzo, M.A., Springer, G.H., Granada, B., and Piston, D.W. (2004). An improved cyan fluorescent protein variant useful for FRET. *Nature Biotechnology* 22, 445-449.
- Roberts, N.J., Morieri, G., Kalsi, G., Rose, A., Stiller, J., Edwards, A., Xie, F., Gresshoff, P.M., Oldroyd, G.E.D., Downie, J.A., and Etzler, M.E. (2013). Rhizobial and mycorrhizal symbioses in *Lotus japonicus* require lectin nucleotide phosphohydrolase, which acts upstream of calcium signaling. *Plant Physiology* 161, 556-567.
- Robles, L.M., Deslauriers, S.D., Alvarez, A.A., and Larsen, P.B. (2012). A loss-of-function mutation in the nucleoporin AtNUP160 indicates that normal auxin signalling is required for a proper ethylene response in *Arabidopsis*. *Journal of Experimental Botany* 63, 2231-2241.
- Roche, P., Debelle, F., Maillet, F., Lerouge, P., Faucher, C., Truchet, G., Dénarié, J., and Promé, J.-C. (1991). Molecular basis of symbiotic host specificity in rhizobium meliloti: *nodH* and *nodPQ* genes encode the sulfation of lipo-oligosaccharide signals. *Cell* 67, 1131-1143.
- Ródenas, E., González-Aguilera, C., Ayuso, C., and Askjaer, P. (2012). Dissection of the NUP107 nuclear pore subcomplex reveals a novel interaction with spindle assembly checkpoint protein MAD1 in *Caenorhabditis elegans*. *Molecular Biology of the Cell* 23, 930-944.
- Rodrigues, M.A., Gomes, D.A., Nathanson, M.H., and Leite, M.F. (2009). Nuclear calcium signaling: a cell within a cell. *Brazilian Journal of Medical and Biological Research* 42, 17-20.
- Rogers, C., and Oldroyd, G.E.D. (2014). Synthetic biology approaches to engineering the nitrogen symbiosis in cereals. *Journal of Experimental Botany*.
- Routray, P., Miller, J.B., Du, L., Oldroyd, G., and Poovaiah, B.W. (2013). Phosphorylation of S344 in the calmodulin-binding domain negatively affects CCaMK function during bacterial and fungal symbioses. *Plant Journal*, n/a-n/a.
- Ruyter-Spira, C., Al-Babili, S., Van Der Krol, S., and Bouwmeester, H. (2013). The biology of strigolactones. *Trends in Plant Science* 18, 72-83.
- Saito, K., Yoshikawa, M., Yano, K., Miwa, H., Uchida, H., Asamizu, E., Sato, S., Tabata, S., Imaizumi-Anraku, H., Umehara, Y., Kouchi, H., Murooka, Y., Szczyglowski, K., Downie, J.A., Parniske, M., Hayashi, M., and Kawaguchi, M. (2007). NUCLEOPORIN85 is required for calcium spiking, fungal and bacterial symbioses, and seed production in *Lotus japonicus*. *Plant Cell* 19, 610-624.
- Sathyanarayanan, P.V., Cremo, C.R., and Poovaiah, B.W. (2000). Plant chimeric Ca²⁺/calmodulin-dependent protein kinase: Role of the neural visinin-like domain in regulating autophosphorylation and calmodulin affinity. *Journal of Biological Chemistry* 275, 30417-30422.
- Schaarschmidt, S., Gresshoff, P., and Hause, B. (2013). Analyzing the soybean transcriptome during autoregulation of mycorrhization identifies the transcription factors GmNF-YA1a/b as positive regulators of arbuscular mycorrhization. *Genome Biology* 14, R62.

- Schauser, L., Handberg, K., Sandal, N., Stiller, J., Thykjær, T., Pajuelo, E., Nielsen, A., and Stougaard, J. (1998). Symbiotic mutants deficient in nodule establishment identified after T-DNA transformation of *Lotus japonicus*. *Molecular and General Genetics MGG* 259, 414-423.
- Schauser, L., Roussis, A., Stiller, J., and Stougaard, J. (1999). A plant regulator controlling development of symbiotic root nodules. *Nature* 402, 191-195.
- Schüßler, A., Schwarzott, D., and Walker, C. (2001). A new fungal phylum, the *Glomeromycota*: phylogeny and evolution. *Mycological Research* 105, 1413-1421.
- Shaner, N.C., Campbell, R.E., Steinbach, P.A., Giepmans, B.N.G., Palmer, A.E., and Tsien, R.Y. (2004). Improved monomeric red, orange and yellow fluorescent proteins derived from *Discosoma* sp. red fluorescent protein. *Nature Biotechnology* 22, 1567-1572.
- Shaw, S.L., and Long, S.R. (2003). Nod factor elicits two separable calcium responses in *Medicago truncatula* root hair cells. *Plant Physiology* 131, 976-984.
- Sieberer, B.J., Chabaud, M., Fournier, J., Timmers, A.C.J., and Barker, D.G. (2012). A switch in Ca²⁺ spiking signature is concomitant with endosymbiotic microbe entry into cortical root cells of *Medicago truncatula*. *Plant Journal* 69, 822-830.
- Sieberer, B.J., Chabaud, M., Timmers, A.C., Monin, A., Fournier, J., and Barker, D.G. (2009). A nuclear-targetedameleon demonstrates intranuclear Ca²⁺ spiking in *Medicago truncatula* root hairs in response to rhizobial nodulation factors. *Plant Physiology* 151, 1197-1206.
- Siltberg-Liberles, J., Grahn, J.A., and Liberles, D.A. (2011). The evolution of protein structures and structural ensembles under functional constraint. *Genes* 2, 748-762.
- Singh, S., Katzer, K., Lambert, J., Cerri, M., and Parniske, M. (2014). CYCLOPS, a DNA-Binding transcriptional activator, orchestrates symbiotic root nodule development. *Cell Host & Microbe* 15, 139-152.
- Singh, S., and Parniske, M. (2012). Generation of calcium spiking and activation of Calcium and calmodulin-dependent protein kinase (CCaMK), the central regulator of plant root endosymbiosis. *Current Opinion in Plant Biology*.
- Siniosoglou, S., Wimmer, C., Rieger, M., Doye, V., Tekotte, H., Weise, C., Emig, S., Segref, A., and Hurt, E.C. (1996). A novel complex of nucleoporins, which includes Sec13p and a Sec13p homolog, is essential for normal nuclear pores. *Cell* 84, 265-275.
- Smit, P., Raedts, J., Portyanko, V., Debelle, F., Gough, C., Bisseling, T., and Geurts, R. (2005). NSP1 of the GRAS protein family is essential for rhizobial Nod factor-induced transcription. *Science* 308, 1789-1791.
- Smith, S.E., and Read, D.J. (2008). *Mycorrhizal symbiosis*. London: Academic Press.
- Smith, S.E., and Smith, F.A. (2011). Roles of arbuscular mycorrhizas in plant nutrition and growth: new paradigms from cellular to ecosystem scales. *Annual Review of Plant Biology* 62, 227-250.
- Soltis, D.E., Soltis, P.S., Chase, M.W., Mort, M.E., Albach, D.C., Zanis, M., Savolainen, V., Hahn, W.H., Hoot, S.B., Fay, M.F., Axtell, M., Swensen, S.M., Prince, L.M., Kress, W.J., Nixon, K.C., and Farris, J.S. (2000). Angiosperm phylogeny inferred from 18S rDNA, *rbcL*, and *atpB* sequences. *Botanical Journal of the Linnean Society* 133, 381-461.
- Soullam, B., and Worman, H.J. (1995). Signals and structural features involved in integral membrane protein targeting to the inner nuclear membrane. *The Journal of Cell Biology* 130, 15-27.
- Soyano, T., Kouchi, H., Hirota, A., and Hayashi, M. (2013). NODULE INCEPTION directly targets NF-Y subunit genes to regulate essential processes of root nodule development in *Lotus japonicus*. *PLoS Genet* 9, e1003352.
- Sprent, J.I. (2007). Evolving ideas of legume evolution and diversity: a taxonomic perspective on the occurrence of nodulation. *New Phytologist* 174, 11-25.
- Sprent, J.I., and James, E.K. (2007). Legume evolution: where do nodules and mycorrhizas fit in? *Plant Physiology* 144, 575-581.

- Staehelein, C., Xie, Z.-P., Illana, A., and Vierheilig, H. (2011). Long-distance transport of signals during symbiosis: are nodule formation and mycorrhization autoregulated in a similar way? *Plant Signaling & Behavior* 6, 372-377.
- Stoffler, D., Feja, B., Fahrenkrog, B., Walz, J., Typke, D., and Aebi, U. (2003). Cryo-electron tomography provides novel insights into nuclear pore architecture: implications for nucleocytoplasmic transport. *Journal of Molecular Biology* 328, 119-130.
- Stougaard, J., Abildsten, D., and Marcker, K. (1987). The *Agrobacterium rhizogenes* pRi TL-DNA segment as a gene vector system for transformation of plants. *Molecular and General Genetics MGG* 207, 251-255.
- Stracke, S., Kistner, C., Yoshida, S., Mulder, L., Sato, S., Kaneko, T., Tabata, S., Sandal, N., Stougaard, J., Szczyglowski, K., and Parniske, M. (2002). A plant receptor-like kinase required for both bacterial and fungal symbiosis. *Nature* 417, 959-962.
- Strambio-De-Castillia, C., Niepel, M., and Rout, M.P. (2010). The nuclear pore complex: bridging nuclear transport and gene regulation. *Nat Rev Mol Cell Biol* 11, 490-501.
- Strawn, L.A., Shen, T., Shulga, N., Goldfarb, D.S., and Went, S.R. (2004). Minimal nuclear pore complexes define FG repeat domains essential for transport. *Nat Cell Biol* 6, 197-206.
- Subramanian, S., Stacey, G., and Yu, O. (2007). Distinct, crucial roles of flavonoids during legume nodulation. *Trends in Plant Science* 12, 282-285.
- Swainsbury, D.J.K., Zhou, L., Oldroyd, G.E.D., and Bornemann, S. (2012). Calcium ion binding properties of *Medicago truncatula* calcium/calmodulin-dependent protein kinase. *Biochemistry* 51, 6895-6907.
- Syed, N.H., Kalyna, M., Marquez, Y., Barta, A., and Brown, J.W.S. (2012). Alternative splicing in plants – coming of age. *Trends in Plant Science* 17, 616-623.
- Takezawa, D., Ramachandiran, S., Paranjape, V., and Poovaiah, B.W. (1996). Dual regulation of a chimeric plant serine/threonine kinase by calcium and calcium/calmodulin. *Journal of Biological Chemistry* 271, 8126-8132.
- Tamura, K., Fukao, Y., Iwamoto, M., Haraguchi, T., and Hara-Nishimura, I. (2010). Identification and characterization of nuclear pore complex components in *Arabidopsis thaliana*. *Plant Cell* 22, 4084-4097.
- Tirichine, L., Imaizumi-Anraku, H., Yoshida, S., Murakami, Y., Madsen, L.H., Miwa, H., Nakagawa, T., Sandal, N., Albrechtsen, A.S., Kawaguchi, M., Downie, A., Sato, S., Tabata, S., Kouchi, H., Parniske, M., Kawasaki, S., and Stougaard, J. (2006). Deregulation of a Ca²⁺/calmodulin-dependent kinase leads to spontaneous nodule development. *Nature* 441, 1153-1156.
- Tirichine, L., Sandal, N., Madsen, L.H., Radutoiu, S., Albrechtsen, A.S., Sato, S., Asamizu, E., Tabata, S., and Stougaard, J. (2007). A gain-of-function mutation in a cytokinin receptor triggers spontaneous root nodule organogenesis. *Science* 315, 104-107.
- Tóth, K., Stratil, T.F., Madsen, E.B., Ye, J., Popp, C., Antolín-Llovera, M., Grossmann, C., Jensen, O.N., Schüßler, A., Parniske, M., and Ott, T. (2012). Functional domain analysis of the remorin protein LjSYMREM1 in *Lotus japonicus*. *PLoS ONE* 7, e30817.
- Trinick, M.J. (1973). Symbiosis between *Rhizobium* and the non-legume, *Trema aspera*. *Nature* 244, 459-460.
- Turgay, Y., Ungrecht, R., Rothballer, A., Kiss, A., Csucs, G., Horvath, P., and Kutay, U. (2010). A classical NLS and the SUN domain contribute to the targeting of SUN2 to the inner nuclear membrane. 29, 2262-2275.
- Udvardi, M.K., Tabata, S., Parniske, M., and Stougaard, J. (2005). *Lotus japonicus*: legume research in the fast lane. *Trends in Plant Science* 10, 222-228.
- Untergasser, A., Cutcutache, I., Koressaar, T., Ye, J., Faircloth, B.C., Remm, M., and Rozen, S.G. (2012). Primer3—new capabilities and interfaces. *Nucleic Acids Research* 40, e115.
- Urbański, D.F., Małolepszy, A., Stougaard, J., and Andersen, S.U. (2012). Genome-wide LORE1 retrotransposon mutagenesis and high-throughput insertion detection in *Lotus japonicus*. *Plant Journal* 69, 731-741.

- Van Brussel, A.a.N., Bakhuizen, R., Van Spronsen, P.C., Spaink, H.P., Tak, T., Lugtenberg, B.J.J., and Kijne, J.W. (1992). Induction of pre-infection thread structures in the leguminous host plant by mitogenic lipo-oligosaccharides of *Rhizobium*. *Science* 257, 70-72.
- Van De Vosse, D., Wan, Y., Lapetina, D., Chen, W.-M., Chiang, J.-H., Aitchison, J., and Wozniak, R. (2013). A role for the nucleoporin Nup170p in chromatin structure and gene silencing. *Cell* 152, 969-983.
- Van De Vosse, D.W., Wan, Y., Wozniak, R.W., and Aitchison, J.D. (2011). Role of the nuclear envelope in genome organization and gene expression. *Wiley Interdisciplinary Reviews: Systems Biology and Medicine* 3, 147-166.
- Venkateshwaran, M., Cosme, A., Han, L., Banba, M., Satyshur, K.A., Schleiff, E., Parniske, M., Imaizumi-Anraku, H., and Ané, J.-M. (2012). The recent evolution of a symbiotic ion channel in the legume family altered ion conductance and improved functionality in calcium signaling. *Plant Cell* 24, 2528-2545.
- Venkateshwaran, M., Volkening, J.D., Sussman, M.R., and Ané, J.-M. (2013). Symbiosis and the social network of higher plants. *Current Opinion in Plant Biology* 16, 118-127.
- Vernié, T., Moreau, S., De Billy, F., Plet, J., Comber, J.-P., Rogers, C., Oldroyd, G., Frugier, F., Niebel, A., and Gamas, P. (2008). EFD is an ERF transcription factor involved in the control of nodule number and differentiation in *Medicago truncatula*. *Plant Cell* 20, 2696-2713.
- Voinnet, O., Rivas, S., Mestre, P., and Baulcombe, D. (2003). An enhanced transient expression system in plants based on suppression of gene silencing by the p19 protein of tomato bushy stunt virus. *Plant Journal* 33, 949-956.
- Walter, M., Chaban, C., Schütze, K., Batistic, O., Weckermann, K., Näke, C., Blazevic, D., Grefen, C., Schumacher, K., Oecking, C., Harter, K., and Kudla, J. (2004). Visualization of protein interactions in living plant cells using bimolecular fluorescence complementation. *Plant Journal* 40, 428-438.
- Walther, T.C., Alves, A., Pickersgill, H., Lo1 Odice, I., Hetzer, M., Galy, V., Hülsmann, B.B., Köcher, T., Wilm, M., Allen, T., Mattaj, I.W., and Doye, V. (2003). The conserved Nup107-160 complex is critical for nuclear pore complex assembly. *Cell* 113, 195-206.
- Wang, E., Schornack, S., Marsh, John f., Gobbato, E., Schwessinger, B., Eastmond, P., Schultze, M., Kamoun, S., and Oldroyd, Giles e.D. (2012). A common signaling process that promotes mycorrhizal and oomycete colonization of plants. *Current Biology* 22, 2242-2246.
- Wen, W., Meinkotht, J.L., Tsien, R.Y., and Taylor, S.S. (1995). Identification of a signal for rapid export of proteins from the nucleus. *Cell* 82, 463-473.
- Wente, S.R., and Rout, M.P. (2010). The nuclear pore complex and nuclear transport. *Cold Spring Harbor Perspectives in Biology* 2.
- Weston, L., and Mathesius, U. (2013). Flavonoids: their structure, biosynthesis and role in the rhizosphere, including allelopathy. *Journal of Chemical Ecology* 39, 283-297.
- White, J., Prell, J., James, E., and Poole, P. (2007). Nutrient sharing between symbionts. *Plant Physiology* 144, 604-614.
- Wiermer, M., Cheng, Y.T., Imkampe, J., Li, M., Wang, D., Lipka, V., and Li, X. (2012). Putative members of the *Arabidopsis* Nup107-160 nuclear pore sub-complex contribute to pathogen defense. *Plant Journal*.
- Wozniak, R., Burke, B., and Doye, V. (2010). Nuclear transport and the mitotic apparatus: an evolving relationship. *Cellular and Molecular Life Sciences* 67, 2215-2230.
- Wu, W., Lin, F., and Worman, H.J. (2002). Intracellular trafficking of MAN1, an integral protein of the nuclear envelope inner membrane. *Journal of Cell Science* 115, 1361-1371.
- Xie, F., Murray, J.D., Kim, J., Heckmann, A.B., Edwards, A., Oldroyd, G.E.D., and Downie, J.A. (2012). Legume pectate lyase required for root infection by rhizobia. *Proceedings of the National Academy of Sciences* 109, 633-638.
- Xiong, T.C., Jauneau, A., Ranjeva, R., and Mazars, C. (2004). Isolated plant nuclei as mechanical and thermal sensors involved in calcium signalling. *The Plant Journal* 40, 12-21.

- Xu, X.M., Rose, A., Muthuswamy, S., Jeong, S.Y., Venkatakrishnan, S., Zhao, Q., and Meier, I. (2007). NUCLEAR PORE ANCHOR, the *Arabidopsis* homolog of Tpr/Mlp1/Mlp2/Megator, is involved in mRNA export and SUMO homeostasis and affects diverse aspects of plant development. *The Plant Cell* 19, 1537-1548.
- Xue, B., Dunbrack, R.L., Williams, R.W., Dunker, A.K., and Uversky, V.N. (2010). PONDR-FIT: A meta-predictor of intrinsically disordered amino acids. *Biochimica et Biophysica Acta (BBA) - Proteins and Proteomics* 1804, 996-1010.
- Yano, K., Yoshida, S., Muller, J., Singh, S., Banba, M., Vickers, K., Markmann, K., White, C., Schuller, B., Sato, S., Asamizu, E., Tabata, S., Murooka, Y., Perry, J., Wang, T.L., Kawaguchi, M., Imaizumi-Anraku, H., Hayashi, M., and Parniske, M. (2008). CYCLOPS, a mediator of symbiotic intracellular accommodation. *Proceedings of the National Academy of Sciences, USA* 105, 20540-20545.
- Yokota, K., Fukai, E., Madsen, L.H., Jurkiewicz, A., Rueda, P., Radutoiu, S., Held, M., Hossain, M.S., Szczyglowski, K., Morieri, G., Oldroyd, G.E.D., Downie, J.A., Nielsen, M.W., Rusek, A.M., Sato, S., Tabata, S., James, E.K., Oyaizu, H., Sandal, N., and Stougaard, J. (2009). Rearrangement of actin cytoskeleton mediates invasion of *Lotus japonicus* roots by *Mesorhizobium loti*. *Plant Cell* 21, 267-284.
- Yoneyama, K., Xie, X., Kim, H., Kisugi, T., Nomura, T., Sekimoto, H., Yokota, T., and Yoneyama, K. (2012). How do nitrogen and phosphorus deficiencies affect strigolactone production and exudation? *Planta* 235, 1197-1207.
- Young, N.D., Debelle, F., Oldroyd, G.E.D., Geurts, R., Cannon, S.B., Udvardi, M.K., Benedito, V.A., Mayer, K.F.X., Gouzy, J., Schoof, H., Van De Peer, Y., Proost, S., Cook, D.R., Meyers, B.C., Spannagl, M., Cheung, F., De Mita, S., Krishnakumar, V., Gundlach, H., Zhou, S., Mudge, J., Bharti, A.K., Murray, J.D., Naoumkina, M.A., Rosen, B., Silverstein, K.a.T., Tang, H., Rombauts, S., Zhao, P.X., Zhou, P., Barbe, V., Bardou, P., Bechner, M., Bellec, A., Berger, A., Berges, H., Bidwell, S., Bisseling, T., Choisine, N., Couloux, A., Denny, R., Deshpande, S., Dai, X., Doyle, J.J., Dudez, A.-M., Farmer, A.D., Fouteau, S., Franken, C., Gibelin, C., Gish, J., Goldstein, S., Gonzalez, A.J., Green, P.J., Hallab, A., Hartog, M., Hua, A., Humphray, S.J., Jeong, D.-H., Jing, Y., Jocker, A., Kenton, S.M., Kim, D.-J., Klee, K., Lai, H., Lang, C., Lin, S., Macmil, S.L., Magdelenat, G., Matthews, L., Mccorison, J., Monaghan, E.L., Mun, J.-H., Najar, F.Z., Nicholson, C., Noirot, C., O/Bleness, M., Paule, C.R., Poulain, J., Prion, F., Qin, B., Qu, C., Retzel, E.F., Riddle, C., Sallet, E., Samain, S., Samson, N., Sanders, I., Saurat, O., Scarpelli, C., Schiex, T., Segurens, B., Severin, A.J., Sherrier, D.J., Shi, R., Sims, S., Singer, S.R., Sinharoy, S., Sterck, L., Viollet, A., Wang, B.-B., et al. (2011). The *Medicago* genome provides insight into the evolution of rhizobial symbioses. *Nature* 480, 520-524.
- Yu, N., Luo, D., Zhang, X., Liu, J., Wang, W., Jin, Y., Dong, W., Liu, J., Liu, H., Yang, W., Zeng, L., Li, Q., He, Z., Oldroyd, G.E.D., and Wang, E. (2014). A DELLA protein complex controls the arbuscular mycorrhizal symbiosis in plants. *Cell Research* 24, 130-133.
- Zapata-Hommer, O., and Griesbeck, O. (2003). Efficiently folding and circularly permuted variants of the Sapphire mutant of GFP. *BMC Biotechnology* 3, 5.
- Zhang, Y., and Li, X. (2005). A putative Nucleoporin 96 is required for both basal defense and constitutive resistance responses mediated by *suppressor of npr1-1, constitutive 1*. *Plant Cell* 17, 1306-1316.
- Zheng, X., Yang, S., Han, Y., Zhao, X., Zhao, L., Tian, T., Tong, J., Xu, P., Xiong, C., and Meng, A. (2012). Loss of zygotic NUP107 protein causes missing of pharyngeal skeleton and other tissue defects with impaired nuclear pore function in zebrafish embryos. *Journal of Biological Chemistry* 287, 38254-38264.
- Zhu, H., Riely, B.K., Burns, N.J., and Ané, J.-M. (2006). Tracing nonlegume orthologs of legume genes required for nodulation and arbuscular mycorrhizal symbioses. *Genetics* 172, 2491-2499.
- Zuleger, N., Korfali, N., and Schirmer, E.C. (2008). Inner nuclear membrane protein transport is mediated by multiple mechanisms. *Biochemical Society Transactions* 36, 1373-1377.